

Accepted Manuscript

Synthesis and SAR of new isoxazole-triazole bis-heterocyclic compounds as analogues of natural lignans with antiparasitic activity

Lara A. Zimmermann, Milene H. de Moraes, Rafael da Rosa, Eduardo B. de Melo, Fávero R. Paula, Eloir P. Schenkel, Mario Steindel, Lílian S.C. Bernardes

PII: S0968-0896(18)31167-2
DOI: <https://doi.org/10.1016/j.bmc.2018.08.025>
Reference: BMC 14512

To appear in: *Bioorganic & Medicinal Chemistry*

Received Date: 21 June 2018
Revised Date: 7 August 2018
Accepted Date: 17 August 2018

Please cite this article as: Zimmermann, L.A., de Moraes, M.H., da Rosa, R., de Melo, E.B., Paula, F.R., Schenkel, E.P., Steindel, M., Bernardes, L.S.C., Synthesis and SAR of new isoxazole-triazole bis-heterocyclic compounds as analogues of natural lignans with antiparasitic activity, *Bioorganic & Medicinal Chemistry* (2018), doi: <https://doi.org/10.1016/j.bmc.2018.08.025>

This is a PDF file of an unedited manuscript that has been accepted for publication. As a service to our customers we are providing this early version of the manuscript. The manuscript will undergo copyediting, typesetting, and review of the resulting proof before it is published in its final form. Please note that during the production process errors may be discovered which could affect the content, and all legal disclaimers that apply to the journal pertain.



Synthesis and SAR of new isoxazole-triazole bis-heterocyclic compounds as analogues of natural lignans with antiparasitic activity

Lara A. Zimmermann[†], Milene H. de Moraes^{*}, Rafael da Rosa[†], Eduardo B. de Melo[#], Fávero R. Paula^{||}, Eloir P. Schenkel[†], Mario Steindel^{*} and Lílian S. C. Bernardes^{†*}.

[†] Department of Pharmaceutical Sciences, Federal University of Santa Catarina, 88040-900, Florianópolis, 88040-900, SC, Brazil.

^{*} Department of Microbiology, Immunology and Parasitology, Federal University of Santa Catarina, Florianópolis, 88040-900, SC, Brazil.

[#] Department of Pharmacy, Western Paraná State University, Cascavel, 858119-110, PR, Brazil.

^{||} Course of Pharmacy, Federal University of Pampa, Uruguaiana, 97500-970, RS, Brazil.

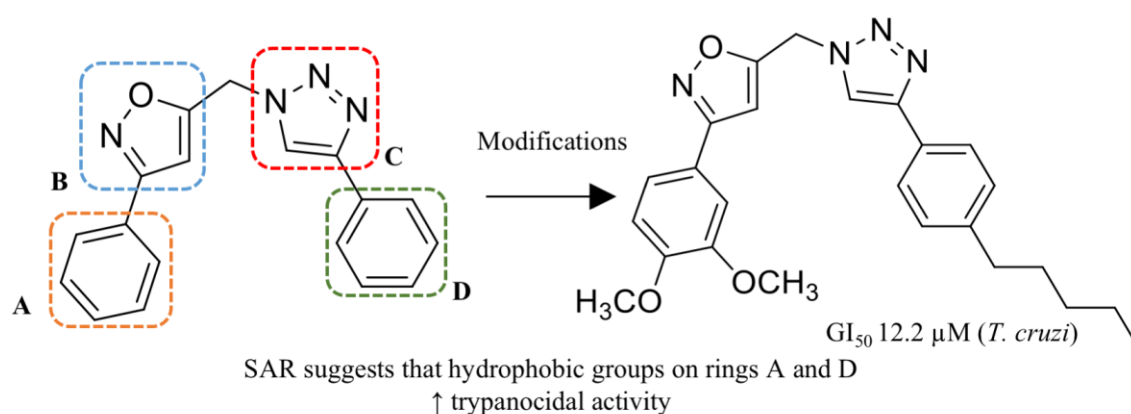
*Corresponding author: l.bernardes@ufsc.br

ABSTRACT Despite the impressive scientific and technological advances of recent decades, no effective treatment is currently available for Chagas disease. Our research group has been studying the design and synthesis of analogues of natural lignans aiming to identify compounds with antiparasitic activity. This article reports the synthesis of 42 novel bis-heterocyclic derivatives and the structure-activity relationship study conducted based on results of biological assays against *Trypanosoma cruzi* amastigotes. Thirty-seven compounds were active, and eight of them had GI₅₀ values lower than 100 μM (GI₅₀ 88.4–12.2 μM). A qualitative structure activity relationship study using three dimensional descriptors was carried out and showed a correlation between growth inhibitory potency and the presence of bulky hydrophobic groups located at rings A and D of the compounds. Compound 3-(3,4-dimethoxyphenyl)-5-((4-(4-pentylphenyl)-1H-1,2,3-triazol-1-yl)methyl)isoxazole (**31**) was the most active in the series (GI₅₀ 12.2 μM), showing, *in vitro*, low toxicity and potency similar to benznidazole (GI₅₀ 10.2 μM). These results suggest that this compound can be a promising scaffold for the design of new trypanocidal compounds.

KEYWORDS isoxazole, triazole, anti-trypanosomatid agents, *Trypanosoma cruzi*, *Leishmania amazonensis*.

ABBREVIATIONS %GI: percentage of parasite growth inhibition at 100 μM; GI₅₀: 50% growth inhibition concentration; Bnz: benznidazole; MW: microwave; NA: not active at the tested concentration; ND: not determined due to absence of trypanocidal activity; SI: selectivity index (CC₅₀ THP-1 cells/GI₅₀); (r)TR: (recombinant) trypanothione reductase.

GRAPHICAL ABSTRACT



HIGHLIGHTS

42 bis-heterocyclic analogues of natural lignans were synthesized.

All compounds had their trypanocidal and leishmanicidal activities evaluated.

The most active compounds were evaluated against (r)TR.

SAR showed a correlation between growth inhibition and the presence of bulky hydrophobic groups.

1. INTRODUCTION

Chagas disease and leishmaniasis caused by protozoan parasites *Trypanosoma cruzi* and *Leishmania* spp., respectively, are tropical and subtropical diseases that affect millions of people worldwide and are major causes of mortality and morbidity, especially in Latin America^{1,2}. Current treatments have major drawbacks, such as variable efficacy, long therapy duration, prolonged hospitalization, high costs, and the potential development of drug resistance. Thus, there is an urgent need to discover new drugs candidate for the treatment of these parasitic diseases³⁻⁵.

The study of natural products is a promising strategy in drug development for obtaining lead compounds. Of all drugs approved between 1981 and 2014 for the treatment of human diseases, about 56% are related to natural products⁶. Furthermore, the search for plant-derived compounds with high antiparasitic activity has received much attention because of the structural diversity of these secondary metabolites^{7,8}.

Our research group has been studying the design and synthesis of analogues of the trypanocidal natural lignans veraguensin (**1**) and grandisin (**2**) using different strategies of molecular modification, aiming to identify *hit* compounds with appropriate chemical and biological properties⁹⁻¹¹. Recently, we have described the synthesis of a series of derivatives containing the isoxazole ring as a bioisosteric replacement of the central tetrahydrofuran ring of natural lignans **1** and **2**⁹. As a continuation of our studies, considering promising molecules previously identified (**4-6**)⁹, we synthesized a series of bis-heterocyclic derivatives containing the isoxazole moiety and a triazole ring as a spacer group between the aromatic units (**Figure 1**). These heterocyclic systems are found in several drugs and show interesting properties because of their chemical characteristics, biological and pharmacological applications¹²⁻¹⁴. The five-membered heterocyclic ring triazole was selected because of its ability to act as both hydrogen bond acceptor (HBA) and donor (HBD), structure rigidity and stability under oxidative and reductive conditions¹⁵. These aspects combined contribute to ongoing SAR studies on trypanocidal lignan derivatives and for designing chemically more complex compounds without considerable negative effects on druglikeness.

In this work, compounds were planned by modifying rings **A** and **D** of the proposed scaffold (**7**) using the different substitution patterns seen in natural derivatives (lignans **1-3**), which contain methoxy and methylenedioxy groups, and by varying the substituent groups on ring **D** regarding their electronic and structural diversity. Presenting the synthesis of 42 new compounds, this article describes the structure-activity relationship (SAR) studies that were carried out based on the results of biological assays against *T. cruzi* amastigotes. Additionally, the most promising synthesized compounds were evaluated against Trypanothione reductase enzyme, considering that it is a trypanosomatid-specific target involved in the redox metabolism of the parasite and is essential for its survival¹⁶⁻²¹.

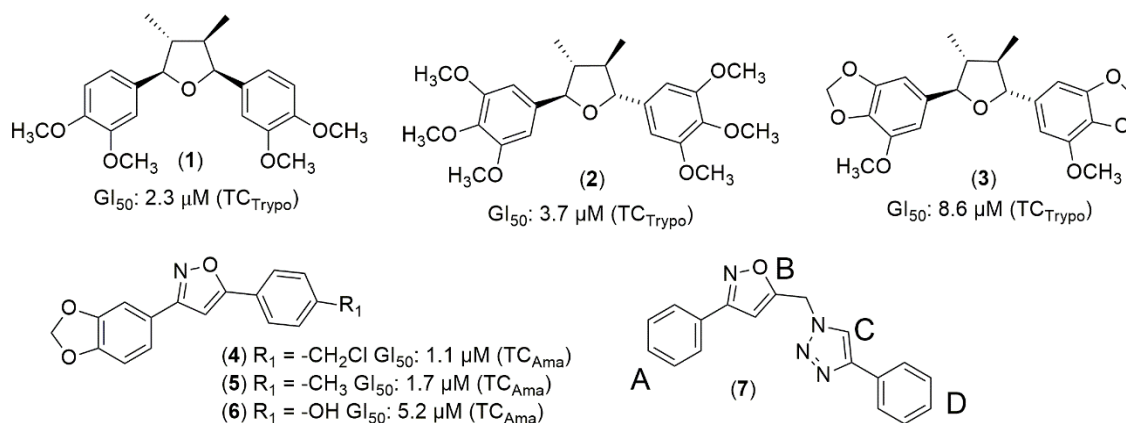
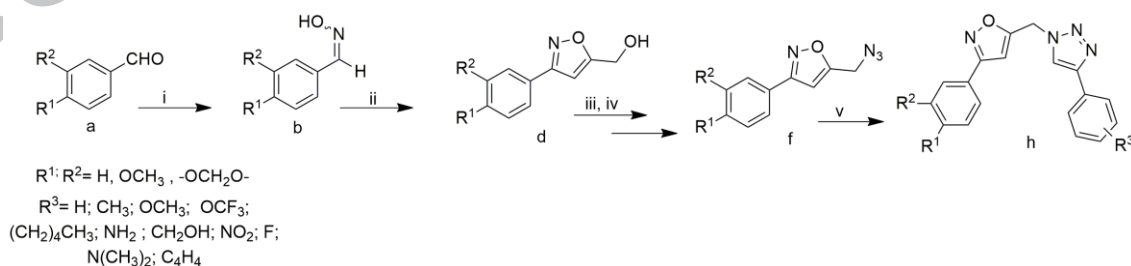


Figure 1. Natural neolignans veraguensin (1), grandisin (2), and 6,6'-((2*R*,3*R*,4*R*,5*R*)-3,4-dimethyltetrahydrofuran-2,5-diyl)bis(4-methoxybenzo[d][1,3]dioxole) (3), 3,5-disubstituted isoxazoles (4-6) and scaffold of the proposed bis-heterocyclic derivatives (7). TC_{Trypo}: *T. cruzi* trypomastigotes; TC_{Ama}: *T. cruzi* amastigotes.

2. RESULTS AND DISCUSSION

2.1. SYNTHESIS

The synthetic route was designed to be economically feasible and reproducible and to allow the rapid preparation of a library of structurally diverse compounds in good yields (Scheme 1). Initially, an aldoxime (b) was synthesized in 98% yield by microwave irradiation of a commercial aldehyde (a) and hydroxylamine hydrochloride²². Subsequently, this aldoxime was reacted with *N*-chlorosuccinimide, generating in situ the corresponding arylcarboximidoyl chloride, which was reacted with propargyl alcohol in the presence of copper sulfate to form a 3,5-disubstituted isoxazole derivative (d)²³. This compound was tosylated and reacted with sodium azide under microwave irradiation, giving intermediate azide f in 85% yield^{24,25}. Finally, the bis-heterocyclic compounds (h) were obtained by copper(I)-catalyzed azide–alkyne cycloadditions (CuAAC) under microwave irradiation in yields ranging from 38 to 99%. The compounds 7–48 were characterized by ¹H and ¹³C NMR and mass spectrometry. Spectral data are available in the Supplementary Material. The compounds were evaluated for drug-likeness using Lipinski's Rule of Five, and most of them had the properties necessary for good oral bioavailability (Table S1, Supplementary Material)^{26,27}.

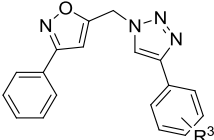


Scheme 1. Synthetic route of bis-heterocyclic compounds. (i) NH₂OH.HCl, DABCO, MW: 70 °C, 100 W, 1 min (60-98%); (ii) NCS, DMF, sodium ascorbate, CuSO₄, NaHCO₃, t-BuOH:H₂O, propargyl alcohol, r.t, 4 h (82%) or NCS, DMF, sodium ascorbate, CuSO₄, NaHCO₃, DMF, propargyl alcohol, MW: 35 °C, 150 W, 11 min (54-76%); (iii) TsCl, Et₃N, K₂CO₃, CH₂Cl₂:H₂O, 1 h (49-76%); (iv) NaN₃, DMF, MW: 70 °C, 150 W, 10 min (89-80%); (v) CuSO₄, sodium ascorbate, alkyne, DMF, 70 °C, 100 W, 10 min (38-89%).

2.2. BIOLOGIC INVESTIGATION AND STRUCTURE-ACTIVITY RELATIONSHIP STUDY

Compounds were tested in vitro on THP-1 cells (human monocytic leukaemia cell line) infected with *T. cruzi* amastigotes. Cytotoxicity assays were performed on THP-1 cells. These results are shown in Tables 1-3. All compounds were additionally evaluated against amastigotes of *Leishmania amazonensis*; however, no compound showed promising activity at 100 μM (Table S2, Supplementary Material).

Table 1. Inhibitory activity of the first series of compounds at 100 μM against *Trypanosoma cruzi* amastigotes.



Compound	R ₃	Yield (%) ^a	%GI ^b	GI ₅₀ (μM) ^b	CC ₅₀ (μM)	SI
7	H	76	33.7 \pm 0.8	>100	ND	-
8	4-OCH ₃	38	43.3 \pm 6.3	>100	ND	-
9	2-OCH ₃	88	12.4 \pm 1.7	>100	ND	-
10	3,5-OCH ₃	76	95.3 \pm 0.7	54.5 \pm 2.1	142.8 \pm 10.9	2.6
11	4-CH ₃	84	45.2 \pm 4.4	>100	ND	-
12	2,4,5-CH ₃	49	89.5 \pm 0.9	88.4 \pm 4.8	200.5 \pm 60.0	2.3
13	2-CH ₃ ,4-OCH ₃	92	18.6 \pm 2.5	>100	ND	-
14	2,5-CH ₃	88	0.0 \pm 0.0	NA ^d	ND	-
15	3-C ₂ H ₂ C(OCH ₃)CH-4	99	43.1 \pm 2.5	>100	ND	-
16	4-NO ₂	89	46.9 \pm 4.5	>100	ND	-
17	4-OCF ₃	77	28.7 \pm 2.4	>100	ND	-
18	4-F	68	0.00 \pm 0.0	NA ^d	ND	-
19	4-N(CH ₃) ₂	87	32.6 \pm 6.9	>100	ND	-
20	4-NH ₂	47	0.0 \pm 0.0	NA ^d	ND	-
21	4-CH ₂ OH	42	0.0 \pm 0.0	NA ^d	ND	-
22	4-(CH ₂) ₄ CH ₃	97	0.0 \pm 0.0	NA ^d	ND	-
Bnz			93.0 \pm 0.6 ^c	10.2 \pm 0.1	>500	>49.02

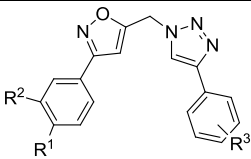
^aYield of the CuAAC reaction. ^bResults are expressed as mean \pm SD of an experiment performed in triplicate. ^cBnz: percentage of growth inhibition of *T. cruzi* amastigotes at 20 μM . ^dNA, not active at the tested concentration. SI: selectivity index = CC₅₀ THP-1/GI₅₀.

The first series of molecules synthesized had an unsubstituted **A** ring and variations of substituent groups on ring **D**. As compound **7** had the most simplified scaffold of the bis-heterocyclic derivatives, we considered its percentage of parasite growth inhibition (33.7%) to compare and discuss the SAR data of other compounds. Biological data suggest that the substitution of hydrogens for methoxy (OMe) groups affects the inhibitory activity according to the position of the group. The presence of 4-OMe contributed to a slight increase in activity (compound **8**, GI 43.3%), whereas the presence of 2-OMe led to a decrease in activity (compound **9**, GI 12.4%). The presence of 3,5-OMe (compound **10**) led to an increase in activity (GI 95.3%, GI₅₀ 54.5 μM , SI 2.6). In addition to the influence of the position of the methoxy groups, we investigated the trypanocidal activity of derivatives with a substituted methyl group on ring **D**. The addition of a 4-methyl group also led to a slight increase in activity (compound **11**, GI 45.2%), similar to the observed for the 4-OMe derivative (**8**). Compound **12**, which received a 2,4,5-trimethyl substitution, had an increase in activity (GI 89.5%, GI₅₀ 88.4 μM , SI 2.3). The combination of a methyl group at the 2-position and a methoxy group at the 4-position (compound **13**) decreased activity (GI 18.6%).

These results demonstrate the contribution of methoxy and methyl groups to compound activity, especially for derivatives with rings substituted at the 3,5 or 4,5 positions; these groups probably occupy and act on a hydrophobic region of a putative molecular target. We also observed a small decrease in activity for derivatives with a 2-methyl group, which may be related to the conformational restriction caused by the presence of *ortho* substituents in bis-aromatic compounds, altering their conformation and, consequently, influencing how they bind to a target. However, the presence of a 3,4-dimethyl substituent (compound **12**) contributed to inhibitory activity. The activity of compounds **9**, **13**, and, **14** suggests that a 2-substituent may decrease activity, but the combination of hydrophobic substituents at positions 3,5 or 4,5 has a positive effect on inhibitory activity. Furthermore, the 6-methoxy- β -naphthalene group, present in compound **15** (GI 43.1%), also seemed to be unfavorable for biological activity; because of its rigidity, this group might prevent the molecule from adopting an appropriate conformation to interact with a molecular target, even though it can form hydrophobic interactions. By analyzing the effects of electron-donor or electron-withdrawing groups at the *para* position of ring **D**, we observed that, for compounds **16–18**, the increase in biological activity was directly proportional to the increase in the electron-withdrawing capacity of the substituent. Most compounds containing electron-donor groups were able to inhibit parasite growth (**8**, **11** and **19**), with the exception of those that have *ortho* substituents (**9**; **14**) and compounds **20** (4-NH₂) and **21** (4-CH₂OH), which have polar substituents that would hinder possible hydrophobic interactions.

Based on the chemical structure of the most active compounds of the first series (**10** and **12**) and considering that the different active natural lignans (**1–3**) have methoxy or methylenedioxy groups as substituents on ring **A**^{28,29}, a second series of molecules was synthesized and evaluated against amastigotes of *T. cruzi* (**23–28**) (Table 2).

Table 2. Inhibitory activity of the second series of compounds at 100 μ M against *Trypanosoma cruzi* amastigotes.



Compound	R ₁	R ₂	R ₃	Yield (%) ^a	%GI ^b	GI ₅₀ (μ M) ^b	CC ₅₀ (μ M)	SI
23	OCH ₃	H	2,4,5-CH ₃	89	33.4 \pm 2.8	>100	ND	-
24	OCH ₃	H	3,5-OCH ₃	82	3.6 \pm 0.7	>100	ND	-
25	OCH ₃	OCH ₃	2,4,5-CH ₃	94	89.6 \pm 0.3	55.2 \pm 5.0	> 500	> 9.0
26	OCH ₃	OCH ₃	3,5-OCH ₃	96	74.8 \pm 3.7	30.3 \pm 4.3	> 500	> 16.5
27		OCH ₂ O	2,4,5-CH ₃	88	13.4 \pm 0.4	>100	ND	-
28		OCH ₂ O	3,5-OCH ₃	60	87.9 \pm 1.1	49.9 \pm 8.9	207.6 \pm 9.3	4.2
Bnz					93.0 \pm 0.6 ^c	10.2 \pm 0.1	>500	>49.0

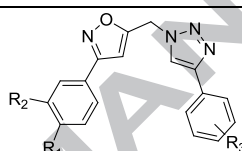
^aYield of the CuAAC reaction. ^bResults are expressed as mean \pm SD of an experiment performed in triplicate. ^cBnz: percentage of growth inhibition of *T. cruzi* amastigotes at 20 μ M. SI: selectivity index = CC₅₀ THP-1/GI₅₀

Regarding analogues containing the 2,4,5-trimethylphenyl ring, we observed that the 3,4-OMe substitution on ring **A** led to an increase both in trypanocidal potency and in selectivity. Similar results were obtained with derivatives containing the 3,5-

dimethoxyphenyl ring. Of these, compounds **26** and **28** were more potent and selective than the compound **10**. These results suggest that the presence of substituents at positions *meta* and *para* of ring **A** are important for biological activity.

On the basis of these observations, a third series of compounds (**29–42**) was synthesized (Table 3). In the new series, the 3,4-dimethoxy substitution pattern on ring **A** was maintained and the effect of modifying substituent groups on ring **D** was evaluated. Comparison of compounds **29**, **30**, and **31**, which have the 4-OCH₃, 4-OCF₃, and 4-(CH₂)₄CH₃ substituents on the **D** ring, respectively, to their analogues (**8**, **17**, and **22**) (Table 1) showed that the insertion of a dimethoxylated substituent on ring **A** favored trypanocidal activity. However, no significant change in activity was observed for analogues **43–48** (Table 3), which contained the 4-methoxy or 3,4-methylenedioxy substituents on ring **A**, corroborating the idea that, for the bis-heterocyclic derivatives presented herein, the presence of the 3,4-dimethoxyphenyl **A** ring is important for biological activity.

Table 3. Inhibitory activity of the third series of compounds at 100 μ M against *Trypanosoma cruzi* amastigotes



Compound	R ₁	R ₂	R ₃	Yield ^a (%)	%GI ^b	GI ₅₀ (μ M) ^b	CC ₅₀ (μ M)	SI
29	OCH ₃	OCH ₃	4-OCH ₃	62	81.9 \pm 2.0	22.7 \pm 3.5	> 500	> 22.0
30	OCH ₃	OCH ₃	4-OCF ₃	89	78.5 \pm 1.8	40.1 \pm 3.5	227.2 \pm 56.3	5.7
31	OCH ₃	OCH ₃	4-(CH ₂) ₄ CH ₃	94	80.2 \pm 0.2	12.2 \pm 1.9	> 500	> 41.0
32	OCH ₃	OCH ₃	4-NH ₂	50	42.8 \pm 1.1	>100	ND	-
33	OCH ₃	OCH ₃	4-CH ₂ OH	87	43.4 \pm 3.3	>100	ND	-
34	OCH ₃	OCH ₃	H	92	12.2 \pm 3.3	>100	ND	-
35	OCH ₃	OCH ₃	4-CH ₃	93	7.6 \pm 0.3	>100	ND	-
36	OCH ₃	OCH ₃	2-OCH ₃	95	43.7 \pm 3.8	>100	ND	-
37	OCH ₃	OCH ₃	2-CH ₃ ,4-OCH ₃	82	13.6 \pm 1.2	>100	ND	-
38	OCH ₃	OCH ₃	2,5-CH ₃	97	4.0 \pm 0.7	>100	ND	-
39	OCH ₃	OCH ₃	4-NO ₂	78	37.8 \pm 4.4	>100	ND	-
40	OCH ₃	OCH ₃	4-F	88	32.0 \pm 1.6	>100	ND	-
41	OCH ₃	OCH ₃	4-N(CH ₃) ₂	65	33.9 \pm 3.5	>100	ND	-
42	OCH ₃	OCH ₃	3-C ₂ H ₂ C(OCH ₃)CH-4	92	26.2 \pm 0.8	>100	ND	-
43	OCH ₃	H	OCH ₃	89	43.2 \pm 3.6	>100	ND	-
44	OCH ₂ O		OCH ₃	85	9.9 \pm 0.0	>100	ND	-
45	OCH ₃	H	OCF ₃	94	26.0 \pm 2.8	>100	ND	-
46	OCH ₂ O		OCF ₃	99	26.8 \pm 1.4	>100	ND	-
47	OCH ₃	H	(CH ₂) ₄ CH ₃	96	13.4 \pm 0.4	>100	ND	-
48	OCH ₂ O		(CH ₂) ₄ CH ₃	91	48.9 \pm 0.9	>100	ND	-
Bnz					93.0 \pm 0.6 ^c	10.2 \pm 0.1	>500	>49.0

^aYield of the CuAAC reaction. ^bResults are expressed as mean \pm SD of an experiment performed in triplicate. ^cBnz: percentage of growth inhibition of *T. cruzi* amastigotes at 20 μ M. SI: selectivity index = CC₅₀ THP-1/GI₅₀

Compounds **29**, **30**, and **31** showed similar percentages of parasite growth inhibition to those of compounds **25** and **26**. However, the comparison between their GI₅₀ values showed that derivatives **29** and **31** were the most active in the series and

presented good selectivity indexes (**29**: GI_{50} 22.7 μ M, SI >22.0; **31**: GI_{50} 12.2 μ M, SI >41.0). The experimental results showed that the activity of compound **31** was similar to those of the commercially available drug benznidazole (GI_{50} 10.2 μ M, SI >49.1). The presence of the 4-pentyl substituent in the derivative **31** may have been determinant for its increased activity; as this group is hydrophobic and highly flexible, it can adopt a conformation that favors the interaction with the hydrophobic region of the molecular target.

To investigate one of the possible mechanisms of action of our bis-heterocyclic compounds, derivatives that showed $GI_{50} < 100 \mu$ M (**10**, **12**, **25**, **26**, **28**, **29**, **30**, and **31**) were evaluated for their ability to inhibit *T. cruzi* trypanothione reductase. None compound showed significant inhibition at 100 μ M (Table S3, Supplementary Material), suggesting that trypanocidal activity is not related to the inhibition of this enzyme. Complementary studies must be carried out in order to clarify the mechanism of action of this class of compounds.

2.3 STRUCTURE-ACTIVITY RELATIONSHIP STUDY

A qualitative study using three-dimensional descriptors was performed³⁰ to complement the observed SAR data of the synthesized compounds. The objective of this step was to increase the understanding of how the studied compounds could present their activities against the studied strain. Using the fractional factorial design (FFD) approach for variable selection, we obtained a Partial Least Square (PLS) regression model composed of 95 molecular interaction field (MIF) descriptors, which originated two latent variables. The results obtained for the fit of the model ($R^2 = 0.74$; $RMSEC = 0.50$; $F_{2,39} = 55.50$; $critical F = 3.24$) and its internal predictive ability ($Q^2_{LOO} = 0.52$; $RMSECV = 0.68$) indicate that the model explains and predicts information at levels recommended by the literature ($R^2 > 0.6$; $Q^2_{LOO} > 0.5$)³¹. The model is represented graphically in Figure 2, based on compounds **10** (active) and **18** (inactive). Distances between probes that favor activity are presented as red lines, whereas distances between probes that are unfavorable are shown as blue lines. Most of the descriptors that favor activity correspond to distances that match exactly those of rings **A** and **D**, in which the variations of substituent groups were carried out.

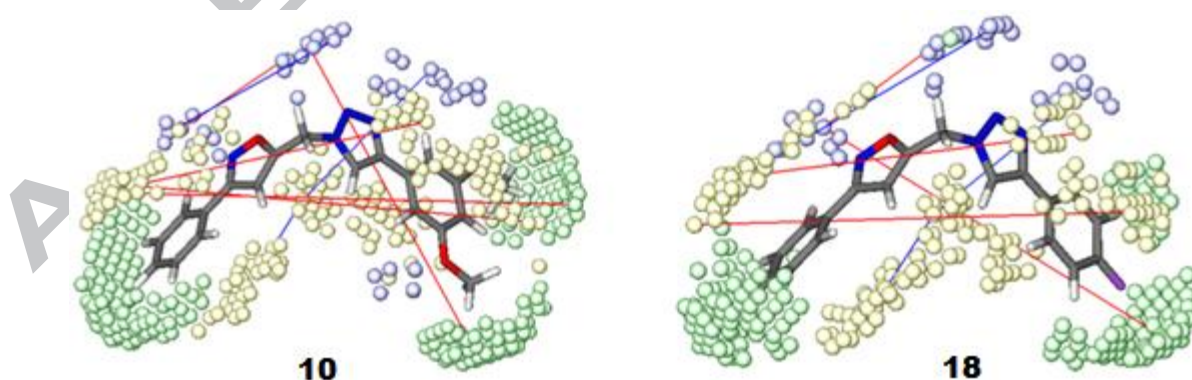


Figure 2. Graphical representation of SAR model obtained using GRIND descriptors. Green spheres: TIP fields; yellow spheres: DRY fields; blue spheres: N1 fields; blue lines: distances between fields (in angstroms) that have a negative impact on activity; red lines: distance between fields that have a positive impact on activity. **10**: compound classified as 1; **18**: compound classified as -1.

The mechanistic interpretation was based on the six most relevant descriptors (Table 4 and Figure S1, Supplementary Material). Spatial characteristics and hydrophobicity are present in four descriptors; the three descriptors that favor inhibitory activity (40_DRY-DRY, 413_DRY-TIP, and 583_N1-TIP) correspond to hydrophobic and steric groups located on rings **A** and **D**. The presence of these DRY and TIP field descriptors in these regions is consistent with that observed for the modifications carried out in compounds **29**, **30** and **31**. These results corroborate the experimental data, showing that the occurrence of activity is highly dependent on hydrophobic and bulky groups located at rings **A** and **D** of the compounds. In 413_DRY-TIP, for example, the distance range of 18.8–19.2 Å is not present in compound **18**. These results are supported by other studies where good antiparasitic activity was related to lipophilicity and the presence of bulky groups^{10,32,33}. Therefore, considering that the model does not contradict the experimental results, and still presents positive correlation with other published studies, it may assist in the development of new derivatives active against the growth of *T. cruzi*.

Table 4. Characteristics of the six most relevant descriptors of the model.

Sign	Descriptor	Field	Distance range (Å)
-	8	DRY-DRY	3.2–3.6
+	40	DRY-DRY	16.0–16.4
-	142	N1-N1	8.0–8.4
-	160	N1-N1	15.2–15.6
+	413	DRY-TIP	18.8–19.2
+	583	N1-TIP	13.6–14.0

3. CONCLUSION

In conclusion, 42 new bis-heterocyclic compounds were synthesized and evaluated for trypanocidal and leishmanicidal activity. The synthetic route established involves four steps of reactions and allows obtaining the analogues quickly and in good yields. On the synthesized series, eight compounds (**10**, **12**, **25**, **26**, **28**, **29**, **30**, and **31**) substantially inhibited the growth of the parasite, showing GI₅₀ values in the of 12.2 to 88.4 μM. Moreover, it was possible to establish the relationship between chemical structure and trypanocidal activity, which was supported by the model generated using GRIND descriptors. Derivative **31** was the most active of the series showing, *in vitro*, low toxicity and a potency in the low micromolar range, similar to that of the reference drug benznidazole. These results suggest that compound **31** can be considered a promising scaffold for the design of new trypanocidal compounds.

4. EXPERIMENTAL SECTION

4.1 Synthesis

Uncorrected melting points were determined by using a MICROQUÍMICA MQAPF-301 apparatus. All ¹H and ¹³C NMR spectra were obtained in Nuclear Brucker Advance DPX 400 MHz and Varian Oxford AS-400 using TMS as internal standard ($\delta = 0.00$ ppm), unless indicated otherwise. Dimethyl sulfoxide-d₆ (DMSO-d₆), Chloroform-d (CDCl₃) and methanol-d₄ (MeOD-d₄) were used as the solvents. In the absence of TMS as standard, chemical shift values (δ) are given in parts per million using residual solvent peaks (¹H NMR: $\delta_{\text{H}} = 7.26$ ppm for CDCl₃, $\delta_{\text{H}} = 2.50$ ppm for DMSO-d₆ and $\delta_{\text{H}} =$

3.31 ppm for MeOD-d4; ^{13}C NMR: $\delta_{\text{C}} = 77.0$ ppm for CDCl_3 , $\delta_{\text{C}} = 39.4$ ppm for DMSO- d_6 and $\delta_{\text{C}} = 49.0$ ppm for MeOD-d4) as internal standard. The residual water peak can be seen in the following chemical shifts: ^1H NMR: $\delta_{\text{H}} = 1.56$ ppm for CDCl_3 , $\delta_{\text{H}} = 3.33$ ppm for DMSO- d_6 and $\delta_{\text{H}} = 4.87$ ppm for MeOD-d4³⁴. When peak multiplicities are reported, the following abbreviations are used: s, singlet; d, doublet; t, triplet; m, multiplet; dd, doublet of doublets. Mass spectra were performed in Agilent's 1100 Series LC linked a Bruker micrOTOF. Reactions under microwave irradiation were conducted in Discovery - CEM Explorer microwave reactor with cooling, pressure and gas addition systems. The solvents were purchased from Tedia® and reagents were purchased from Sigma–Aldrich®, they were treated and purified when necessary according to methodologies in literature³⁵. Thin layer chromatography was performed on silica G60 gel layers SILICYCLE® with fluorescence indicator F-254 and column chromatography was performed using silica gel with particle size: 40-63 and 63-200 μm (Sigma Aldrich) and hexane: ethyl acetate (Tedia) as eluent.

4.1.1. General procedure for preparation of aldoxime **b1** – **b4**.

A mixture of 4-methoxybenzaldehyde (3.7 mmol), hydroxylamine hydrochloride (7.4 mmol) and 1,4-diazabicyclo [2.2.2] octane (DABCO) (3.7 mmol) was irradiated in microwave in a sealed tube during 1 min., at 70 °C and 300 W. To the reaction mixture was added HCl 5% (10.0 mL) and the crude product was extracted with CH_2Cl_2 (2 x 10.0 mL). The organic phase was dried with anhydrous Na_2SO_4 and then the solvent was removed under reduced pressure. The mixture was purified by column chromatography [hexane: ethyl acetate, 70-30% (v/v)] affording (*E*)-4-methoxybenzaldehyde oxime (**b1**) (520.1 mg, 3.4 mmol, 93% yield) as a white solid yielding the expected product.

4.1.1.1. (*E*)-3,4-dimethoxybenzaldehyde oxime (**b2**).

Compound **b2** was prepared as described in general procedure 4.1.1. The product **b2** (468.8 mg; 2.6 mmol, 86% yield) was obtained as a white solid. The spectral data for the title compound are in agreement with the reference already reported²².

4.1.1.2. (*E*)-benzaldehyde oxime (**b3**).

Compound **b3** was prepared as described in general procedure 4.1.1. The product **b3** (2.3 mg; 2.3 mmol, 98% yield) was obtained as a white solid²². The spectral data of this compound was compared with the commercially available compound.

4.1.1.3. (*E*)-benzo [1,3] dioxole-5-carbaldehyde oxime (**b4**).

Compound **b4** was prepared as described in general procedure 4.1.1. The product **b4** (338.5 mg, 2.0 mmol, 60% yield) was obtained as a white solid. The spectral data for the title compound are in agreement with the reference already reported³⁶.

4.1.2. Synthesis of isoxazole (3-(4-methoxyphenyl)isoxazol-5-yl)methanol (**d1**).

To a solution of (*E*)-4-methoxybenzaldehyde oxime (**b1**) (790.0 mg; 5.3 mmol) in DMF (15.8 mL), was slowly added a small quantity of N-chlorosuccinimide (NCS). The reaction temperature increased (if this did not happen, add 50.0 μL de HCl 1N and the temperature should increase). After, the other amount of NCS (774.2 mg, 5.8 mmol) was added. The reaction was stirred for one hour at room temperature and controlled by TLC. The reaction was quenched by addition of ethyl ether (20.0 mL) and washed with NaCl (2 x 20.0 mL). The organic phase was dried with anhydrous Na_2SO_4 and then the solvent was rotaevaporated. The carboxyimidoyl chloride obtained was diluted in

t-BuOH:H₂O (1:1) (3.8 mL) and then propargylic alcohol (340.0 μ L, 5.8 mmol), CuSO₄ (7.5 mg; 0.05 mmol, diluted in 50.0 μ L of water), sodium ascorbate (104.40 mg; 0.5 mmol) and NaHCO₃ (1.3 g; 15.8 mmol) were added. The reaction was stirred for 4 hours, then diluted in ethyl acetate (20.0 mL) and washed with H₂O (2 x 20.0 mL). The organic phase was dried with anhydrous Na₂SO₄ and then the solvent was removed under reduced pressure. The purified compound (**d1**) was obtained after column chromatography [hexane: ethyl acetate, 8:2 (v/v)]. Light yellow solid (890.0 mg; 4.3 mmol, 82% yield). **Mp.**: 90-92 °C. Rf.:0.40 [hexane: ethyl acetate, 60:40 % (v/v)]. **IR (KBr)**: 3352, 2837, 1610, 1527, 1431, 1259, 1082, 840, 802 cm⁻¹. **¹H NMR (400 MHz, CDCl₃)** δ 7.74 (d, *J*= 8.5 Hz, 2H), 6.98 (d, *J*= 8.5 Hz, 2H), 6.52 (s, 1H), 4.81 (s, 2H), 3.86 (s, 3H). **¹³C NMR (100 MHz, CDCl₃)** δ 171.5, 162.1, 161.0, 128.2, 121.4, 114.3, 99.8, 56.7, 55.4⁹.

4.1.3. General procedure for preparation of isoxazoles **d2-d4**.

Under microwave irradiation, to a solution of oxime (1.03 mmol) in DMF (0.3 mL), was added NCS (1.1 mmol) and the mixture was irradiated in a sealed tube during 1 min., at 35 °C and 150 W. After that, propargylic alcohol (1.1 mmol), CuSO₄ (0.01 mmol) dilute in 50.0 μ L of water, sodium ascorbate (0.10 mmol) and NaHCO₃ (4.10 mmol) were added to the tube. The reaction was irradiated again during 10 min., in the same conditions above. When reaction time was over, the mixture was diluted in EtOAc (20.0 mL) and washed with NaCl (2 x 20.0 mL). The organic phase was dried with anhydrous Na₂SO₄ and the solvent was removed under reduced pressure yielding the expected product.

4.1.3.1. (3-(3,4-dimethoxyphenyl)isoxazol-5-yl)methanol (**d2**).

Compound **d2** was prepared as described in general procedure 4.1.3. The product **d2** (259.66 mg, 1.1 mmol, 55% yield) was obtained as a white solid. The spectral data for the title compound are in agreement with the reference already reported⁹.

4.1.3.2. (3-phenylisoxazol-5-yl)methanol (**d3**).

Compound **d3** was prepared as described in general procedure 4.1.3. The product **d3** (27.36 mg, 0.2 mmol, 76% yield) was obtained as a light yellow solid. The spectral data for the title compound are in agreement with the reference already reported⁹.

4.1.3.3. (3-(benzo[d][1,3]dioxol-5-yl)isoxazol-5-yl)methanol (**d4**).

Compound **d3** was prepared as described in general procedure 4.1.3. The product **d3** (144.6 mg, 0.7 mmol, 54% yield) was obtained as a light yellow solid. The spectral data for the title compound are in agreement with the reference already reported⁹.

4.1.4. General procedure for preparation of tosylates **e1-e4**.

To a solution of the isoxazol (**d**) (0.1 mmol) in CH₂Cl₂:H₂O (1:1) at molar concentration 10⁴ mol/L, were added: triethylamine (TEA) (0.01 mmol), K₂CO₃ (0.2 mmol) and, finally, 4-toluenesulfonyl chloride (0.2 mmol) divided in 6 equal parts added every 10 min. The pH was monitored and adjusted by addition of NaOH to 10-11. The reaction was stirred for 8 hours at room temperature. At the end of the reaction, 50.0 μ L of TEA was added and the reaction further stirred for 10 min. Then, the solution was quenched with CH₂Cl₂ (20.0 mL) and washed with saturated solution of NaCl (2 x 20.0 mL). The organic phase was dried with anhydrous Na₂SO₄ and the solvent was removed under reduced pressure. The mixture was purified by chromatography [Hexane:EtOAc 80:20 % (v/v) yielding the expected product.

4.1.4.1. (3-(4-methoxyphenyl)isoxazol-5-yl)methyl 4-methylbenzenesulfonate (**e1**).

Compound **e1** was prepared as described in general procedure 4.1.4. The product **e1** (27.3 mg, 0.1 mmol, 76 % yield) was obtained as a white solid. The spectral data for the title compound are in agreement with the reference already reported⁹.

4.1.4.2. (3-(3,4-dimethoxyphenyl)isoxazol-5-yl)methyl 4-methylbenzenesulfonate (**e2**).

White solid (26.3mg, 0.1 mmol, 63% yield). **Mp.:** 112- 113 °C. **Rf.:** 0.24 [Hexane:EtOAc, 60:40 % (v/v)]. **IR (KBr):** 2837, 1583, 1525, 1469, 1355, 1174, 1018, 964, 813, 779, 734 cm⁻¹. **¹H NMR (400 MHz, CDCl₃)** δ 7.82 (d, *J*= 8.4 Hz, 2H), 7.35 (d, *J*= 2.0 Hz, 1H), 7.35 (d, *J*= 8.4 Hz, 2H), 7.22 (dd, *J*= 8.3, 2.0 Hz, 1H), 6.92 (d, *J*= 8.3 Hz, 1H), 6.54 (s, 1H), 5.17 (s, 2H), 3.94 (s, 3H), 3.93 (s, 3H), 2.42 (s, 3H).

4.1.4.3. (3-phenylisoxazol-5-yl)methyl 4-methylbenzenesulfonate (**e3**).

White solid (40.7mg, 1.2 mmol, 49% yield). **Mp.:** 93-94 °C. **Rf.:** 0.50 [Hexane:EtOAc, 60:40 % (v/v)]. **IR (KBr):** 3115, 1957, 1469, 1436, 1357, 1172, 1095, 939, 817, 767, 694cm⁻¹. **¹H NMR (300 MHz, CDCl₃)** δ: 7.81 (d, *J*= 8 Hz, 2H), 7.76 – 7.68 (m, 2H), 7.49 – 7.42 (m, 3H), 7.34 (d, *J*= 8 Hz, 2H), 6.55 (s, 1H), 5.19 (s, 2H), 2.40 (s, 3H). **HSQC (¹H: 300 MHz, ¹³C: 75 MHz, CDCl₃)** δ_C 130.0, 129.1, 128.1, 126.8, 103.1, 61.1, 21.6.

4.1.4.4. (3-(benzo[d][1,3]dioxol-5-yl)isoxazol-5-yl)methyl 4-methylbenzenesulfonate (**e4**).

Light yellow solid (51.7mg, 0.1 mg, 57% yield). **Mp.:** 84-85 °C. **Rf.:** 0.6 [Hexane:EtOAc, 60:40 % (v/v)]. **IR (KBr):** 3126, 2781, 1597, 1516, 1465, 1423, 1359, 1244, 1180, 1095, 1035, 954, 929, 873, 812, 744cm⁻¹. **¹H NMR (400 MHz, CDCl₃)** δ 7.81 (d, *J*= 8.3 Hz, 2H), 7.35 (d, *J*= 8.3 Hz, 2H), 7.25 (d, *J*= 2.0 Hz, 1H), 7.19 (dd, *J*=8.4, 2.0 Hz, 1H), 6.87 (d, *J*= 8.4 Hz, 1H), 6.46 (s, 1H), 6.03 (s, 2H), 5.30 (s, 1H), 5.17 (s, 2H), 2.43 (s, 3H).

4.1.5. General procedure for preparation of azides **f1-f4**.

To a solution of the tosylate (**e**) (0.1 mmol) in 0.2 mL of DMF sodium azide (NaN₃) (0.6 mmol) was added. The reaction was irradiated in microwave in a sealed tube during 10 min., at 70 °C and 150 W. At the end, the reaction was quenched with EtOAc (20.0 mL) and washed with saturated solution of NaCl (2 x 20.0 mL). The organic phase was dried with anhydrous Na₂SO₄ and was removed under reduced pressure. The mixture was purified by chromatography [hexane: ethyl acetate, 90:10 % (v/v)] yielding the expected product.

4.1.5.1. 5-(azidomethyl)-3-(4-methoxyphenyl)isoxazole (**f1**).

Compound **f1** was prepared as described in general procedure 4.1.5. The product **f1** (11.4 mg, 0.05 mmol, 89% yield) was obtained as a white solid. The spectral data for the title compound are in agreement with the reference already reported⁹.

4.1.5.2. 5-(azidomethyl)-3-(3,4-dimethoxyphenyl)isoxazole (**f2**).

White solid (386.0 mg, 1.5 mmol, 80% yield). **Mp.:** 88–89 °C. **Rf.:** 0.8 [Hexane:EtOAc, 60:40 % (v/v)]. **IR (KBr):** 2839, 2098, 1612, 1583, 1525, 1471, 1234, 1020, 912, 871, 854, 765 cm⁻¹. **¹H NMR (300 MHz, CDCl₃)** δ 7.42 (d, *J*= 2.0 Hz, 1H), 7.30 (dd, *J*= 8.3, 2.0 Hz, 1H), 6.94 (d, *J*= 8.3 Hz, 1H), 6.57 (s, 1H), 4.50 (s, 2H), 3.96 (s, 3H), 3.94 (s, 3H).

4.1.5.3. 5-(azidomethyl)-3-phenylisoxazole (**f3**).

White solid (209.6 mg, 1.0 mmol, 85% yield). **Mp.:** 51-52 °C. **Rf.:** 0.9 [Hexane:EtOAc, 60:40 % (v/v)]. **IR (KBr):** 3120, 2999, 2106, 1604, 1577, 1469, 1444, 1404, 1290, 1251, 1080, 950, 883, 773, 694 cm⁻¹. **¹H NMR (300 MHz, CDCl₃)** δ 7.88 – 7.76 (m, 2H), 7.53 – 7.40 (m, 3H), 6.60 (s, 1H), 4.50 (s, 2H). **HSQC (¹H: 300 MHz, ¹³C: 75 MHz, CDCl₃)** δ_C 126.9, 129.5, 101.2, 45.5.

4.1.5.4. 5-(azidomethyl)-3-(benzo[d][1,3]dioxol-5-yl)isoxazole (**f4**).

Light yellow solid (230.6 mg, 0.94 mmol, 87% yield). **Mp.:** 55-56 °C. **Rf.:** 0.7 [Hexane:EtOAc, 60:40 % (v/v)]. **IR (KBr):** 3126, 2781, 2137, 2102, 1597, 1516, 1465, 1423, 1359, 1244, 1180, 1095, 1035, 954, 929, 873, 812, 744 cm⁻¹. **¹H NMR (400 MHz, CDCl₃)** δ 7.33 (d, *J* = 1.7 Hz, 1H), 7.27 (q, *J* = 8.1, 1.7 Hz, 1H), 6.89 (d, *J* = 8.1 Hz, 1H), 6.52 (s, 1H), 6.04 (s, 2H), 4.49 (s, 2H). **¹³C NMR (100 MHz, CDCl₃)** δ 166.9, 162.7, 149.4, 148.3, 122.5, 121.3, 108.7, 106.9, 101.5, 101.1, 45.5.

4.1.6. General procedure for synthesis of triazole derivatives (**h**).

To a solution of the azide intermediate (0.1 mmol) in 0.2 mL of DMF in a microwave tube, CuSO₄ (0.05 mmol) diluted in 50.0 μL of water, sodium ascorbate (0.025 mmol) and the alkyne (0.2 mmol) were added. The tube was sealed and the solution was irradiated (70 °C, 150 W) for 10 min and, then, TLC analysis showed the complete consumption of the starting material. The reaction was diluted with 15 mL of brine, extracted with ethyl acetate (3 x 10 mL), dried by anhydrous Na₂SO₄ and concentrated under reduced pressure. The resulting crude product was purified by column chromatography on silica gel [hexane: ethyl acetate, 60:40 % (v/v)] yielding the expected product.

4.1.6.1. 3-phenyl-5-((4-phenyl-1H-1,2,3-triazol-1-yl)methyl)isoxazole (**7**).

White solid (28.8 mg, 0.09 mmol, 76% yield). **M.P.:** 175-176 °C. **R.f.:** 0.59 [Hexane:EtOAc, 60:40 % (v/v)]. **IR (KBr):** 3116, 1612, 1579, 1462, 1442, 1406, 1218, 1082, 761, 690 cm⁻¹. **¹H NMR (400 MHz, CDCl₃)** δ 7.95 (s, 1H, H-triazole), 7.83 (d, *J* = 7.4 Hz, 2H, Ar), 7.77-7.75 (m, 2H, Ar), 7.45-7.41 (m, 6H, Ar), 6.61 (s, 1H, H-isoxazole), 5.77 (s, 2H, CH₂). **¹³C NMR (100 MHz; CDCl₃)** δ 165.6, 163.1, 148.9, 130.6, 130.2, 129.2, 129.1, 128.7, 128.3, 127.0, 126.0, 120.0, 102.7, 45.5. **HRMS (ESI-TOF) m/z: [M + H]⁺ Calcd for C₁₈H₁₅N₄O 303.1246, found 303.1301 [M + H]⁺.**

4.1.6.2. 5-((4-(4-methoxyphenyl)-1H-1,2,3-triazol-1-yl)methyl)-3-phenylisoxazole (**8**).

Light yellow solid (15.9 mg, 0.05 mmol, 38% yield). **M.P.:** 210-211 °C. **R.f.:** 0.55 [Hexane:EtOAc, 60:40 % (v/v)]. **IR (KBr):** 3174, 2968, 2837, 1608, 1577, 1548, 1465, 1253, 1068, 758, 696 cm⁻¹. **¹H NMR (400 MHz, CDCl₃)** δ 8.36 (dd, *J* = 7.7, 1.7 Hz, 1H, Ar), 8.23 (s, 1H, H-triazole), 7.79 – 7.74 (m, 2H, Ar), 7.47 – 7.43 (m, 3H, Ar), 7.34 (dd, *J* = 7.5, 1.7 Hz, 1H, Ar), 7.09 (td, *J* = 7.6, 1.0 Hz, 1H, Ar), 6.99 (d, *J* = 8.4 Hz, 1H, Ar), 6.56 (s, 1H, H-isoxazole), 3.95 (s, 3H, Ar-OCH₃). **¹³C NMR (125 MHz, DMSO- d₆)** δ 167.3, 162.2, 155.4, 142.1, 130.4, 129.1, 128.1, 126.7, 126.6, 124.5, 120.7, 118.7, 111.6, 102.0, 55.5, 44.5. **HRMS (ESI-TOF) m/z: [M + H]⁺ Calcd for C₁₉H₁₇N₄O₂ 333.1352, found 333.1410 [M + H]⁺.**

4.1.6.3. 5-((4-(2-methoxyphenyl)-1H-1,2,3-triazol-1-yl)methyl)-3-phenylisoxazole (**9**).

Light yellow solid (36.0 mg, 0.10 mmol, 88% yield). **M.P.:** 210-211 °C; **R.f.:** 0.36 [Hexane:EtOAc, 60:40 % (v/v)]. **IR (KBr):** 3172, 2968, 2837, 1658, 1583, 1548, 1442, 1253, 1068, 777, 758, 698 cm⁻¹. **¹H NMR (300 MHz, CDCl₃)** δ 8.36 (dd, *J* = 7.7, 1.7 Hz, 1H, Ar), 8.22 (s, 1H, H-triazole), 7.79 – 7.75 (m, 2H, Ar), 7.48 – 7.43 (m, 3H, Ar), 7.34

(ddd, $J=7,7, 8,5, 1.0$ Hz, 1H, Ar), 7.10 (ddd, $J=8.5, 8.0, 1.7$ Hz, 1H, Ar), 6.99 (dd, $J=8.0, 1.0$ Hz, 1H, Ar), 6.57 (s, 1H, H-isoxazole), 5.79 (s, 2H, CH₂), 3.95 (s, 3H, Ar-OCH₃). **HSQC** (¹H: 300 MHz, ¹³C: 75 MHz, CDCl₃) δ_C 127.8, 123.4, 126.8, 130.3, 129.0, 129.1, 121.0, 110.9, 102.1, 45.3, 55.4. **HRMS (ESI-TOF) m/z: [M + H]⁺ Calcd for C₁₉H₁₇N₄O₂ 333.1352, found 333.1371 [M + H]⁺.**

4.1.6.4. 5-((4-(3,5-dimethoxyphenyl)-1H-1,2,3-triazol-1-yl)methyl)-3-phenylisoxazole (10).

White solid (34.3 mg, 0.09 mmol, 76% yield). **M.P:** 119-120 °C. **R.f:** 0.31 [Hexane:EtOAc, 60:40 % (v/v)]. **IR (KBr):** 3128, 2839, 1593, 1556, 1427, 1207, 1157, 1066, 833, 773, 696, 688 cm⁻¹. **¹H NMR (300 MHz, CDCl₃)** δ 7.93 (s, 1H, H-triazole), 7.78-7.75 (m, 2H, Ar), 7.49 – 7.42 (m, 3H, Ar), 7.00 (d, $J= 2.3$ Hz, 2H, Ar), 6.61 (s, 1H, H-isoxazole), 6.46 (t, $J=2.3$ Hz, 1H, Ar), 5.77 (s, 2H, CH₂), 3.84 (s, 6H, Ar-OCH₃). **HSQC** (¹H: 300 MHz, ¹³C: 75 MHz, CDCl₃) δ_C 129.1, 126.9, 120.2, 103.7, 102.3, 101.0, 55.5, 45.4. **HRMS (ESI-TOF) m/z: [M + H]⁺ Calcd for C₂₀H₁₈N₄O₃ 363.1457, found 363.1882 [M + H]⁺.**

4.1.6.5. 3-phenyl-5-((4-(p-tolyl)-1H-1,2,3-triazol-1-yl)methyl)isoxazole (11).

White solid (33.0 mg, 0.10 mmol, 84% yield). **M.P:** 171-172 °C. **R.f:** 0.57 [Hexane:EtOAc, 60:40 % (v/v)]. **IR (KBr):** 3113, 2920, 2852, 1610, 1581, 1498, 1444, 1228, 819, 769, 688 cm⁻¹. **¹H NMR (400 MHz, CDCl₃)** δ 7.90 (s, 1H, H-triazole), 7.77-7.74 (m, 2H, Ar), 7.72 (d, $J= 8.0$ Hz, 2H, Ar), 7.45-7.46 (m, 3H, Ar), 7.23 (d, $J= 8.0$ Hz, 2H, Ar), 6.60 (s, 1H, H-isoxazole), 5.74 (s, 2H, CH₂), 2.37 (s, 3H, AR-CH₃). **¹³C NMR (100 MHz, CDCl₃)** δ 165.7, 163.1, 149.0, 138.5, 130.7, 129.7, 129.2, 128.3, 127.4, 127.0, 125.9, 119.6, 102.4, 45.5, 21.4. **HRMS (ESI-TOF) m/z: [M + H]⁺ Calcd for C₁₉H₁₇N₄O 317.1402, found 317.1462 [M + H]⁺.**

4.1.6.6. 3-phenyl-5-((4-(2,4,5-trimethylphenyl)-1H-1,2,3-triazol-1-yl)methyl)isoxazole (12).

White solid (21.1 mg, 0.06 mmol, 49% yield). **M.P:** 200-201 °C. **R.f:** 0.63 [Hexane:EtOAc, 60:40 % (v/v)], **IR (KBr):** 3163, 2966, 2883, 1614, 1573, 1504, 1442, 1230, 945, 871, 771, 734, 698 cm⁻¹. **¹H NMR (300 MHz, CDCl₃)** δ 7.84 (s, 1H, H-triazole), 7.80 – 7.75 (m, 2H, Ar), 7.53 (s, 1H, Ar), 7.48-7.45 (m, 3H, Ar), 7.30 (s, 1H, Ar), 7.05 (s, 1H, Ar), 6.66 (s, 1H, H-isoxazol), 5.80 (s, 2H, CH₂), 2.39 (s, 3H, AR-CH₃), 2.27 (s, 3H, AR-CH₃). **HSQC** (¹H: 300 MHz, ¹³C: 75 MHz, CDCl₃) δ_C 132.2, 129.9, 129.1, 126.9, 121.9, 102.3, 45.2, 20.6, 19.2, **HRMS (ESI-TOF) m/z: [M + H]⁺ Calcd for C₂₁H₂₁N₄O 345.1715, found 345.1750 [M + H]⁺.**

4.1.6.7. 5-((4-(4-methoxy-2-methylphenyl)-1H-1,2,3-triazol-1-yl)methyl)-3-phenylisoxazole (13).

White solid (31.2 mg, 0.09 mmol, 92% yield). **M.P:** 127-128 °C. **R.f:** 0.46 [Hexane:EtOAc, 60:40 % (v/v)]. **IR (KBr):** 3140, 2960, 1606, 1577, 1492, 1444, 1406, 1236, 1205, 1039, 848, 829, 770, 692 cm⁻¹. **¹H NMR (300 MHz, CDCl₃)** δ 7.79-7.75 (m, 3H, Ar/H-triazol), 7.69 (d, $J= 9.3$ Hz, 1H, Ar), 7.50 – 7.43 (m, 2H, Ar), 6.82 (dd, $J= 9.3, 2.4$ Hz, 1H, Ar), 6.81 (d, $J= 2.4$ Hz, 1H, Ar) 6.62 (s, 1H, H-isoxazol), 5.78 (s, 2H, CH₂), 3.83 (s, 3H, Ar-OCH₃), 2.44 (s, 3H, Ar-CH₃). **HSQC** (¹H: 300 MHz, ¹³C: 75 MHz, CDCl₃) δ_C 130.2, 129.2, 126.9, 121.4, 116.3, 111.5, 102.3, 55.3, 45.2, 21.5. **HRMS (ESI-TOF) m/z: [M + H]⁺ Calcd for C₂₀H₁₉N₄O₂ 347.1508, found 347.1763 [M + H]⁺.**

4.1.6.8. 5-((4-(2,5-dimethylphenyl)-1H-1,2,3-triazol-1-yl)methyl)-3-phenylisoxazole (14).

White solid (29.0 mg, 0.09 mmol, 88% yield). **M.P.**: 136-137 °C. **R.f.**: 0.46 [Hexane:EtOAc, 60:40 % (v/v)]. **IR (KBr)**: 3107, 1614, 1581, 1440, 1404, 1864, 815, 769, 690 cm⁻¹. **¹H NMR (300 MHz, CDCl₃)** δ 7.83 (s, 1H, H-triazole), 7.81 – 7.74 (m 2H, Ar), 7.62 (d, *J* = 1.4 Hz, 1H, Ar), 7.49 – 7.43 (m, 3H, Ar), 7.16 (d, *J* = 7.8 Hz, 1H, Ar), 7.09 (dd, *J* = 7.8, 1.4 Hz, 1H, Ar), 6.62 (s, 1H, H-isoxazol), 5.79 (s, 2H, CH₂), 2.42 (s, 3H, Ar-CH₃), 2.36 (s, 3H, Ar-CH₃). **HSQC (¹H: 300 MHz, ¹³C: 75 MHz, CDCl₃)** δ_C 130.8, 129.5, 129.2, 129.2, 126.9, 122.0, 102.2, 45.3, 20.9, 20.9, **HRMS (ESI-TOF) m/z: [M + H]⁺ Calcd for C₂₀H₁₉N₄O 331.1559, found 3331.1787 [M + H]⁺.**

4.1.6.9. **5-((4-(6-methoxynaphthalen-2-yl)-1H-1,2,3-triazol-1-yl)methyl)-3-phenylisoxazole (15).**

Light yellow solid (38.0 mg, 0.10 mmol, 99% yield). **M.P.**: 197-198 °C. **R.f.**: 0.6 [Hexane:EtOAc, 60:40 % (v/v)]. **IR (KBr)**: 3118, 2962, 1610, 1546, 1508, 1469, 1440, 1224, 1211, 1029, 902, 856, 821, 767, 686 cm⁻¹. **¹H NMR (300 MHz, CDCl₃)** δ 8.28 (s, 1H, Ar), 8.02 (s, 1H, H-triazole), 7.89 (dd, *J* = 8.0, 1.0 Hz, 1H, Ar), 7.83 – 7.76 (m, 4H, Ar), 7.51 – 7.43 (m, 3H, Ar), 7.19 (d, *J* = 2.0 Hz, 1H, Ar), 7.15 (s, 1H, Ar), 6.64 (s, 1H, H-isoxazole), 5.81 (s, 2H, CH₂), 3.94 (s, 3H, Ar-OCH₃). **HSQC (¹H: 300 MHz, ¹³C: 75 MHz, CDCl₃)** δ_C 129.7, 129.1, 127.1, 124.6, 124.3, 119.7, 119.4, 105.8, 102.4, 55.3, 45.4. **HRMS (ESI-TOF) m/z: [M + H]⁺ Calcd for C₂₃H₁₉N₄O₂ 383.1508, found 383.1780 [M + H]⁺.**

4.1.6.10. **5-((4-(4-nitrophenyl)-1H-1,2,3-triazol-1-yl)methyl)-3-phenylisoxazole (16).**

White solid (30.8 mg, 0.09 mmol, 89% yield). **M.P.**: 131-132 °C. **R.f.**: 0.43 [Hexane:EtOAc, 60:40 % (v/v)]. **IR (KBr)**: 3115, 2922, 850, 1612, 1581, 1467, 1408, 1226, 839, 808, 765, 688 cm⁻¹. **¹H NMR (300 MHz, CDCl₃)** δ 8.31 (d, *J* = 9.0 Hz, 2H, Ar), 8.10 (s, 1H, H-triazole), 8.03 (d, *J* = 9.0 Hz, 2H, Ar), 7.81 – 7.76 (m, 2H, Ar), 7.50 – 7.45 (m, 3H, Ar), 6.69 (s, 1H, H-isoxazole), 5.83 (s, 2H, CH₂). **HSQC (¹H: 400 MHz, ¹³C: 100 MHz, CDCl₃)** δ_C 130.6, 129.0, 126.9, 126.4, 124.6, 121.2, 102.8, 45.3. **HRMS (ESI-TOF) m/z: [M + H]⁺ Calcd for C₁₈H₁₄N₅O₃ 348.1097, found 348.1391 [M + H]⁺.**

4.1.6.11. **3-phenyl-5-((4-(4-(trifluoromethoxy)phenyl)-1H-1,2,3-triazol-1-yl)methyl)isoxazole (17).**

White solid (30.0 mg, 0.08 mmol, 77% yield). **M.P.**: 182-183 °C. **R.f.**: 0.37 [Hexane:EtOAc, 60:40 % (v/v)]. **IR (KBr)**: 3113, 3089, 1614, 1581, 1556, 1309, 1209, 850, 810, 767, 694 cm⁻¹. **¹H NMR (300 MHz, CDCl₃)** δ 7.90 (s, 1H, H-triazole), 7.81 (d, *J* = 8.5 Hz, 2H, Ar), 7.74 – 7.69 (m, 2H, Ar), 7.43-7.38 (m, 3H, Ar), 7.23 (d, *J* = 8.5 Hz, 2H, Ar), 6.58 (s, 1H, H-isoxazole), 5.73 (s, 2H, CH₂). **¹³C NMR (75 MHz, CDCl₃)** δ 165.3, 163.2, 149.4 (d, ²J_{CF} = 1.5 Hz), 147.6, 130.7, 129.2, 129.0, 128.3, 127.4, 127.0, 121.6, 120.8 (d, ¹J_{CF} = 257.6 Hz), 120.2, 102.6, 45.5. **HRMS (ESI-TOF) m/z: [M + H]⁺ Calcd for C₁₉H₁₄F₃N₄O₂ 387.1069, found 387.1032 [M + H]⁺.**

4.1.6.12. **5-((4-(4-fluorophenyl)-1H-1,2,3-triazol-1-yl)methyl)-3-phenylisoxazole (18).**

White solid (21.9 mg, 0.07 mmol, 68% yield). **M.P.**: 195-196 °C. **R.f.**: 0.57 [Hexane:EtOAc, 60:40 % (v/v)]. **IR (KBr)**: 3101, 1612, 1560, 1496, 1406, 1228, 1082, 833, 781, 767, 692 cm⁻¹. **¹H NMR (300 MHz, CDCl₃)** δ 7.91 (s, 1H, H-triazole), 7.80 (m, 4H, Ar), 7.53 – 7.43 (m, 3H, Ar), 7.15-7.10 (m, 2H, Ar), 6.63 (s, 1H, H-isoxazole), 5.78 (s, 2H, CH₂). **¹³C NMR (75 MHz, CDCl₃)** δ: 165.3, 163.0, 162.6 (d, ¹J_{CF} = 257.7 Hz), 147.9, 130.5, 129.1, 128.1, 127.6 (d, ³J_{CF} = 8.2 Hz), 126.8, 126.3, 119.6, 115.9 (d, ²J_{CF} = 21.9 Hz), 102.4, 45.4. **HRMS (ESI-TOF) m/z: [M + H]⁺ Calcd for C₁₈H₁₄N₄O 321.1152, found 321.1417 [M + H]⁺.**

4.1.6.13. *N,N*-dimethyl-4-(1-((3-phenylisoxazol-5-yl)methyl)-1*H*-1,2,3-triazol-4-yl)aniline (**19**).

Light yellow solid (29.9 mg, 0.09 mmol, 87% yield). **M.P:** 160-161 °C. **R.f:** 0,54 [Hexane:EtOAc, 60:40 % (v/v)]. **IR (KBr):** 3124, 2987, 2808, 1618, 1606, 1556, 1508, 1454, 1442, 1359, 1224, 948, 821, 773, 698 cm⁻¹. **¹H NMR (300 MHz, CDCl₃)** δ 7.80 (s, 1H, H-triazole), 7.78 – 7.74 (m, 2H, Ar), 7.70 (d, *J* = 8.9 Hz, 2H, Ar), 7.47 – 7.42 (m, 3H, Ar), 6.76 (d, *J* = 8.9 Hz, 2H, Ar), 6.58 (s, 1H, H-isoxazole), 5.73 (s, 2H, CH₂), 2.99 (s, 6H, N-CH₃). **HSQC (¹H: 300 MHz, ¹³C: 75 MHz, CDCl₃)** δ_C 129.1, 126.9, 118.4, 112.5, 102.2, 45.3, 40.5. **HRMS (ESI-TOF) m/z: [M + H]⁺ Calcd for C₂₀H₂₀N₅O** 346.1668, found 346.1960 [M + H]⁺.

4.1.6.14. 4-(1-((3-phenylisoxazol-5-yl)methyl)-1*H*-1,2,3-triazol-4-yl)aniline (**20**).

Light yellow solid (15.0 mg, 0.05 mmol, 47% yield). **M.P:** 220- 221 °C. **R.f:** 0.15 [Hexane:EtOAc, 60:40 % (v/v)], **IR (KBr):** 3460, 3360, 3223, 3122, 1730, 1631, 1614, 1566, 1502, 1442, 1404, 1296, 1045, 833, 771, 688 cm⁻¹. **¹H NMR (300 MHz, CDCl₃)** δ 7.80 (s, 1H, H-triazole), 7.79 – 7.74 (m, 2H, Ar), 7.63 (d, *J* = 8.2 Hz, 2H, Ar), 7.46 (m, 3H, Ar), 6.74 (d, *J* = 8.2 Hz, 2H, Ar), 6.59 (s, 1H, H-isoxazole), 5.75 (s, 2H, CH₂). **¹³C NMR (125 MHz, MeOD)** δ 164.2, 146.5, 131.3, 129.9, 127.7, 121.7, 120.7, 116.1, 103.1, 45.9. **HRMS (ESI-TOF) m/z: [M + H]⁺ Calcd for C₁₈H₁₆N₅O** 318.1355, found 318.1628 [M + H]⁺.

4.1.6.15. (4-(1-((3-phenylisoxazol-5-yl)methyl)-1*H*-1,2,3-triazol-4-yl)phenyl)methanol (**21**).

White solid (17.4 mg, 0.05 mmol, 42% yield). **M.P:** 170-171 °C. **R.f:** 0.13 [Hexane:EtOAc, 60:40 % (v/v)]. **IR (KBr):** 3228, 3115, 3091, 2904, 1612, 1581, 1548, 1444, 1404, 1203, 10493 1004, 763, 688 cm⁻¹. **¹H NMR (400 MHz, MeOD)** δ 8.40 (s, 1H, H-triazole), 7.83 – 7.80 (m, 4H, Ar), 7.49 – 7.46 (m, 3H, Ar), 7.44 (d, *J* = 8.5 Hz, 2H, Ar), 6.89 (s, 1H, H-isoxazole), 5.92 (s, 2H, CH₂), 4.65 (s, 2H, CH₂). **¹³C NMR (100 MHz, MeOD)** δ 165.5, 163.0, 148.4, 141.7, 130.5, 129.0, 128.7, 128.0, 127.4, 126.8, 125.8, 120.4, 102.5, 64.1, 45.3. **HRMS (ESI-TOF) m/z: [M + H]⁺ Calcd for C₁₉H₁₇N₄O₂** 333.1352, found 333.1409 [M + H]⁺.

4.1.6.16. 5-((4-(4-pentylphenyl)-1*H*-1,2,3-triazol-1-yl)methyl)-3-phenylisoxazole (**22**).

White solid (36.0 mg, 0.09 mmol, 97% yield). **M.P:** 201-202 °C. **R.f:** 0.31 [Hexane:EtOAc, 60:40 % (v/v)]. **IR (KBr):** 3118, 1606, 1581, 1514, 1352, 1232, 860, 779, 694 cm⁻¹. **NMR ¹H (300 MHz, CDCl₃)** δ 7.90 (s, 1H, H-triazole), 7.78-7.73 (m, 2H, Ar), 7.74 (d, *J* = 8.1 Hz, 2H, Ar), 7.49 – 7.42 (m, 3H, Ar), 7.24 (d, *J* = 8.1 Hz, 2H, Ar), 6.60 (s, 1H, H-isoxazole), 5.76 (s, 2H, CH₂), 2.68 – 2.57 (m, 2H, CH₂), 1.67 – 1.57 (m, 2H, CH₂), 1.38 – 1.29 (m, 4H, CH₂-CH₂), 0.89 (t, *J* = 6.8 Hz, 3H, CH₂-CH₃). **HSQC (¹H: 400 MHz, ¹³C: 75 MHz, CDCl₃)** δ_C 128.9, 128.9, 126.0, 119.5, 102.2, 45.4, 35.7, 31.5, 31.0, 22.5, 14.0. **HRMS (ESI-TOF) m/z: [M + H]⁺ Calcd for C₂₃H₂₅N₄O** 373.2028, found 373.2338 [M + H]⁺.

4.1.6.17. 3-(4-methoxyphenyl)-5-((4-(2,4,5-trimethylphenyl)-1*H*-1,2,3-triazol-1-yl)methyl)isoxazole (**23**).

White solid (38.0 mg, 0,09, 97% yield). **Mp:** 127-128 °C. **IR (KBr):** 2835, 1610, 1531, 1427, 1255, 1176, 1033, 829 cm⁻¹. **¹H NMR (300 MHz, CDCl₃)** δ 7.80 (s,1H, triazole), 7.71 (d, *J*=8.9 Hz, 2H, Ar), 7.58 (s, 1H, Ar), 7.04 (s, 1H, Ar), 6.96 (d, *J* = 8.9 Hz, 2H, Ar), 6.56 (s,1H, Isoxazole), 5.77 (s, 2H, CH₂), 3.85 (s, 3H, Ar-OCH₃), 2.40 (s, 3H, CH₃),

2.26 (s, 6H, CH₃). ¹³C NMR (100 MHz, CDCl₃) δ 165.5, 162.7, 161.5, 148.2, 137.0, 134.4, 132.8, 132.4, 130.1, 128.4, 126.9, 121.8, 120.9, 114.6, 102.1, 55.5, 45.5, 20.9, 19.5, 19.3. HRMS (ESI-TOF) m/z: [M + H]⁺ Calcd for C₂₂H₂₃N₄O₂ 375.1816, found 375.1999 [M + H]⁺.

4.1.6.18. 5-((4-(3,5-dimethoxyphenyl)-1H-1,2,3-triazol-1-yl)methyl)-3-(4-methoxyphenyl)isoxazole (**24**).

Light yellow solid (32.2mg, 0.08 mmol, 82% yield). Mp:142–143 °C. IR (KBr): 2837, 1620, 1591, 1529, 1429, 1255, 1157, 1043, 860, 831, 730 cm⁻¹. ¹H NMR (300 MHz, CDCl₃) δ 7.92 (s, 1H, H-triazole), 7.71 (d, J = 8.8 Hz, 2H, Ar), 7.00 (d, J = 2.3 Hz, 2H, Ar), 6.96 (d, J = 8.8 Hz, 2H, Ar), 6.56 (s, 1H, H-isoxazole), 6.46 (t, J = 2.3 Hz, 1H, Ar), 5.75 (s, 2H, CH₂), 3.85 (s, 3H, Ar-OCH₃), 3.84 (s, 6H, Ar-OCH₃). ¹³C NMR (100 MHz, CDCl₃) δ 165.2, 162.7, 161.5, 161.4, 148.7, 132.0, 128.4, 120.8, 120.3, 114.6, 103.9, 102.2, 101.2, 55.7, 55.5, 45.5. HRMS (ESI-TOF) m/z: [M + H]⁺ Calcd for C₂₁H₂₁N₄O 393.1563, found 393.1803 [M + H]⁺.

4.1.6.19. 3-(3,4-dimethoxyphenyl)-5-((4-(2,4,5-trimethylphenyl)-1H-1,2,3-triazol-1-yl)methyl)isoxazole (**25**).

White solid (38.0 mg, 0.09 mmol, 97 % yield). M.P: 98–99 °C. R.f: 0,18[Hexane:EtOAc, 60:40 % (v/v)], IR (KBr): 2831, 1618, 1589, 1525, 1475, 1435, 1259, 1234, 1153, 1029, 893, 796, 742 cm⁻¹, ¹H NMR (400 MHz, CDCl₃) δ 7.80 (s, 1H, H-triazole), 7.58 (s, 1H, Ar), 7.37 (d, J = 1.9 Hz, 1H, Ar), 7.26 (dd, J = 8.4, 1.9 Hz, 2H, Ar), 7.04 (s, 1H, Ar), 6.91 (d, J = 8.4 Hz, 1H, Ar), 6.57 (s, 1H, H-isoxazole), 5.77 (s, 2H, CH₂), 3.93 (s, 3H, CH₃), 3.92 (s, 3H, Ar-OCH₃), 2.40 (s, 3H, AR-CH₃), 2.27 (s, 3H, AR-CH₃) 2.26 (s, 3H, AR-CH₃). ¹³C NMR (100 MHz, CDCl₃) δ 165.6, 162.8, 151.1, 149.6, 148.2, 137.0, 134.4, 132.8, 132.5, 130.1, 126.8, 121.8, 121.1, 120.2, 111.3, 109.4, 102.2, 56.2, 56.1, 45.5, 21.0, 19.5, 19.3. HRMS (ESI-TOF) m/z: [M + H]⁺ Calcd for C₂₃H₂₅N₄O₃ 405.1927, found 405.2223 [M + H]⁺.

4.1.6.20. 3-(3,4-dimethoxyphenyl)-5-((4-(3,5-dimethoxyphenyl)-1H-1,2,3-triazol-1-yl)methyl)isoxazole (**26**).

White solid (40.0 mg, 0.09 mmol, 96% yield). M.P: 145–146 °C. R.f: 0.07 [Hexane:EtOAc, 60:40 % (v/v)]. IR (KBr): 2841, 1654, 1591, 1527, 1477, 1419, 1157, 1060, 842, 821 cm⁻¹. ¹H NMR (400 MHz, CDCl₃) δ 7.92 (s, 1H, H-triazole), 7.36 (d, J = 1.9 Hz, 1H, Ar), 7.25 (dd, J = 8.3, 1.9 Hz, 1H, Ar), 7.00 (d, J = 2.3 Hz, 2H, Ar), 6.91 (d, J = 8.3 Hz, 1H, Ar), 6.56 (s, 1H, H-isoxazole), 6.46 (t, J = 2.3 Hz, 1H, Ar), 5.75 (s, 2H, CH₂), 3.93 (s, 3H, Ar-OCH₃), 3.92 (s, 3H, Ar-OCH₃), 3.84 (s, 6H, Ar-OCH₃). ¹³C NMR (100 MHz, CDCl₃) δ 165.3, 162.8, 161.4, 151.2, 149.6, 148.7, 132.0, 121.0, 120.3, 120.2, 111.3, 109.5, 103.9, 102.3, 101.1, 56.2, 56.1, 55.7, 45.6. HRMS (ESI-TOF) m/z: [M + H]⁺ Calcd for C₂₂H₂₃N₄O 423.1668, found 423.2027 [M + H]⁺.

4.1.6.21. 3-(benzo[d][1,3]dioxol-5-yl)-5-((4-(2,4,5-trimethylphenyl)-1H-1,2,3-triazol-1-yl)methyl)isoxazole (**27**).

White solid (28.2 mg, 0.07 mmol, 88% yield). M.P: 170-171 °C. R.f: 0.38 [Hexane:EtOAc, 60:40 % (v/v)]. IR (KBr): 3120, 2862, 1604, 1517, 1463, 1240, 1043, 939, 869, 812 cm⁻¹. ¹H NMR (400 MHz, CDCl₃) δ 7.72 (s, 1H, H-triazole), 7.50 (s, 1H, Ar), 7.21 (d, J = 1.8 Hz, 1H, Ar), 7.15 (dd, J = 8.1, 1.8 Hz, 1H, Ar), 6.97 (s, 1H, Ar), 6.79 (d, J = 8.1 Hz, 1H, Ar), 6.45 (s, 1H, H-isoxazole), 5.94 (s, 2H, O-CH₂-O), 5.68 (s, 2H, CH₂), 2.32 (s, 3H, Ar-CH₃), 2.19 (s, 3H, Ar-CH₃), 2.19 (s, 3H, Ar-CH₃) ¹³C NMR (100

MHz, CDCl₃) δ 165.54, 162.62, 149.61, 148.45, 148.16, 137.04, 134.42, 132.74, 132.42, 130.05, 126.76, 122.23, 121.87, 121.49, 108.82, 107.00, 102.21, 101.70, 77.48, 77.16, 76.84, 45.41, 20.91, 19.54, 19.29. **HRMS (ESI-TOF) m/z: [M + H]⁺ Calcd for C₂₂H₂₁N₄O₃ 389.1614, found 389.1952 [M + H]⁺.**

4.1.6.22. *3-(benzo[d][1,3]dioxol-5-yl)-5-((4-(3,5-dimethoxyphenyl)-1H-1,2,3-triazol-1-yl)methyl)isoxazole (28).*

White solid (20.1 mg, 0.05 mmol, 60% yield). **M.P:** 100–101 °C. **R.f:** 0.3 [Hexane:EtOAc, 60:40 % (v/v)]. **IR (KBr):** 3118, 2839, 1741, 1591, 1517, 1462, 1357, 1240, 1157, 1041, 939, 869, 808, 773, 682 cm⁻¹. **¹H NMR (500 MHz, DMSO-*d*₆)** δ 8.76 (s, 1H, H-triazole), 7.44 – 7.41 (m, 3H, Ar), 7.09 (s, 1H, H-isoxazol), 7.07 (d, *J* = 2.3 Hz, 2H, Ar), 7.05 (d, *J* = 8.5 Hz, 1H, Ar), 6.49 (t, *J* = 2.3 Hz, 1H, Ar), 6.11 (s, 2H, O-CH₂-O), 5.97 (s, 2H, CH₂), 3.81 (s, 6H, Ar-OCH₃). **¹³C NMR (125 MHz, DMSO-*d*₆)** δ 166.6, 161.9, 160.9, 149.0, 148.0, 146.7, 132.2, 122.4, 121.9, 121.2, 108.8, 106.5, 103.2, 102.2, 101.6, 100.1, 55.3, 44.7. **HRMS (ESI-TOF) m/z: [M + H]⁺ Calcd for C₂₁H₁₈N₄O₅ 407.1355, found 407.1348 [M + H]⁺.**

4.1.6.23. *3-(3,4-dimethoxyphenyl)-5-((4-(4-methoxyphenyl)-1H-1,2,3-triazol-1-yl)methyl)isoxazole (29).*

White solid (23.0 mg, 0.06 mmol, 62% yield). **M.P:** 135–136 °C. **R.f:** 0.13 [Hexane:EtOAc, 60:40 % (v/v)]. **IR (KBr):** 2833, 1608, 1579, 1529, 1465, 1247, 1139, 1031, 975, 858, 821, 763 cm⁻¹. **¹H NMR (400 MHz, CDCl₃)** δ 7.85 (s, 1H, H-triazole), 7.77 (d, *J* = 8.8 Hz, 2H, Ar), 7.37 (d, *J* = 1.7 Hz, 1H, Ar), 7.25 (dd, *J* = 8.4, 1.7 Hz, 1H, Ar), 6.97 (d, *J* = 8.8 Hz, 2H, Ar), 6.92 (1H, d, *J* = 8.4 Hz), 6.56 (s, 1H, H-isoxazole), 5.76 (s, 2H, CH₂), 3.94 (s, 3H, Ar-OCH₃), 3.93 (s, 3H, Ar-OCH₃), 3.85 (s, 3H, Ar-OCH₃). **¹³C NMR (100 MHz, CDCl₃)** δ 165.5, 162.8, 160.0, 151.2, 149.6, 148.7, 127.3, 122.9, 121.0, 120.2, 119.2, 114.5, 111.3, 109.5, 102.2, 56.2, 56.1, 55.5, 45.5. **HRMS (ESI-TOF) m/z: [M + H]⁺ Calcd for C₂₁H₂₁N₄O 393.1563, found 393.1975 [M + H]⁺.**

4.1.6.24. *3-(3,4-dimethoxyphenyl)-5-((4-(4-(trifluoromethoxy)phenyl)-1H-1,2,3-triazol-1-yl)methyl)isoxazole (30).*

White solid (38.0 mg, 0.08 mmol, 89% yield). **M.P:** 148–149 °C. **R.f:** 0.15 [Hexane:EtOAc, 60:40 % (v/v)]. **IR (KBr):** 2837, 1606, 1587, 1529, 1473, 1276, 1159, 1026, 854, 806 cm⁻¹. **¹H NMR (400 MHz, CDCl₃)** δ 7.95 (s, 1H, H-triazole), 7.87 (d, *J* = 8.8 Hz, 2H, Ar), 7.37 (d, *J* = 1.9 Hz, 1H, Ar), 7.28 (d, *J* = 8.8 Hz, 2H, Ar), 7.26 (dd, *J* = 8.4, 1.9 Hz, 1H, Ar), 6.92 (d, *J* = 8.4 Hz, 1H, Ar), 6.60 (s, 1H, H-isoxazole), 5.78 (s, 2H, CH₂), 3.94 (s, 3H, Ar-OCH₃), 3.93 (s, 3H, Ar-OCH₃). **¹³C NMR (100 MHz, CDCl₃)** δ 165.1, 162.9, 151.2, 149.6, 149.4, 147.6, 129.0, 127.4, 121.6, 120.9, 120.7 (d, ¹*J*_{CF} = 257.4 Hz), 120.3, 120.2, 111.3, 109.4, 102.4, 56.2, 56.1, 45.5. **HRMS (ESI-TOF) m/z: [M + H]⁺ Calcd for C₂₁H₁₈F₃N₄O₄ 447.1280, found 447.1659 [M + H]⁺.**

4.1.6.25. *3-(3,4-dimethoxyphenyl)-5-((4-(4-pentylphenyl)-1H-1,2,3-triazol-1-yl)methyl)isoxazole (31).*

White solid (39.3 mg, 0.09 mmol, 94% yield). **M.P:** 78–79 °C. **R.f:** 0.12 [Hexane:EtOAc, 60:40 % (v/v)]. **IR (KBr):** 2852, 1747, 1604, 1585, 1529, 1471, 1433, 1230, 1147, 854, 820 cm⁻¹. **¹H NMR (300 MHz, CDCl₃)** δ 7.84 (s, 1H, H-triazole), 7.67 (d, *J* = 8.1 Hz, 2H, Ar), 7.29 (d, *J* = 1.9 Hz, 1H, Ar), 7.18 (dd, *J* = 8.3, 1.9 Hz, 1H, Ar), 7.16 (d, *J* = 8.1 Hz, 1H, Ar), 6.84 (d, *J* = 8.3 Hz, 1H, Ar), 6.48 (s, 1H, H-isoxazole), 5.69 (s, 2H, CH₂), 3.86 (Ar-OCH₃), 3.85 (Ar-OCH₃), 2.60 – 2.51 (m, 2H, CH₂), 1.61 – 1.50 (m, 2H, CH₂), 1.32 – 1.18 (m, 4H, CH₂), 0.82 (t, *J* = 6.8 Hz, 3H, CH₃). **¹³C NMR (100 MHz,**

CDCl_3) δ 165.5, 162.8, 151.1, 149.6, 149.0, 143.7, 129.1, 127.6, 125.9, 121.0, 120.2, 119.7, 111.3, 109.5, 102.2, 56.2, 56.1, 45.6, 35.9, 31.6, 31.2, 22.7, 14.1. **HRMS (ESI-TOF) m/z: [M + H]⁺ Calcd for C₂₅H₂₉N₄O₃ 433.2240, found 433.2650 [M + H]⁺.**

4.1.6.26. *4-(1-((3-(3,4-dimethoxyphenyl)isoxazol-5-yl)methyl)-1H-1,2,3-triazol-4-yl)aniline (32).*

White solid (18.0 mg, 0.05mmol, 50% yield). **M.P:**167–168 °C. **R.f:** 0.12 [Hexane:EtOAc, 60:40 % (v/v)]. **IR (KBr):** 3325, 3062, 1651, 1585, 1438, 1359, 1280, 1178, 960, 837, 819 cm⁻¹. **¹H NMR (300 MHz, CDCl₃)** δ 7.79 (s, 1H, H-triazole), 7.63 (d, *J* = 8.5 Hz, 2H, Ar), 7.36 (d, *J* = 1.8 Hz, 1H, Ar), 7.25 (dd, *J* = 8.4, 1.8 Hz, 2H, Ar), 6.91 (d, *J* = 8.4 Hz, 1H, Ar), 6.73 (d, *J* = 8.5 Hz, 2H, Ar), 6.53 (s, 1H, H-isoxazole), 5.73 (s, 2H, CH₂), 3.93 (s, 3H, Ar-OCH₃), 3.92 (s, 3H, Ar-OCH₃). **¹³C NMR (100 MHz, CDCl₃)** δ 165.5, 162.7, 151.0, 149.4, 149.1, 146.8, 127.1, 120.9, 120.5, 120.1, 118.5, 115.2, 111.2, 109.3, 102.0, 56.1, 56.0, 45.4. **HRMS (ESI-TOF) m/z: [M + H]⁺ Calcd for C₂₀H₂₀N₅O₃ 378.1566, found 378.1904 [M + H]⁺.**

4.1.6.27. *(4-(1-((3-(3,4-dimethoxyphenyl)isoxazol-5-yl)methyl)-1H-1,2,3-triazol-4-yl)phenyl)methanol (33).*

White solid (32.6 mg, 0.08 mmol, 87% yield). **M.P:** 109–110 °C. **R.f:** 0.10 [Hexane:EtOAc, 60:40 % (v/v)]. **IR (KBr):** 3560, 2853, 1614, 1587, 1529, 1458, 1433, 1230, 1155, 1022, 900, 839, 800 cm⁻¹. **¹H NMR (400 MHz, CDCl₃)** δ 7.94 (s, 1H, H-triazole), 7.82 (d, *J* = 8.0 Hz, 2H, Ar), 7.43 (d, *J* = 8.0 Hz, 2H, Ar), 7.36 (d, *J* = 1.8 Hz, 1H, Ar), 7.25 (dd, *J* = 8.3, 1.8 Hz, 1H, Ar), 6.91 (d, *J* = 8.3 Hz, 1H, Ar), 6.58 (s, 1H, H-isoxazole), 5.76 (s, 2H, CH₂), 4.73 (s, 2H, CH₂), 3.93 (s, 3H, Ar-OCH₃), 3.92 (s, 3H, Ar-OCH₃). **¹³C NMR (100 MHz, CDCl₃)** δ 165.3, 162.8, 151.1, 149.5, 148.5, 141.7, 129.0, 127.5, 125.9, 120.8, 120.2, 111.3, 109.4, 102.3, 64.5, 56.1, 56.0, 45.4. **HRMS (ESI-TOF) m/z: [M + H]⁺ Calcd for C₂₁H₂₁N₄O 393.1563, found 393.1993 [M + H]⁺.**

4.1.6.28. *3-(3,4-dimethoxyphenyl)-5-((4-phenyl-1H-1,2,3-triazol-1-yl)methyl)isoxazole (34).*

Light yellow solid (32.0 mg, 0.09 mmol, 92% yield). **M.P:** 158–159 °C. **R.f:** 0.15 [Hexane:EtOAc, 60:40 % (v/v)]. **IR (KBr):** 2839, 1602, 1587, 1529, 1421, 1230, 1138, 1018, 902, 850, 763 cm⁻¹. **¹H NMR (400 MHz, CDCl₃)** δ 7.94 (s, 1H, H-triazole), 7.84 (dd, *J* = 8.0, 1.3 Hz, 2H, Ar), 7.44 (dd, *J* = 7.58, 1.3 Hz, 3H, Ar), 7.37 (d, *J* = 2.0 Hz, 1H, Ar), 7.37 (dd, *J* = 8.3, 2.0 Hz, 2H, Ar), 6.92 (d, *J* = 8.3 Hz, 1H, Ar), 6.57 (s, 1H, H-isoxazole), 5.78 (s, 2H, CH₂), 3.94 (s, 3H, Ar-OCH₃), 3.93 (s, 3H, Ar-OCH₃). **¹³C NMR (100 MHz, CDCl₃)** δ 165.4, 162.83, 151.2, 149.6, 148.9, 130.2, 129.1, 128.7, 126.0, 121.0, 120.2, 120.0, 111.3, 109.5, 102.3, 56.2, 56.1, 45.6. **HRMS (ESI-TOF) m/z: [M + H]⁺ Calcd for C₂₀H₁₉N₄O₃ 363.1457, found 362.1828 [M + H]⁺.**

4.1.6.29. *3-(3,4-dimethoxyphenyl)-5-((4-(*p*-tolyl)-1H-1,2,3-triazol-1-yl)methyl)isoxazole (35).*

Light yellow solid (33.8 mg, 0.09 mmol, 93% yield). **M.P:** 176–177 °C. **R.f:** 0.18 [Hexane:EtOAc, 60:40 % (v/v)]. **IR (KBr):** 2841, 1604, 1585, 1527, 1421, 1265, 1228, 1139, 1018, 906, 854, 815, 765 cm⁻¹. **¹H NMR (400 MHz, CDCl₃)** δ 7.90 (s, 1H, H-triazole), 7.72 (d, *J* = 8.0 Hz, 2H, Ar), 7.36 (d, *J* = 1.65 Hz, 1H, Ar), 7.27 – 7.21 (m, 3H, Ar), 6.90 (d, *J* = 8.3 Hz, 1H, Ar), 6.56 (s, 1H, H-isoxazole), 3.93 (s, 3H, Ar-OCH₃), 3.91 (s, 3H, Ar-OCH₃), 2.37 (s, 3H, Ar-CH₃). **¹³C NMR (100 MHz, CDCl₃)** δ 165.5, 162.8, 151.1, 149.6, 148.9, 138.5, 129.7, 127.4, 125.9, 121.0, 120.2, 119.7, 111.3, 109.4, 102.2, 56.2, 56.1, 45.5, 21.4. **HRMS (ESI-TOF) m/z: [M + H]⁺ Calcd for C₂₁H₂₁N₄O₃ 377.1614, found 377.1981 [M + H]⁺.**

4.1.6.30. 3-(3,4-dimethoxyphenyl)-5-((4-(2-methoxyphenyl)-1H-1,2,3-triazol-1-yl)methyl)isoxazole (**36**).

Light yellow solid (36.0 mg, 0.09 mmol, 95% yield). **M.P.:** 136–137°C. **R.f:** 0.32 [Hexane: EtOAc, 60:40 % (v/v)]. **IR (KBr):** 2827, 1622, 1583, 1527, 1477, 1435, 1257, 1163, 1033, 833, 796, 742 cm⁻¹. **¹H NMR (400 MHz, CDCl₃)** δ 8.26 (dd, *J*=7.8, 1.8 Hz, 1H, Ar), 8.12 (s, 1H, H-triazole), 7.26 (d, *J*= 1.8 Hz, 1H, Ar), 7.22 (dd, *J*= 8.3, 1.6 Hz, 1H, Ar), 7.15 (dd, *J*= 8.4, 1.6 Hz, 1H, Ar), 6.99 (1H, dd, *J*= 8.3, 7.4 Hz), 6.91 (1H, d, *J*= 8.4 Hz), 6.83 (1H, d, *J*= 8.3 Hz), 6.44 (s, 1H, H-isoxazole), 5.69 (s, 2H, CH₂), 3.87 (s, 3H, Ar-OCH₃), 3.86 (s, 3H, Ar-OCH₃), 3.84 (s, 3H, Ar-OCH₃). **¹³C NMR (100 MHz, CDCl₃)** δ 166.0, 162.8, 155.9, 151.1, 149.6, 144.2, 129.4, 127.8, 123.5, 121.2, 121.1, 120.2, 119.1, 111.3, 111.0, 109.5, 101.9, 56.2, 56.1, 55.6, 45.5. **HRMS (ESI-TOF) m/z: [M + H]⁺ Calcd for C₂₁H₂₁N₄O₄ 393.1563, found 393.1855 [M + H]⁺.**

4.1.6.31. 3-(3,4-dimethoxyphenyl)-5-((4-(4-methoxy-2-methylphenyl)-1H-1,2,3-triazol-1-yl)methyl)isoxazole (**37**).

Light yellow solid (32.2 mg, 0.08 mmol, 82% yield). **M.P.:** 124–125 °C. **R.f:** 0.10 [Hexane: EtOAc, 60:40 % (v/v)]. **IR (KBr):** 2839, 1606, 1583, 1527, 1444, 1419, 1267, 1134, 1039, 1022, 850, 825, 796 cm⁻¹. **¹H NMR (400 MHz, CDCl₃)** δ 7.77 (s, 1H, H-triazole), 7.70 (d, *J*= 7.4 Hz, 1H, Ar), 7.38 (d, *J*= 1.9 Hz, 1H, Ar), 7.26 (dd, *J*= 8.3, 1.9 Hz, 1H, Ar), 6.92 (d, *J*= 8.3 Hz, 1H, Ar), 6.84-6.81 (m, 2H, Ar), 6.58 (s, 1H, H-isoxazole), 5.77 (s, 2H, CH₂), 3.94 (s, 3H, Ar-OCH₃), 3.93 (s, 3H, Ar-OCH₃), 3.83 (s, 3H, Ar-OCH₃), 2.45 (s, 3H, Ar-CH₃). **¹³C NMR (100 MHz, CDCl₃)** δ 165.5, 162.8, 159.8, 151.1, 149.6, 148.0, 137.4, 130.4, 122.3, 121.5, 121.0, 120.2, 116.5, 111.7, 111.3, 109.4, 102.2, 56.2, 56.1, 55.4, 45.5, 21.7. **HRMS (ESI-TOF) m/z: [M + H]⁺ Calcd for C₂₂H₂₃N₄O₄ 407.1719, found 407.2078 [M + H]⁺.**

4.1.6.32. 3-(3,4-dimethoxyphenyl)-5-((4-(2,5-dimethylphenyl)-1H-1,2,3-triazol-1-yl)methyl)isoxazole (**38**).

White solid (36.5 mg, 0.09 mmol, 97% yield). **M.P.:** 163-164 °C. **R.f:** 0.17 [Hexane: EtOAc, 60:40 % (v/v)]. **IR (KBr):** 2837, 1610, 1581, 1523, 1431, 1232, 1020, 902, 817, 779 cm⁻¹. **¹H NMR (300 MHz, CDCl₃)** δ 7.83 (s, 1H, H-triazole), 7.63 (d, *J*= 1.2 Hz, 1H, Ar), 7.38 (d, *J*= 2.0 Hz, 1H, Ar), 7.26 (dd, *J*= 8.3, 2.0 Hz, 1H, Ar), 7.17 (d, *J*= 7.8 Hz, 1H, Ar), 7.09 (dd, *J*= 7.8, 1.2 Hz, 1H, Ar), 6.92 (d, *J*= 8.3 Hz, 1H, Ar), 6.58 (s, 1H, H-isoxazole), 5.79 (s, 2H, CH₂), 3.94 (s, 3H, Ar-OCH₃), 3.93 (s, 3H, Ar-OCH₃), 2.43 (s, 3H, Ar-CH₃), 2.36 (s, 3H, Ar-CH₃). **¹³C NMR (100 MHz, CDCl₃)** δ 165.5, 162.8, 151.16, 149.6, 148.2, 135.8, 132.5, 131.0, 129.6, 129.3, 129.3, 122.1, 121.0, 120.2, 111.3, 109.4, 102.2, 56.2, 56.1, 45.5, 21.0, 21.0. **HRMS (ESI-TOF) m/z: [M + H]⁺ Calcd for C₂₂H₂₃N₄O₃ 391.1770, found 391.2101 [M + H]⁺.**

4.1.6.33. 3-(3,4-dimethoxyphenyl)-5-((4-(4-nitrophenyl)-1H-1,2,3-triazol-1-yl)methyl)isoxazole (**39**).

Yellow solid (30.5 mg, 0.07 mmol, 78% yield). **M.P.:** 167–168 °C. **R.f:** 0.07 [Hexane: EtOAc, 60:40 % (v/v)]. **IR (KBr):** 2839, 1604, 1590, 1527, 1514, 1431, 1336, 1267, 1141, 1024, 908, 854, 804, 767 cm⁻¹. **¹H NMR (300 MHz, CDCl₃)** δ 8.24 (d, *J*= 8.9 Hz, 2H, Ar), 8.03 (s, 1H, H-triazole), 7.95 (d, *J*= 8.9 Hz, 2H, Ar), 7.31 (d, *J*= 1.9 Hz, 1H, Ar), 7.20 (dd, *J*= 8.3, 1.9 Hz, 2H, Ar), 6.86 (d, *J*= 8.3 Hz, 1H, Ar), 6.58 (s, 1H, H-isoxazol), 5.74 (s, 2H, CH₂), 3.87 (s, 3H, Ar-OCH₃), 3.86 (s, 3H, Ar-OCH₃). **¹³C NMR (100 MHz, CDCl₃)** δ 164.9, 162.8, 151.0, 149.3, 147.5, 146.3, 136.2, 126.3, 124.3, 122.1, 120.6,

120.2, 111.2, 109.3, 102.5, 55.9, 55.8, 45.3. **HRMS (ESI-TOF) m/z: [M + H]⁺ Calcd for C₂₀H₁₈N₅O₅ 408.1308, found 408.1751 [M + H]⁺,**

4.1.6.34. **3-(3,4-dimethoxyphenyl)-5-((4-(4-fluorophenyl)-1H-1,2,3-triazol-1-yl)methyl)isoxazole (40).**

White solid (32.3 mg, 0.08 mmol, 88% yield). **M.P:** 173–174 °C. **R.f:** 0.12 [Hexane:EtOAc, 60:40 % (v/v)], **IR (KBr):** 2839, 1604, 1587, 1529, 1496, 1421, 1232, 1138, 1028, 898, 831, 767 cm⁻¹. **¹H NMR (300 MHz, CDCl₃)** δ 7.91 (s, 1H, H-triazole), 7.83 – 7.78 (m, 2H, Ar), 7.37 (d, *J* = 1.8 Hz, 1H, Ar), 7.26 (dd, *J* = 8.3, 1.8 Hz, 1H, Ar), 7.15 – 7.09 (m, 2H, Ar), 6.91 (d, *J* = 8.3 Hz, 1H, Ar), 6.59 (s, 1H, H-isoxazole), 5.76 (s, 2H, CH₂), 3.93 (s, 3H, Ar-OCH₃), 3.92 (s, 3H, Ar-OCH₃). **¹³C NMR (125 MHz, CDCl₃)** δ 165.2, 162.9 (d, ¹J_{CF} = 255.2 Hz), 162.8, 151.1, 149.5, 147.9, 127.7 (d, ³J_{CF} = 8.2 Hz), 126.2, 120.8, 120.2, 120.0, 116.0 (d, ²J_{CF} = 22.0 Hz), 111.3, 109.4, 102.4, 56.1, 56.0, 45.4. **HRMS (ESI-TOF) m/z: [M + H]⁺ Calcd for C₂₀H₁₈FN₄O₃ 381.1363, found 381.1761 [M + H]⁺.**

4.1.6.35. **4-(1-((3-(3,4-dimethoxyphenyl)isoxazol-5-yl)methyl)-1H-1,2,3-triazol-4-yl)-N,N-dimethylaniline (41).**

White solid (25.5 mg, 0.062 mmol, 65% yield). **M.P:** 164–165 °C. **R.f:** 0.07 [Hexane:EtOAc, 60:40 % (v/v)], **IR (KBr):** 2806, 1612, 1556, 1525, 1506, 1261, 1024, 854, 813 cm⁻¹. **¹H NMR (300 MHz, CDCl₃)** δ 7.81 (s, 1H, H-triazole), 7.72 (d, *J* = 8.8 Hz, 2H, Ar), 7.36 (d, *J* = 1.6 Hz, 2H, Ar), 7.25 (dd, *J* = 8.3, 1.6 Hz, 2H, Ar), 6.91 (d, *J* = 8.8 Hz, 2H, Ar), 6.84 (d, *J* = 8.3 Hz, 2H, Ar), 6.54 (s, 1H, H-isoxazole), 5.73 (s, 2H, CH₂), 3.93 (s, 3H, Ar-OCH₃), 3.92 (s, 3H, Ar-OCH₃), 3.01 (s, 6H, N-CH₃). **¹³C NMR (100 MHz, CDCl₃)** δ 165.8, 162.8, 151.1, 150.8, 149.6, 149.4, 126.9, 121.1, 120.2, 118.5, 118.4, 112.6, 111.3, 109.5, 102.1, 56.2, 56.1, 45.5, 40.6. **HRMS (ESI-TOF) m/z: [M + H]⁺ Calcd for C₂₂H₂₄N₅O₃ 406.1879, found 406.2239 [M + H]⁺.**

4.1.6.36. **3-(3,4-dimethoxyphenyl)-5-((4-(6-methoxynaphthalen-2-yl)-1H-1,2,3-triazol-1-yl)methyl)isoxazole (42).**

Light yellow solid (39.3 mg, 0.09 mmol, 92% yield). **M.P:** 185–186 °C. **R.f:** 0.30 [EtOAc: Hexane 60:40% (v/v)]. **IR (KBr):** 28843, 1604, 1587, 1527, 1467, 1232, 1147, 1020, 893, 864, 823 cm⁻¹. **¹H NMR (300 MHz, CDCl₃)** δ 8.26 (s, 1H, Ar), 8.00 (s, 1H, H-triazole), 7.88 (dd, *J* = 8.4, 1.6 Hz, 1H, Ar), 7.77 (dd, *J* = 8.7, 3.7 Hz, 2H, Ar), 7.37 (d, *J* = 1.8 Hz, 1H, Ar), 7.25 (dd, *J* = 8.3, 1.8 Hz, 1H, Ar), 7.16 (dd, *J* = 8.7, 2.5 Hz, 1H, Ar), 7.15 – 7.12 (m, 1H, Ar), 6.90 (d, *J* = 8.3 Hz, 1H, Ar), 6.58 (s, 1H, H-isoxazole), 5.77 (s, 2H, CH₂), 3.93 (s, 6H, Ar-OCH₃), 3.91 (s, 3H, Ar-OCH₃). **¹³C NMR (100 MHz, CDCl₃)** δ 165.5, 162.9, 158.3, 151.2, 149.6, 149.1, 134.7, 129.9, 129.1, 127.6, 125.4, 124.7, 124.4, 121.0, 120.3, 119.9, 119.6, 111.3, 109.5, 106.0, 102.3, 100.1, 56.2, 56.1, 55.5, 45.6. **HRMS (ESI-TOF) m/z: [M + H]⁺ Calcd for C₂₅H₂₃N₄O₄ 443.1719, found 443.2177 [M + H]⁺.**

4.1.6.37. **3-(4-methoxyphenyl)-5-((4-(4-methoxyphenyl)-1H-1,2,3-triazol-1-yl)methyl)isoxazole (43).**

White solid (89% yield). **Mp:** 196.0–198.0 °C. **IR (KBr):** 2835, 1614, 1577, 1529, 1435, 1251, 1180, 1029, 827 cm⁻¹. **¹H NMR (400 MHz, CDCl₃):** δ = 7.85 (s, 1H, triazole), 7.76 (d, *J* = 8.8 Hz, 2H, Ar), 7.71 (d, *J* = 8.8 Hz, 2H, Ar), 6.96 (d, *J* = 8.8 Hz, 4H, Ar), 6.55 (s, 1H, isoxazole), 5.75 (s, 2H, CH₂), 3.85 (s, 3H, Ar-OCH₃), 3.85 (s, 3H, Ar-OCH₃). **¹³C NMR (100 MHz, CDCl₃)** δ 165.4, 162.8, 161.5, 160.0, 148.6, 128.4, 127.3, 122.6, 120.6, 119.8, 114.6, 114.6, 102.4, 55.5, 55.4, 45.4. **HRMS (ESI-TOF) m/z: [M + H]⁺ Calcd for C₂₀H₁₉N₄O₃ 363.1457, found 363.1670 [M + H]⁺.**

4.1.6.38. 3-(benzo[d][1,3]dioxol-5-yl)-5-((4-(4-methoxyphenyl)-1H-1,2,3-triazol-1-yl)methyl)isoxazole (**44**).

White solid (19.3 mg, 0.05 mmol, 85% yield). **M.P.**: 181-182 °C. **R.f.**: 0.28 [Hexane:EtOAc, 60:40 % (v/v)], **IR (KBr)**: 3124, 2835, 1604, 1560, 1516, 1454, 1247, 935, 871, 831, 813, 781, 742 cm⁻¹. **¹H NMR (400 MHz, CDCl₃)** δ 7.84 (s, 1H, H-triazole), 7.76 (d, *J* = 8.8 Hz, 2H, Ar), 7.29 (d, *J* = 1.6 Hz, 1H, Ar), 7.22 (dd, *J* = 8.1, 1.6 Hz, 1H, Ar), 6.96 (d, *J* = 8.8 Hz, 2H, Ar), 6.86 (d, *J* = 8.1 Hz, 1H, Ar), 6.52 (s, 1H, H-isoxazole), 6.02 (s, 2H, O-CH₂-O), 5.74 (s, 2H, CH₂), 3.84 (s, 3H, Ar-OCH₃). **¹³C NMR (100 MHz, CDCl₃)** δ 165.5, 162.7, 160.0, 149.7, 148.7, 148.5, 127.3, 122.9, 122.3, 121.5, 119.2, 114.5, 108.8, 107.0, 102.2, 101.7, 55.5, 45.5, **HRMS (ESI-TOF) m/z: [M + H]⁺ Calcd for C₂₀H₁₇N₄O₄ 377.1250, found 377.1409 [M + H]⁺.**

4.1.6.39. 3-(4-methoxyphenyl)-5-((4-(4-(trifluoromethoxy)phenyl)-1H-1,2,3-triazol-1-yl)methyl)isoxazole (**45**).

White solid (42.6 mg, 0.10 mmol, 94% yield). **M.P.**: 191–192 °C. **R.f.**: 0.32 [Hexane:EtOAc, 60:40 % (v/v)]. **IR (KBr)**: 2841, 1612, 1575, 1529, 1435, 1282, 1215, 1161, 1031, 833 cm⁻¹. **¹H NMR (300 MHz, CDCl₃)** δ 7.95 (s, 1H, H-triazole), 7.86 (d, *J* = 8.8 Hz, 2H, Ar), 7.71 (d, *J* = 8.9 Hz, 2H, Ar), 7.29 (d, *J* = 8.8 Hz, 2H, Ar), 6.96 (d, *J* = 8.9 Hz, 2H, Ar), 6.58 (s, 1H, H-isoxazole), 5.77 (s, 2H, CH₂), 3.85 (s, 3H, Ar-OCH₃). **¹³C NMR (125 MHz, CDCl₃)** δ 165.0, 162.7, 161.4, 149.25 (d, ²J_{CF} = 1.5 Hz), 147.3, 128.7, 128.3, 127.3, 121.4, 120.6, 120.5, 120.4 (d, ¹J_{CF} = 256.3 Hz), 114.5, 102.3, 55.3, 45.3. **HRMS (ESI-TOF) m/z: [M + H]⁺ Calcd for C₂₀H₁₆F₃N₄O₃ 417.1175, found 417.1481 [M + H]⁺.**

4.1.6.40. 3-(benzo[d][1,3]dioxol-5-yl)-5-((4-(4-(trifluoromethoxy)phenyl)-1H-1,2,3-triazol-1-yl)methyl)isoxazole (**46**).

White solid (26.0 mg, 0.06 mmol, 98% yield). **M.P.**: 166-167 °C. **R.f.**: 0.43 [Hexane:EtOAc, 60:40 % (v/v)]. **IR (KBr)**: 3115, 1608, 1517, 1350, 1255, 1039, 846, 817, 756 cm⁻¹. **¹H NMR (300 MHz, CDCl₃)** δ 7.95 (s, 1H, H-triazol), 7.87 (d, *J* = 8.5 Hz, 2H, Ar), 7.29 (d, *J* = 1.2 Hz, 1H, Ar), 7.28 (d, *J* = 8.5 Hz, 2H, Ar), 7.23 (dd, *J* = 8.1, 1.2 Hz, 1H, Ar), 6.87 (d, *J* = 8.1 Hz, 1H, Ar), 6.55 (s, 1H, H-isoxazole), 6.03 (s, 2H, O-CH₂-O), 5.77 (s, 2H, CH₂). **¹³C NMR (125 MHz, MeOD)** δ 167.7, 164.1, 163.8, 151.0, 149.9, 130.9, 128.4, 123.2, 122.7, 122.6, 122.0 (d, ¹J_{CF} = 258.8 Hz), 109.8, 107.7, 103.3, 103.1, 46.1. **HRMS (ESI-TOF) m/z: [M + H]⁺ Calcd for C₂₀H₁₄F₃N₄O₄ 431.0967, found 431.1271 [M + H]⁺.**

4.1.6.41. 3-(4-methoxyphenyl)-5-((4-(4-pentylphenyl)-1H-1,2,3-triazol-1-yl)methyl)isoxazole (**47**).

Solid white solid (42,3 mg, 0,11 mmol, 96% yield), **F.M.:** C₂₄H₂₆N₄O₂, **M.M.:** 402,49 g/mol, **M.P.:**150–151 °C, **R.f:** 0,46 [Hexane:EtOAc, 60:40 % (v/v)], **IR (KBr):** 2848, 1614, 1577, 1529, 1440, 1251, 1031, 819, 532 cm⁻¹, **NMR ¹H (300 MHz, CDCl₃)** δ 7.90 (s, 1H, H-triazole), 7.74 (d, *J* = 8.3 Hz, 2H, Ar), 7.70 (d, *J* = 8.9 Hz, 2H, Ar), 7.24 (d, *J* = 8.3 Hz, 2H, Ar), 6.96 (d, *J* = 8.9 Hz, 2H, Ar), 6.54 (s, 1H, H-isoxazole), 5.75 (s, 2H, CH₂), 3.85 (s, 3H, Ar-OCH₃), 2.67 – 2.57 (m, 2H, Ar-CH₂), 1.70 – 1.57 (m, 2H, CH₂), 1.38 – 1.27 (m, 4H, CH₂-CH₂), 0.89 (t, *J* = 6.8 Hz, 3H, CH₂-CH₃). **NMR ¹³C (100 MHz, CDCl₃)** δ 165.4, 162.7, 161.5, 149.0, 143.6, 129.1, 128.4, 127.6, 125.9, 120.8, 119.6, 114.6, 102.2, 55.5, 45.5, 35.9, 31.6, 31.2, 22.7, 14.2, **HRMS (ESI-TOF) m/z: [M + H]⁺ Calcd for C₂₄H₂₇N₄O₂ 403,2134, found 403,2473 [M + H]⁺.**

4.1.6.42. 3-(benzo[d][1,3]dioxol-5-yl)-5-((4-(4-pentylphenyl)-1H-1,2,3-triazol-1-yl)methyl)isoxazole (**48**).

White solid (31.0 mg, 0.07 mmol, 91% yield). **M.P.:** 165-166 °C. **R.f:** 0.54 [Hexane:EtOAc, 60:40 % (v/v)]. **IR (KBr):** 3124, 2854, 1602, 1517, 1488, 1469, 1340, 1242, 1043, 933, 871, 815, 781 cm⁻¹. **¹H NMR (500 MHz, DMSO- d₆)** δ 8.65 (s, 1H, H-triazole), 7.77 (d, *J* = 8.1 Hz, 2H, Ar), 7.41 (d, *J* = 1.7Hz, 1H, Ar), 7.41 (dd, *J* = 8.5, 1.7 Hz, 1H, Ar), 7.27 (d, *J* = 8.1 Hz, 2H, Ar), 7.06 (s, 1H, H-isoxazole), 7.03 (d, *J* = 8.5 Hz, 1H, Ar), 6.10 (s, 2H, O-CH₂-O), 5.95 (s, 2H, CH₂), 2.62 – 2.57 (m, 2H, CH₂), 1.62 – 1.55 (m, 2H, CH₂), 1.34 – 1.23 (m, 4H, CH₂-CH₂), 0.86 (t, *J* = 7.0 Hz, 3H, CH₂-CH₃). **¹³C NMR (125 MHz, DMSO- d₆)** δ 166.7, 161.8, 149.0, 148.0, 146.9, 142.3, 128.8, 127.9, 125.2, 121.9, 121.6, 121.2, 108.8, 106.5, 102.1, 101.6, 44.7, 34.8, 30.8, 30.5, 21.9, 13.9. **HRMS (ESI-TOF) m/z: [M + H]⁺ Calcd for C₂₄H₂₅N₄O₃ 417.1927, found 417.2254 [M + H]⁺.**

4.2. Biological evaluation

4.2.1. Screening against *T. cruzi* amastigote

The *in vitro* tripanocidal activity in amastigote forms of *T. cruzi* was evaluated by a colorimetric beta-galactosidase assay³⁷. The β-galactosidase *T. cruzi*, Tulahuén strain was provided by the Laboratory of Cellular and Molecular Parasitology, Centro de Pesquisas René Rachou, FIOCRUZ, Belo Horizonte. Culture-derived trypomastigotes raised from infected L929 cell line were used to infect differentiated human THP-1 derived macrophage (4.0x10⁶ cells/well) in 96-well microplates in a parasite/cell ratio of 2:1 and incubated overnight at 37°C and 5% CO₂³⁸. The medium containing non-internalized parasites was removed and replaced with 180 μl of fresh complete medium. Infected cell layer were treated by addition of 20.00 μl of each sample (2 μM of DMSO-diluted stock solution in 18 μM of RPMI-1640), in triplicate, with the compounds solubilized in dimethyl sulfoxide (DMSO) diluted at 100 μM, followed by incubation for 72h at 37°C and 5% CO₂. After treatment, cells were carefully washed with PBS and incubated for 4h at 37°C with 250 μl of Chlorophenolred-β-D-galactopyranoside (Sigma-Aldrich Co., St. Louis, MO, USA) (CPRG) at 100 μM and Nonidet P-40 (Amresco Inc, Solon, Ohio, USA) (NP-40) 0,1%. The absorbance was measured at 570 nm and reference at 630 nm in an automated microplate reader. Benznidazole (Sigma Aldrich) was used as positive control. The results are expressed as percentage of parasite growth inhibition.

4.2.2. Screening against *Leishmania amazonensis* amastigote

For the leishmanicidal screening against intracellular *L. amazonensis* amastigotes was used colorimetric methodology. THP-1 (ATCC TIB202) cells (4.0 × 10⁴ per well) were cultivated in 96 well plates in RPMI-1640 medium without phenol red (Sigma-Aldrich, CO. St. Louis, MO, USA) supplemented with 10% FBS (Life Technologies, USA), 12.5 mM HEPES, penicillin (100 U/ml), streptomycin (100 μg/ml), sodium pyruvate (1 mM) (Gibco) and Glutamax (2 mM) (Gibco) and treated with 100 ng/ml of phorbol 12-myristate 13-acetate (PMA, Sigma-Aldrich Co., St. Louis, MO, USA) for 72 h at 34 °C in a 5% CO₂, to allow THP-1 cells differentiation into non-dividing macrophages³⁸. *L. amazonensis* MHOM/BR/77/LTB0016 promastigotes, expressing β-galactosidase, were grown at 26 °C in Schneider's insect medium (Sigma Chemical Co., St. Louis, MO, USA) supplemented with 5% heat inactivated fetal bovine serum FBS and 2% of human urine. Four days old culture promastigotes (40.0 × 10⁶ parasites/ml) were washed with phosphate buffered saline, pH 7.4 (PBS)

an incubated in RPMI-1640 supplemented with 10% human B+ serum heat-inactivated for 1 h at 34 °C to parasite opsonization. THP-1 cells were incubated with a parasite/cell ratio of 10:1 for 3 h at 34 °C and 5% CO₂. After this period, non-adherent parasites were removed by one wash with PBS and infected cells were incubated with 180 µl of full supplemented RPMI-1640 medium for another 24 h to allow the transformation of promastigotes into intracellular amastigotes. The infected cells were treated with 20.00 µl of each compound (2 µM of DMSO-diluted stock solution in 18 µM of RPMI-1640) in triplicate. After treatment, cells were carefully washed with PBS and incubated for 4 h at 37 °C with 250 µl of chlorophenolred-β-D-galactopyranoside (Sigma–Aldrich Co., St. Louis, MO, USA) (CPRG) at 100 µM and Nonidet P-40 (Amresco Inc, Solon, Ohio, USA) (NP-40) 0.1%. Optical density was read at 570/630 nm in an Infinite M200 TECAN, Austria. Amphotericin B (2 µM) (Sigma) was used as positive control and DMSO 1% as negative control.

4.2.3. Human THP-1-derived macrophages

THP-1 cells (human monocytic leukaemia cell line) were grown and cultivated in 96 well plates (4.0 × 10⁶ cells/well), as described above, treated with the compounds (diluted in DMSO) in concentrations ranging from 15.6 µM to 500 µM and incubated for 72 h (37 °C, 5% CO₂). Cell viability was assessed by the MTT assay, which consists in the colorimetric measurement of the metabolization of 3-(4,5-dimethylthiazol-2-yl)-2,5-diphenyltetrazolium bromide (MTT) to formazan by viable cells. DMSO 1% was used as negative control and the optical density was read at 540 nm in an Infinite M200 TECAN microplate reader immediately after the dissolution of formazan crystals with DMSO.

4.2.4. Trypanothione reductase enzyme assay

Trypanothione reductase from *T. cruzi* (TcTR), was expressed in *Escherichia coli* BL21DE3 and purified by affinity chromatography. TryR (1 m-unit), HEPES (40 mM, pH 7.5), NADPH (0.15 mM), DTNB (25 µM) and EDTA (1 mM) were incubated in 96 well plates (final volume= 240 µL) for 5 min (27 °C) before T(S)₂ (1 µM) and the tested compound (diluted in DMSO) were added³⁹. Compounds and controls were pre-incubated at 27 °C for 30 min and 10 µL of DTNB was added to the reaction mixture. Following, absorbance at 412 nm was measured for 30 min to determine the enzymatic activity. Clomipramine was used as positive control and DMSO 1% as negative control.

4.2. Structure-Activity Relationships Study

The structure-activity relationship (SAR) study was carried out using a three-dimensional approach. For this to be possible, three-dimensional structures were built in HyperChem 7 (Hyper Co.), and calculations of MM+ force field, followed by AM1 semi-empirical theory level, were carried out using the same software.

Field descriptors were obtained using the software Pentacle (Molecular Discovery Ltd). This software uses the GRIND approach, that calculate 3D field descriptors in an alignment-independent way. The descriptors were computed using a combination of ALMOND and CLACC algorithms³⁰

Based in the approach used by Ermondi et al., a binary SAR study was carried out. Compounds with inhibition less to 40%, or inactive (24), were set as -1, whereas with inhibition greater or equal to 40% (18) were set as 1⁴⁰. Pentacle generated DRY-DRY (hydrophobic-hydrophobic groups), O-O (hydrogen bond acceptor-hydrogen bond acceptor groups), N1-N1 (hydrogen bond donor-hydrogen bond donor groups), and TIP-TIP (shape-shape groups) descriptors, and the combinations between these (DRY-O, DRY-N1, DRY-TIP, O-N1, O-TIP, and N1-TIP). This initial set was reduced using

the Fractional Factorial Design (FDD) variable selection method³⁰, and the model was built by Partial Least Squares (PLS)^{41,42}. In this step and a step subsequent, descriptors were autoscaled, the most adequate data pre-processing approach for QSAR studies⁴³. Thus, the quality of the model assessed based on its coefficient of determination (R^2), the root mean square error of calibration ($RMSEC$), the F -test, the coefficient of determination of cross-validation (Q^2_{LOO}), and the root mean square error of cross-validation ($RMSECV$)³¹.

SUPPLEMENTARY MATERIAL

Supplementary data associated with this article can be found in These data include experimental details and characterization data for the reported compounds, NMR spectra, mass spectrometry and biological data (PDF)

AUTHOR INFORMATION

CORRESPONDING AUTHOR

E-mail address: l.bernardes@ufsc.br (L.S.C. Bernardes).

FUNDING SOURCES

This work was supported by the Brazilian agencies FAPESC/CNPq, (PRONEX, grant number 2671/2012-9), CAPES, CNPq (Universal, grant number 407626/2016-6), Fundação Araucária, and FAPERGS.

ACKNOWLEDGMENT

We gratefully acknowledge José Carlos Tomaz (FCFRP, USP, Brazil), Vinícius Palaretti (FFLCH, USP, Brazil), Luis Otávio Zamoner (FCFRP, USP, Brazil), Louis Pergaud Sandjo (CIF, UFSC, Brazil), and Ana Luísa Morotti for the spectral analyses.

REFERENCES

1. Bhutta ZA, Sommerfeld J, Lassi ZS, Salam RA, Das JK. Global burden, distribution, and interventions for infectious diseases of poverty. *Infect Dis Poverty*. 2014;3(1):21. doi:10.1186/2049-9957-3-21.
2. WHO. *Investing to Overcome the Global Impact of Neglected Tropical Diseases: Third WHO Report on Neglected Diseases 2015*. Geneva; 2015. doi:ISBN 978 92 4 156486 1.
3. Leal SM. In vitro Antileishmanial, Trypanocidal and Mammalian Cell Activities of Diverse N,N'-Dihetaryl Substituted Diamines and Related Compounds. *Sci Pharm*. 2013;81(1):43-55. doi:10.3797/scipharm.1205-14.
4. No JH. Visceral leishmaniasis: Revisiting current treatments and approaches for future discoveries. *Acta Trop*. 2016;155:113-123. doi:10.1016/j.actatropica.2015.12.016.
5. Scarim CB, Jornada DH, Chelucci RC, de Almeida L, dos Santos JL, Chung MC. Current advances in drug discovery for Chagas disease. *Eur J Med Chem*. 2018;155:824-838. doi:10.1016/j.ejmech.2018.06.040.
6. Newman DJ, Cragg GM. Natural Products as Sources of New Drugs from 1981 to 2014. *J Nat Prod*. 2016;79(3):629-661. doi:10.1021/acs.jnatprod.5b01055.
7. Singh N, Mishra BB, Bajpai S, Singh RK, Tiwari VK. Natural product based leads to fight against leishmaniasis. *Bioorg Med Chem*. 2014;22(1):18-45. doi:10.1016/j.bmc.2013.11.048.
8. Izumi E, Ueda-Nakamura T, Dias Filho BP, Veiga Júnior VF, Nakamura CV. Natural products and Chagas' disease: a review of plant compounds studied for activity against *Trypanosoma cruzi*. *Nat Prod Rep*. 2011;28(4):809. doi:10.1039/c0np00069h.
9. da Rosa R, de Moraes MH, Zimmermann LA, Schenkel EP, Steindel M, Bernardes LSC. Design and synthesis of a new series of 3,5-disubstituted isoxazoles active against *Trypanosoma cruzi* and *Leishmania amazonensis*. *Eur J Med Chem*. 2017;128:25-35. doi:10.1016/j.ejmech.2017.01.029.
10. Hartmann AP, de Carvalho MR, Bernardes LSC, et al. Synthesis and 2D-QSAR studies

- of neolignan-based diaryl-tetrahydrofuran and -furan analogues with remarkable activity against *Trypanosoma cruzi* and assessment of the trypanothione reductase activity. *Eur J Med Chem.* 2017;140:187-199. doi:10.1016/j.ejmech.2017.08.064.
11. Bernardes LSC, Kato MJ, Albuquerque S, Carvalho I. Synthesis and trypanocidal activity of 1,4-bis-(3,4,5-trimethoxy-phenyl)-1,4-butanediol and 1,4-bis-(3,4-dimethoxyphenyl)-1,4-butanediol. *Bioorganic Med Chem.* 2006;14(21):7075-7082. doi:10.1016/j.bmc.2006.07.006.
 12. Dua R, Shrivastava S, Sonwane SK, Srivastava SK. Pharmacological Significance of Synthetic Heterocycles Scaffold: A Review. *Adv Biol Res (Rennes).* 2011;5(3):120-144.
 13. Sysak A, Obmińska-Mrukowicz B. Isoxazole ring as a useful scaffold in a search for new therapeutic agents. *Eur J Med Chem.* 2017;137:292-309. doi:10.1016/j.ejmech.2017.06.002.
 14. Zhu J, Mo J, Lin H zhi, Chen Y, Sun H peng. The recent progress of isoxazole in medicinal chemistry. *Bioorganic Med Chem.* 2018;26(12):3065-3075. doi:10.1016/j.bmc.2018.05.013.
 15. Bonandi E, Christodoulou MS, Fumagalli G, Perdicchia D, Rastelli G, Passarella D. The 1,2,3-triazole ring as a bioisostere in medicinal chemistry. *Drug Discov Today.* 2017;22(10):1572-1581. doi:10.1016/j.drudis.2017.05.014.
 16. Schmidt A, Krauth-Siegel RL. Enzymes of the trypanothione metabolism as targets for antitrypanosomal drug development. *Curr Top Med Chem.* 2002;2(11):1239-1259. doi:10.2174/1568026023393048.
 17. Krauth-Siegel RL, Inhoff O. Parasite-specific trypanothione reductase as a drug target molecule. *Parasitol Res.* 2003;90(SUPPL. 2):S77-S85. doi:10.1007/s00436-002-0771-8.
 18. Krauth-Siegel RL, Bauer H, Schirmer RH. Dithiol Proteins as Guardians of the Intracellular Redox Milieu in Parasites: Old and New Drug Targets in Trypanosomes and Malaria-Causing Plasmodia. *Angew Chemie Int Ed.* 2005;44(5):690-715. doi:10.1002/anie.200300639.
 19. Cavalli A, Bolognesi ML. Neglected Tropical Diseases: Multi-Target-Directed Ligands in the Search for Novel Lead Candidates against *Trypanosoma* and *Leishmania*. *J Med Chem.* 2009;52(23):7339-7359. doi:10.1021/jm9004835.
 20. Lo Presti MS, Bazán PC, Strauss M, Báez AL, Rivarola HW, Paglini-Oliva PA. Trypanothione reductase inhibitors: Overview of the action of thioridazine in different stages of Chagas disease. *Acta Trop.* 2015;145:79-87. doi:10.1016/j.actatropica.2015.02.012.
 21. Field MC, Horn D, Fairlamb AH, et al. Anti-trypanosomatid drug discovery: an ongoing challenge and a continuing need. *Nat Rev Microbiol.* 2017;15(4):217-231. doi:10.1038/nrmicro.2016.193.
 22. Hajipour AR, Rafiee F, Ruoho AE. A rapid and convenient method for the synthesis of aldoximes under microwave irradiation using in situ generated ionic liquids. *J Iran Chem Soc.* 2010;7(1):114-118. doi:10.1007/BF03245867.
 23. Hansen T V., Wu P, Fokin V V. One-pot copper(I)-catalyzed synthesis of 3,5-disubstituted isoxazoles. *J Org Chem.* 2005;70(19):7761-7764. doi:10.1021/jo050163b.
 24. Morita J-I, Nakatsuji H, Misaki T, Tanabe Y. Water-solvent method for tosylation and mesylation of primary alcohols promoted by KOH and catalytic amines. *Green Chem.* 2005;7:711. doi:10.1039/b505345e.
 25. Himo F, Lovell T, Hilgraf R, et al. Copper(I)-catalyzed synthesis of azoles. DFT study predicts unprecedented reactivity and intermediates. *J Am Chem Soc.* 2005;127(1):210-216. doi:10.1021/ja0471525.
 26. Lipinski CA. Drug-like properties and the causes of poor solubility and poor permeability. *J Pharmacol Toxicol Methods.* 2000;44(1):235-249. doi:10.1016/S1056-8719(00)00107-6.
 27. Lipinski CA. Lead- and drug-like compounds: The rule-of-five revolution. *Drug Discov Today Technol.* 2004;1(4):337-341. doi:10.1016/j.ddtec.2004.11.007.
 28. Da Silva Filho AA, Costa ES, Cunha WR, Silva MLA, Nanayakkara NPD, Bastos JK. In vitro antileishmanial and antimalarial activities of tetrahydrofuran lignans isolated from *Nectandra megapotamica* (Lauraceae). *Phyther Res.* 2008;22(10):1307-1310. doi:10.1002/ptr.2486.
 29. Felipe LG, Baldoqui DC, Kato MJ, et al. Trypanocidal tetrahydrofuran lignans from *Peperomia blanda*. *Phytochemistry.* 2008;69(2):445-450. doi:10.1016/j.phytochem.2007.08.012.

30. Pastor M, Cruciani G, McLay I, Pickett S, Clementi S. GRIND-INdependent Descriptors (GRIND): A Novel Class of Alignment-Independent Three-Dimensional Molecular Descriptors. *J Med Chem.* 2000;43(17):3233-3243. doi:10.1021/jm000941m.
31. Roy PP, Roy K. On Some Aspects of Variable Selection for Partial Least Squares Regression Models. *QSAR Comb Sci.* 2008;27(3):302-313. doi:10.1002/qsar.200710043.
32. da Silva Santos J, de Melos JLR, Lima GS, et al. Synthesis, anti-Trypanosoma cruzi activity and quantitative structure relationships of some fluorinated thiosemicarbazones. *J Fluor Chem.* 2017;195:31-36. doi:10.1016/j.jfluchem.2017.01.013.
33. Pauli I, Ferreira LG, de Souza ML, et al. Molecular modeling and structure-activity relationships for a series of benzimidazole derivatives as cruzain inhibitors. *Future Med Chem.* 2017;9(7):641-657. doi:10.4155/fmc-2016-0236.
34. Gottlieb HE, Kotlyar V, Nudelman A. NMR Chemical Shifts of Common Laboratory Solvents as Trace Impurities. *J Org Chem.* 1997;62(21):7512-7515. doi:10.1021/jo971176v.
35. Armarego WLF, Chai CLL. Chemical Methods Used in Purification. In: *Purification of Laboratory Chemicals.* Elsevier. Elsevier; 2009:61-79. doi:10.1016/B978-1-85617-567-8.50010-X.
36. Arshad M, Bhat AR, Pokharel S, et al. Synthesis, characterization and anticancer screening of some novel piperonyl-tetrazole derivatives. *Eur J Med Chem.* 2014;71:229-236. doi:10.1016/j.ejmech.2013.11.008.
37. Buckner FS, Verlinde CLMJ, Flamme ACL a, Voorhis WCV a N. Efficient Technique for Screening Drugs for Activity against. *Microbiology.* 1996;40(11):2592-2597.
38. Schwende H, Fitzke E, Ambs P, Dieter P. Differences in the state of differentiation of THP-1 cells induced by phorbol ester and 1,25-dihydroxyvitamin D3. *J Leukoc Biol.* 1996;59.
39. Hamilton CJ, Saravanamuthu A, Eggleston IM, Fairlamb AH. Ellman's-reagent-mediated regeneration of trypanothione in situ: substrate-economical microplate and time-dependent inhibition assays for trypanothione reductase. *Biochem J.* 2003;369:529-537. doi:10.1042/BJ20021298.
40. Ermondi G, Caron G, Pintos IG, et al. An application of two MIFs-based tools (Volsurf+ and Pentacle) to binary QSAR: The case of a palinurin-related data set of non-ATP competitive Glycogen Synthase Kinase 3 β (GSK-3 β) inhibitors. *Eur J Med Chem.* 2011;46(3):860-869. doi:10.1016/j.ejmech.2010.12.024.
41. Teófilo RF, Martins JPA, Ferreira MMC. Sorting variables by using informative vectors as a strategy for feature selection in multivariate regression. *J Chemom.* 2009;23(1):32-48. doi:10.1002/cem.1192.
42. Eriksson L, Jaworska J, Worth AP, Cronin MTD, McDowell RM, Gramatica P. Methods for Reliability and Uncertainty Assessment and for Applicability Evaluations of Classification- and Regression-Based QSARs. *Environ Health Perspect.* 2003;111(10):1361-1375. doi:10.1289/ehp.5758.
43. Martins JP a, Ferreira MMC. QSAR modeling: um novo pacote computacional open source para gerar e validar modelos QSAR. *Quim Nova.* 2013;36(4):554-560. doi:10.1590/S0100-40422013000400013.

Supporting Information**Synthesis and SAR of new isoxazole-triazole bis-heterocyclic compounds as analogues of natural lignans with antiparasitic activity**

Lara A. Zimmermann[†], Milene H. de Moraes^{*}, Rafael da Rosa[†], Eduardo B. de Melo[#], Fávero R. Paula^{||}, Eloir P. Schenkel[†], Mario Steindel^{*} and Lílian S. C. Bernardes^{†;*}.

[†] Department of Pharmaceutical Sciences, Federal University of Santa Catarina, 88040-900, Florianópolis, 88040-900, SC, Brazil.

^{*} Department of Microbiology, Immunology and Parasitology, Federal University of Santa Catarina, Florianópolis, 88040-900, SC, Brazil.

[#] Department of Pharmacy, Western Paraná State University, Cascavel, 858119-110, PR, Brazil.

^{||} Course of Pharmacy, Federal University of Pampa, Uruguaiana, 97500-970, RS, Brazil.

*Corresponding author: l.bernardes@ufsc.br

ACCEPTED MANUSCRIPT

Table of contents

Figure S1. Best GRIND descriptors associated with compounds 10 and 18	30
Table S1. Molecular properties of (7-48) calculated using StarDrop 5 Program	31
Table S2: Leishmanicidal activity of compounds 7-48 against <i>Leishmania amazonensis</i> intracellular amastigotes	32
Table S3: <i>Trypanosoma cruzi</i> rTR inhibitory activity of compounds 10, 12, 25-26, 28-31.....	33
REPRESENTATIVE SPECTRA.....	34

ACCEPTED MANUSCRIPT

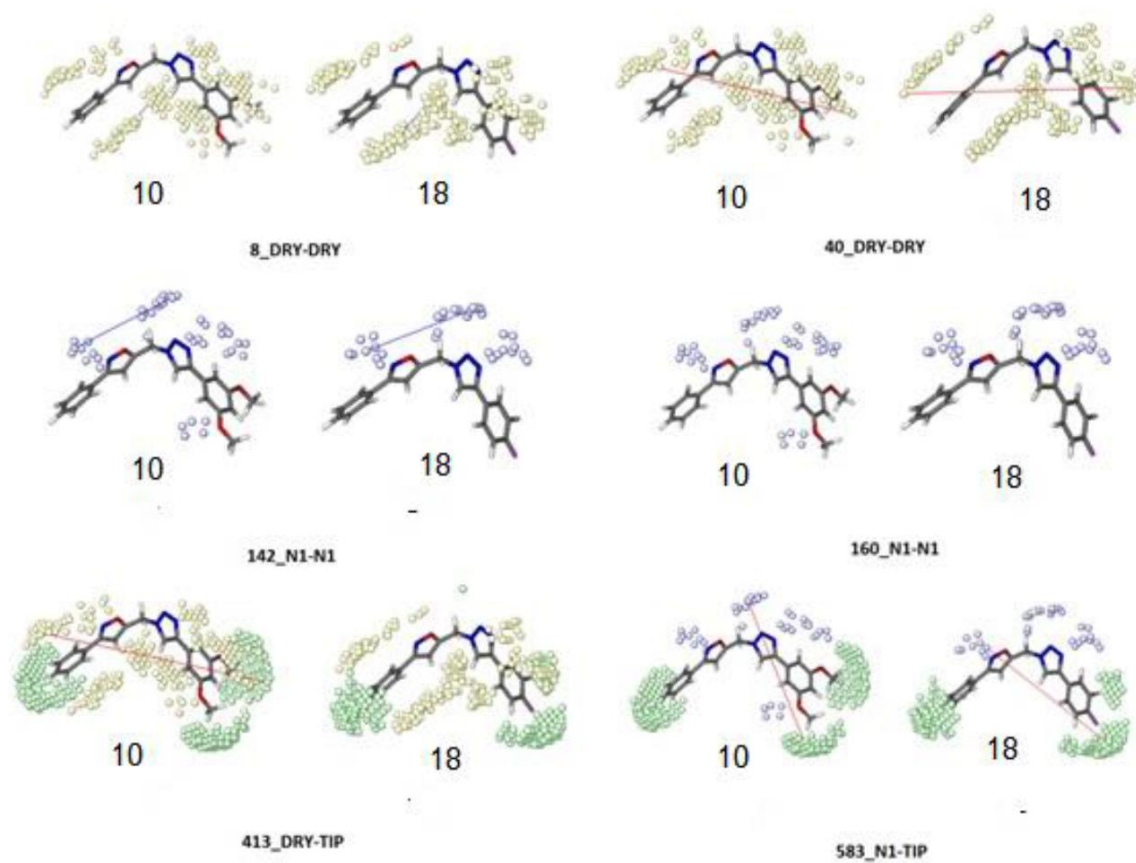


Figure S1. Best GRIND descriptors associated with compounds **10** and **18**.

Table S1. Molecular properties of (7-48) calculated using StarDrop 5 Program.

Compound	MW	LogP	cLogS	PSA	HBD	HBA
7	302.1	4.054 +/- 0.4351	-3.839	56.74 +/- 0	0	5
8	332.1	3.948 +/- 0.4351	-3.857	65.97 +/- 0	0	6
9	332.1	3.914 +/- 0.4351	-3.857	65.97 +/- 0	0	6
10	364.2	3.384 +/- 0.4351	-3.875	75.20 +/- 0	0	7
11	316.1	4.366 +/- 0.4351	-4.183	56.74 +/- 0	0	6
12	344.2	4.977 +/- 0.4351	-4.871	56.74 +/- 0	0	5
13	348.2	3.896 +/- 0.4351	-4.201	65.97 +/- 0	0	6
14	330.1	4.671 +/- 0.4351	-4.527	56.74 +/- 0	0	5
15	382.1	5.036 +/- 0.4351	-5.463	65.97 +/- 0	0	6
16	347.1	3.991 +/- 0.4351	-4.299	102.6 +/- 0	0	8
17	386.1	4.398 +/- 0.4351	-4.862	65.97 +/- 0	0	6
18	320.1	3.905 +/- 0.4351	-4.153	56.74 +/- 0	0	5
19	34.2	3.953 +/- 0.4351	-3.875	59.98 +/- 0	0	6
20	317.1	3.373 +/- 0.4351	-3.915	82.76 +/- 0	1	6
21	332.1	3.122 +/- 0.4351	-3.723	76.97 +/- 0	1	6
22	372.2	5.440 +/- 0.4351	-5.152	56.74 +/- 0	0	5
23	374.2	4.911 +/- 0.4351	-4.889	65.97 +/- 0	0	6
24	392.1	3.647 +/- 0.4351	-3.893	84.43 +/- 0	0	8
25	404.2	4.816 +/- 0.4351	-4.907	75.20 +/- 0	0	7
26	422.2	3.464 +/- 0.4351	-3.911	84.43 +/- 0	0	8
27	388.2	4.389 +/- 0.4351	-5.582	75.20 +/- 0	0	7
28	406.1	3.171 +/- 0.4351	-4.586	93.66 +/- 0	0	9
29	392.1	3.647 +/- 0.4351	-3.893	84.43 +/- 0	0	8
30	446.1	4.131 +/- 0.4351	-4.880	84.43 +/- 0	0	8
31	432.2	5.142 +/- 0.4351	-5.188	75.20 +/- 0	0	7
32	337.1	3.130 +/- 0.4351	-3.951	101.2 +/- 0	1	8
33	392.1	2.943 +/- 0.4351	-3.759	95.43 +/- 0	1	8
34	362.1	3.806 +/- 0.4351	-3.875	75.20 +/- 0	0	7
35	376.2	4.149 +/- 0.4351	-4.219	75.20 +/- 0	0	7
36	392.1	3.631 +/- 0.4351	-3.893	84.43 +/- 0	0	8
37	406.2	4.000 +/- 0.4351	-4.237	84.43 +/- 0	0	8
38	390.2	4.484 +/- 0.4351	-4.563	75.20 +/- 0	0	7
39	407.1	3.665 +/- 0.4351	-4.335	121.0 +/- 0	0	10
40	380.1	3.752 +/- 0.4351	-4.189	75.20 +/- 0	0	7
41	405.2	3.706 +/- 0.4351	-3.911	78.44 +/- 0	0	8
42	442.2	4.630 +/- 0.4351	-5.499	84.43 +/- 0	0	7
43	362.1	3.806 +/- 0.4351	-3.875	75.20 +/- 0	0	7
44	376.1	2.583 +/- 0.4351	-4.568	95.43 +/- 0	1	8
45	416.1	4.283 +/- 0.4351	-4.880	75.20 +/- 0	0	7
46	430.3	3.847 +/- 0.4351	-5.573	84.43 +/- 0	0	8
47	402.2	5.306 +/- 0.4351	-5.170	65.97 +/- 0	0	6
48	416.2	4.854 +/- 0.4351	-5.863	75.20 +/- 0	0	7

MW: molecular weight; LogP: partition coefficient octanol:water; PSA: polar surface area; HBD: hydrogen bond donors; HBA: hydrogen bond acceptors.

Table S2: Leishmanicidal activity of compounds 7-48 against *Leishmania amazonensis* intracellular amastigotes.

Compound	%GI ^{a,b}
44	2.8 ±1.1
48	1.7 ±0,1
Amphotericin B	96.5 ±0.6.

^aResults are expressed as mean ± SD of an experiment performed in triplicate; b %GI: percentage of growth inhibition of *L. amazonensis* amastigotes at 100 µM; Positive control amphotericin B test at 2 µM %GI (*L. amazonensis*). *All bis-heterocyclic compounds were test but did not showed activity at 100 µM.

ACCEPTED MANUSCRIPT

Table S3: *Trypanosoma cruzi* rTR inhibitory activity of compounds 10, 12, 25-26, 28-31.

Compound	<i>T. cruzi</i> rTry % inhibition [100 μM]^a
10	0.0 \pm 0.0
12	0.0 \pm 0.0
25	9.0 \pm 1.0
26	8.9 \pm 2.5
28	0.0 \pm 0.0
29	9.6 \pm 3.8
30	0.0 \pm 0.0
31	0.0 \pm 0.0

^aThe results are averages \pm SD of triplicates. Positive control clomipramine GI₅₀ 14.0 \pm 2.6 μ M.

ACCEPTED MANUSCRIPT

REPRESENTATIVE SPECTRA

Fig. S2. $^1\text{H-NMR}$ spectrum of **compound 7**: 3-phenyl-5-((4-phenyl-1H-1,2,3-triazol-1-yl)methyl)isoxazole (400 MHz, CDCl_3).

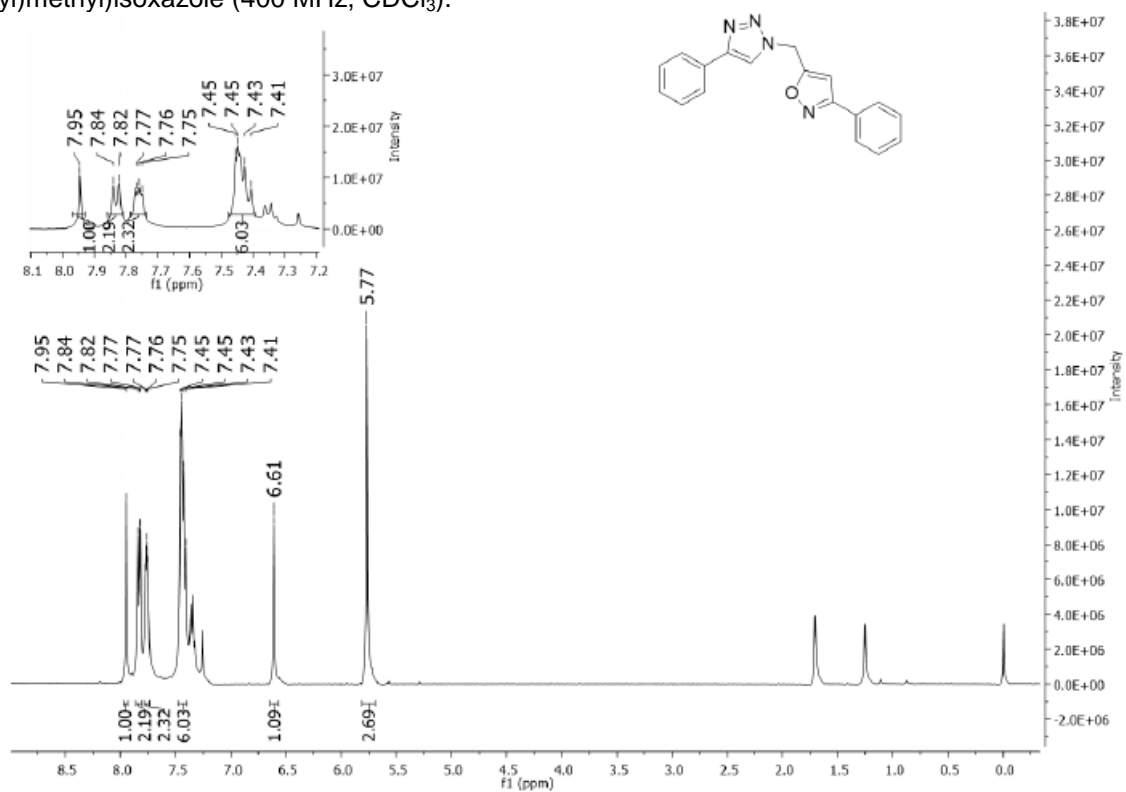


Fig. S3. $^{13}\text{C-NMR}$ spectrum of **compound 7**: 3-phenyl-5-((4-phenyl-1H-1,2,3-triazol-1-yl)methyl)isoxazole (100 MHz, CDCl_3).

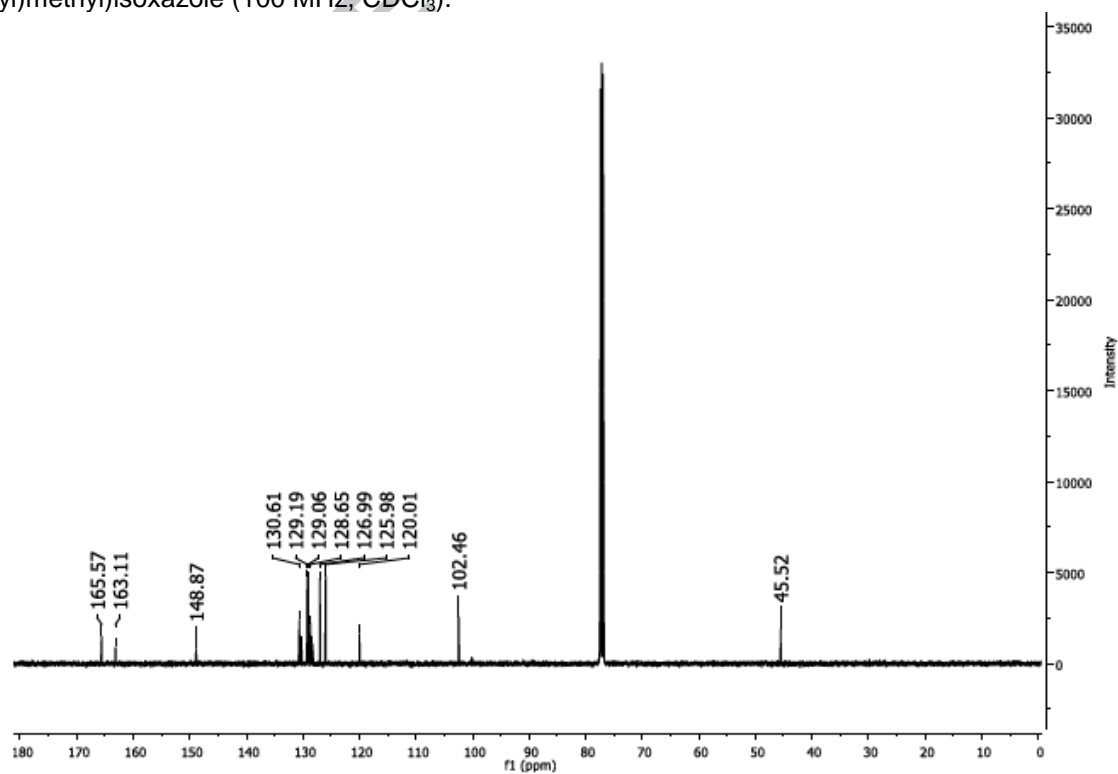


Fig. S4. $^1\text{H-NMR}$ spectrum of **compound 8**: 5-((4-(4-methoxyphenyl)-1H-1,2,3-triazol-1-yl)methyl)-3-phenylisoxazole (400 MHz, CDCl_3).

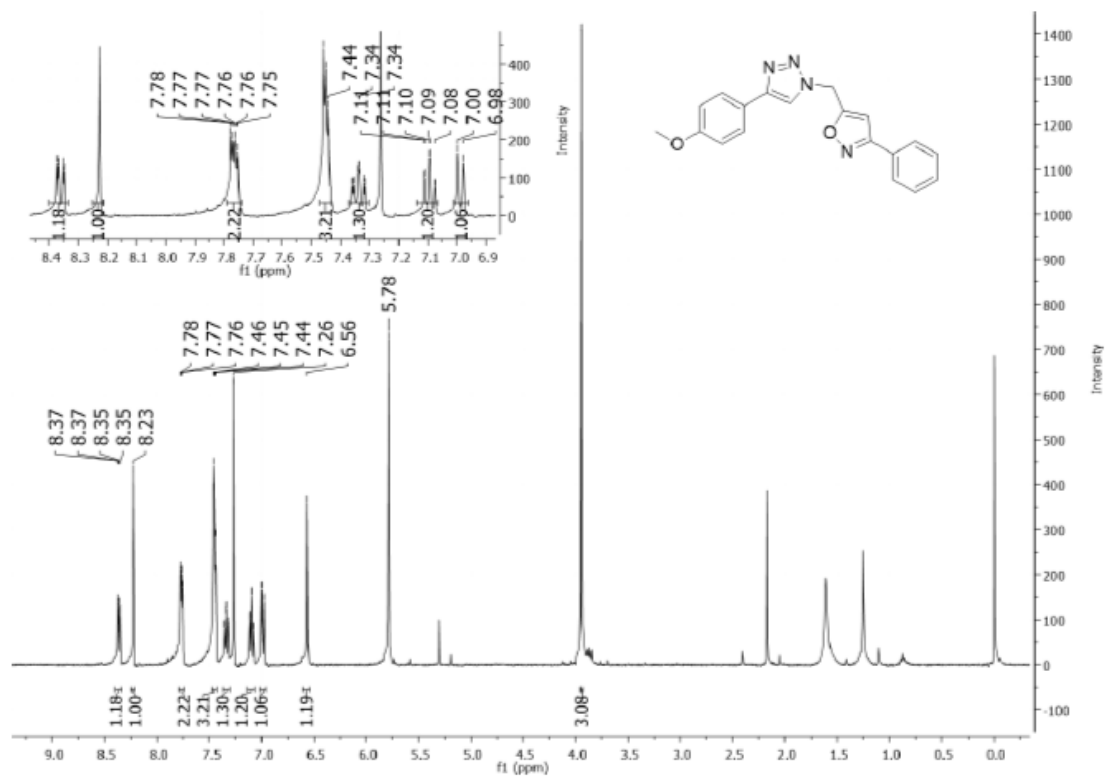


Fig. S5. $^{13}\text{C-NMR}$ spectrum of **compound 8**: 5-((4-(4-methoxyphenyl)-1H-1,2,3-triazol-1-yl)methyl)-3-phenylisoxazole (100 MHz, DMSO-d_6).

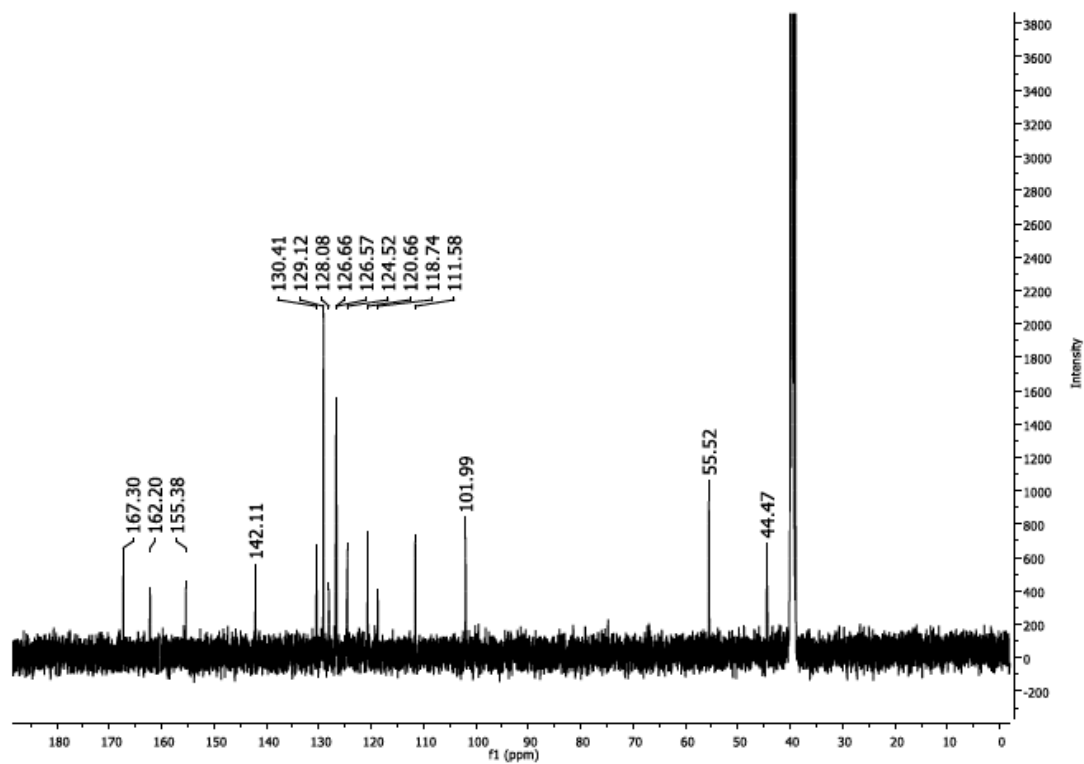


Fig. S6. $^1\text{H-NMR}$ spectrum of **compound 9**: 5-((4-(2-methoxyphenyl)-1H-1,2,3-triazol-1-yl)methyl)-3-phenylisoxazole (300 MHz, CDCl_3).

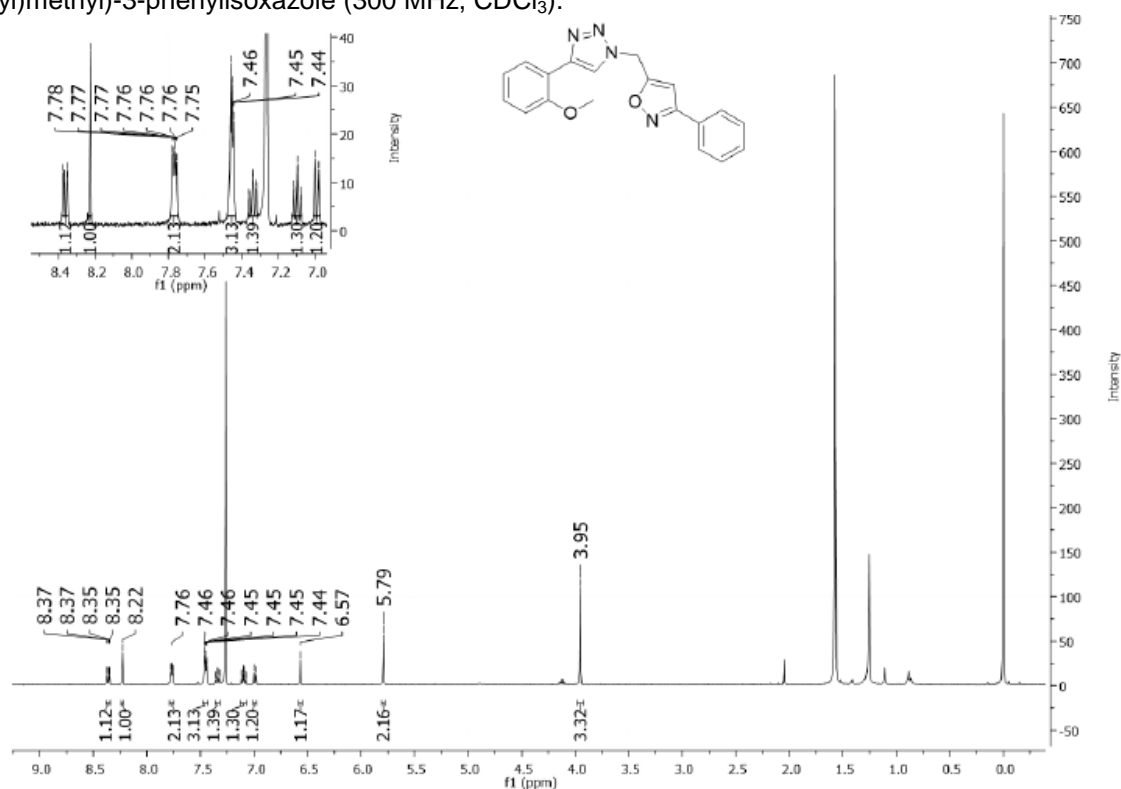


Fig. S7. HSQC spectrum of **compound 9**: 5-((4-(2-methoxyphenyl)-1H-1,2,3-triazol-1-yl)methyl)-3-phenylisoxazole (^1H : 300 MHz, ^{13}C : 75 MHz, CDCl_3).

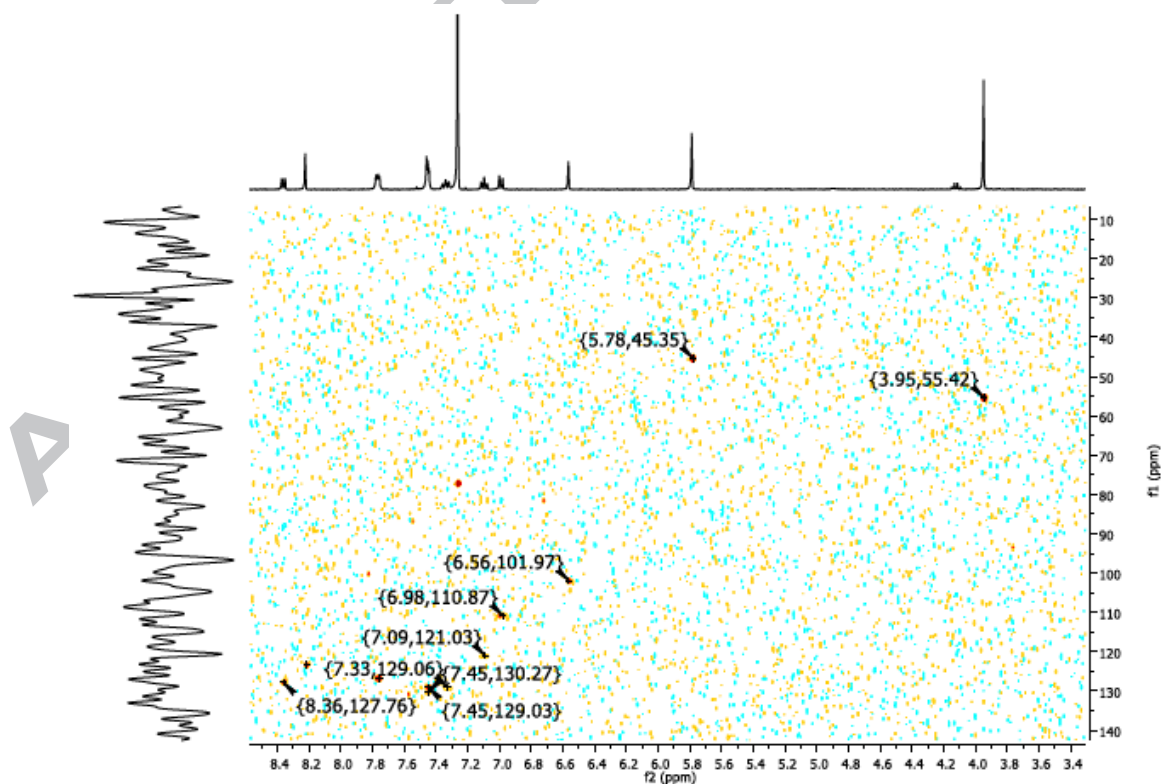


Fig. S8. $^1\text{H-NMR}$ spectrum of **compound 10**: 5-((4-(3,5-dimethoxyphenyl)-1H-1,2,3-triazol-1-yl)methyl)-3-phenylisoxazole (300 MHz, CDCl_3).

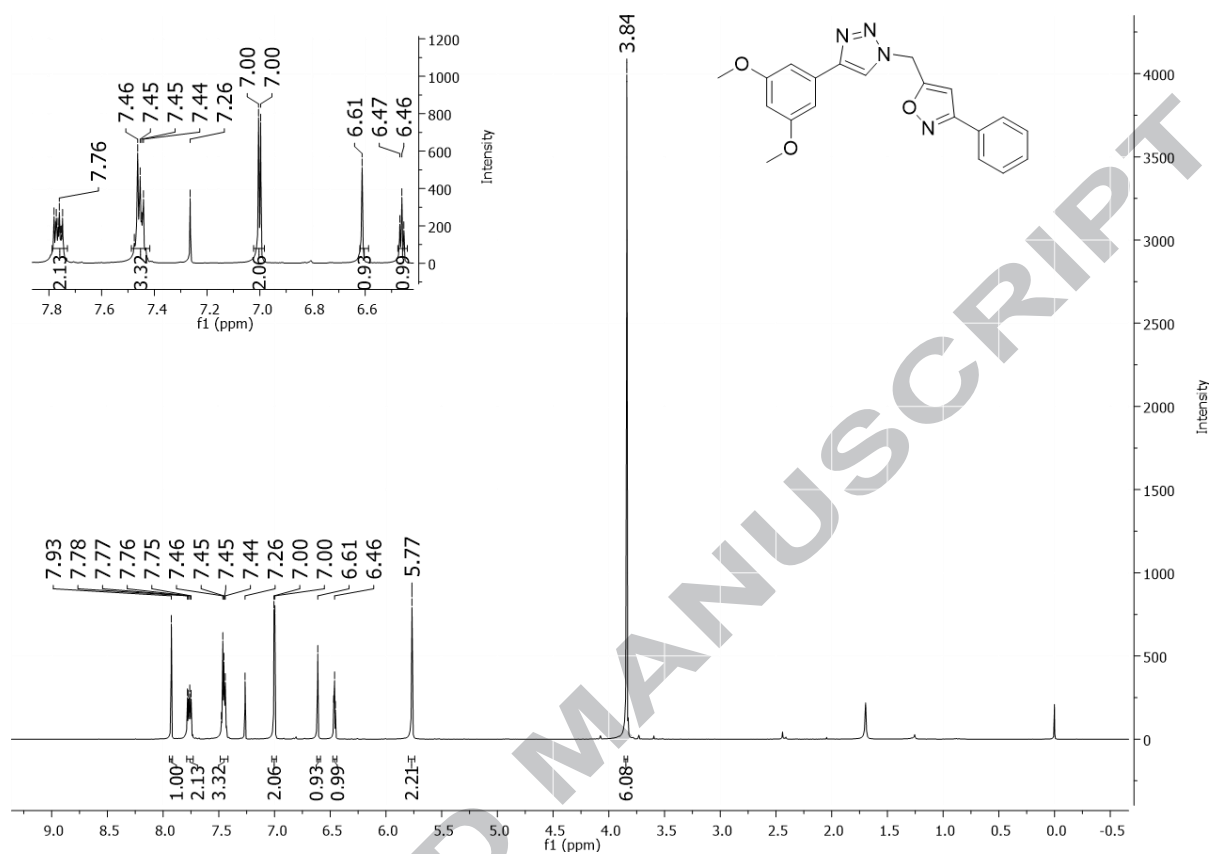


Fig. S9. HSQC spectrum of **compound 10**: 5-((4-(3,5-dimethoxyphenyl)-1H-1,2,3-triazol-1-yl)methyl)-3-phenylisoxazole (^1H : 300 MHz, ^{13}C : 75 MHz, CDCl_3).

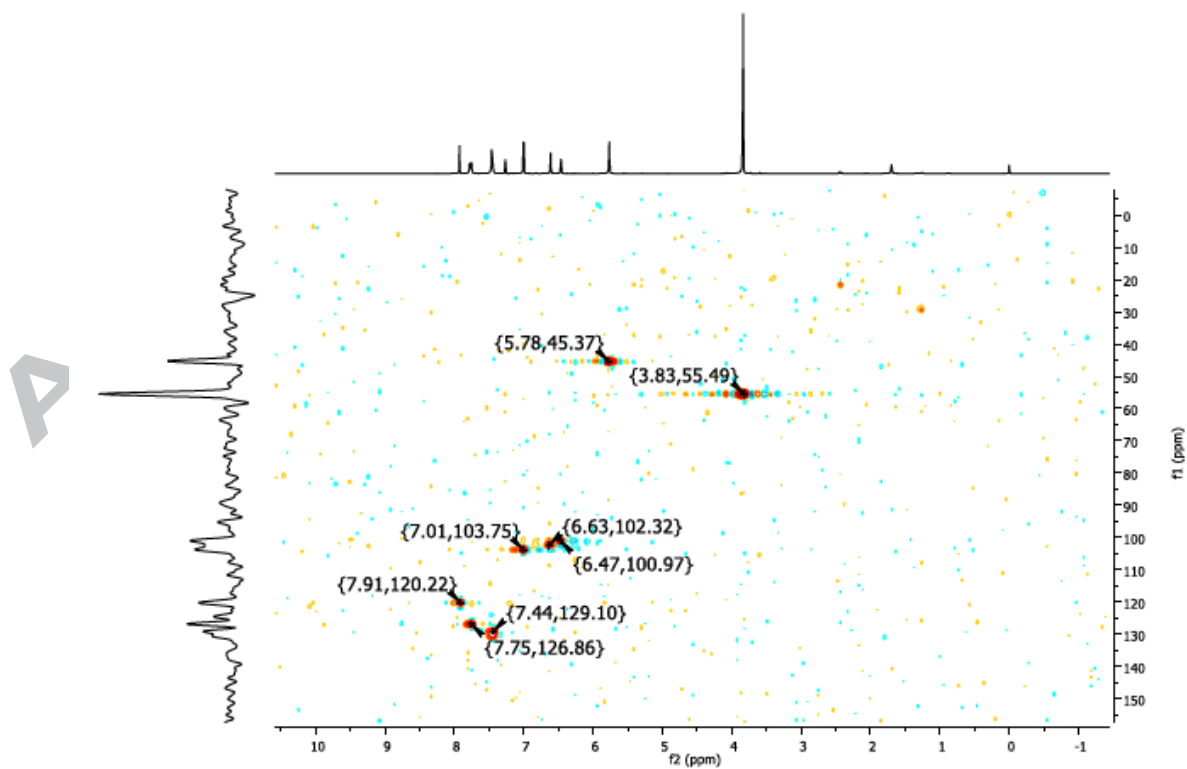


Fig. S10. $^1\text{H-NMR}$ spectrum of **compound 11**: 3-phenyl-5-((4-(p-tolyl)-1H-1,2,3-triazol-1-yl)methyl)isoxazole (400 MHz, CDCl_3).

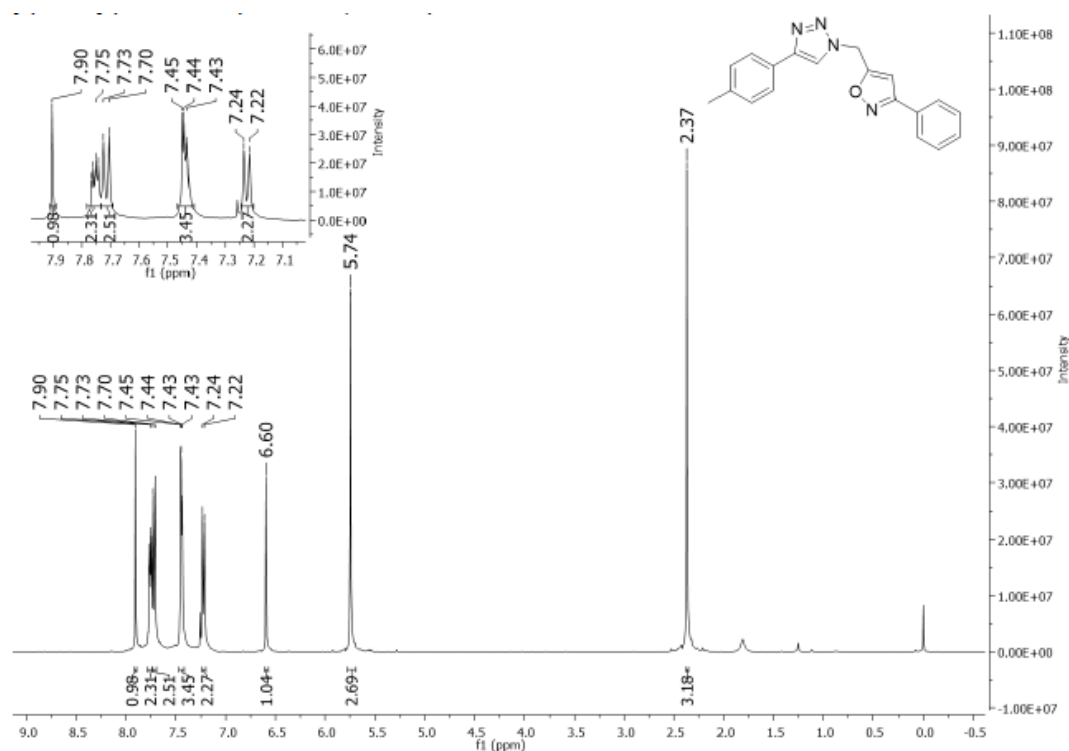


Fig. S11. $^{13}\text{C-NMR}$ spectrum of **compound 11**: 3-phenyl-5-((4-(p-tolyl)-1H-1,2,3-triazol-1-yl)methyl)isoxazole (100 MHz, CDCl_3).

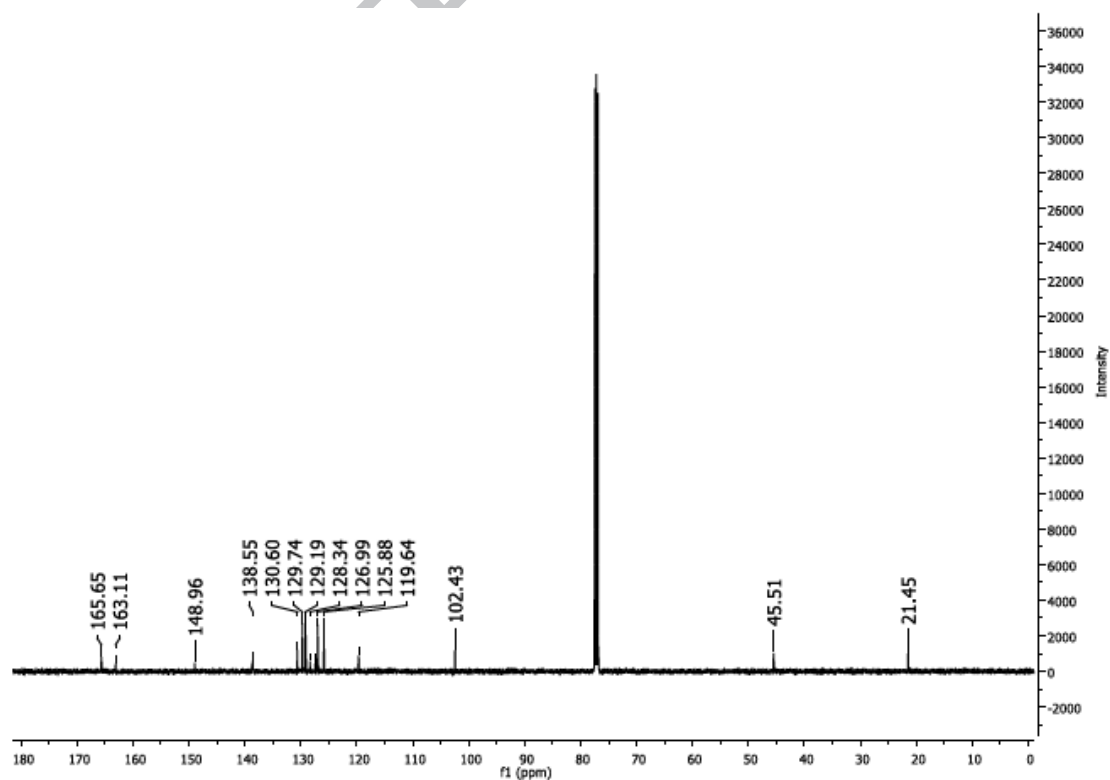


Fig. S12. $^1\text{H-NMR}$ spectrum of **compound 12**: 3-phenyl-5-((4-(2,4,5-trimethylphenyl)-1H-1,2,3-triazol-1-yl)methyl)isoxazole (300 MHz, CDCl_3).

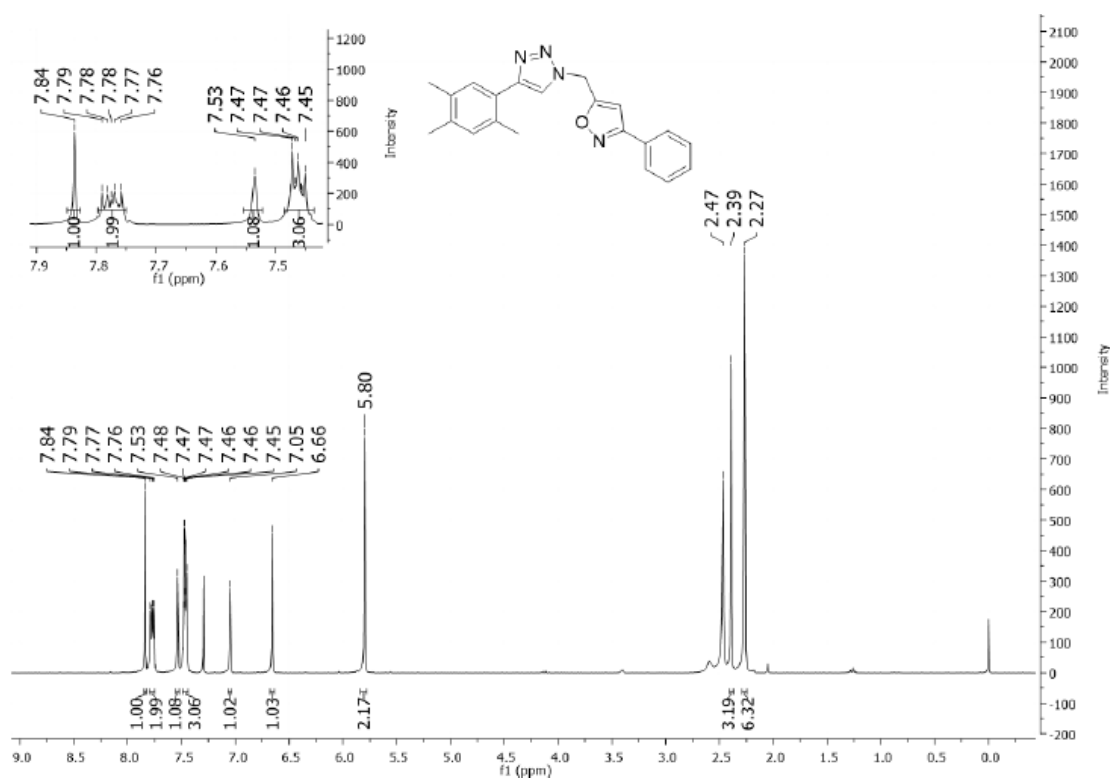


Fig. S13. HSQC spectrum of **compound 12**: 3-phenyl-5-((4-(2,4,5-trimethylphenyl)-1H-1,2,3-triazol-1-yl)methyl)isoxazole (^1H : 300 MHz, ^{13}C : 75 MHz, CDCl_3).

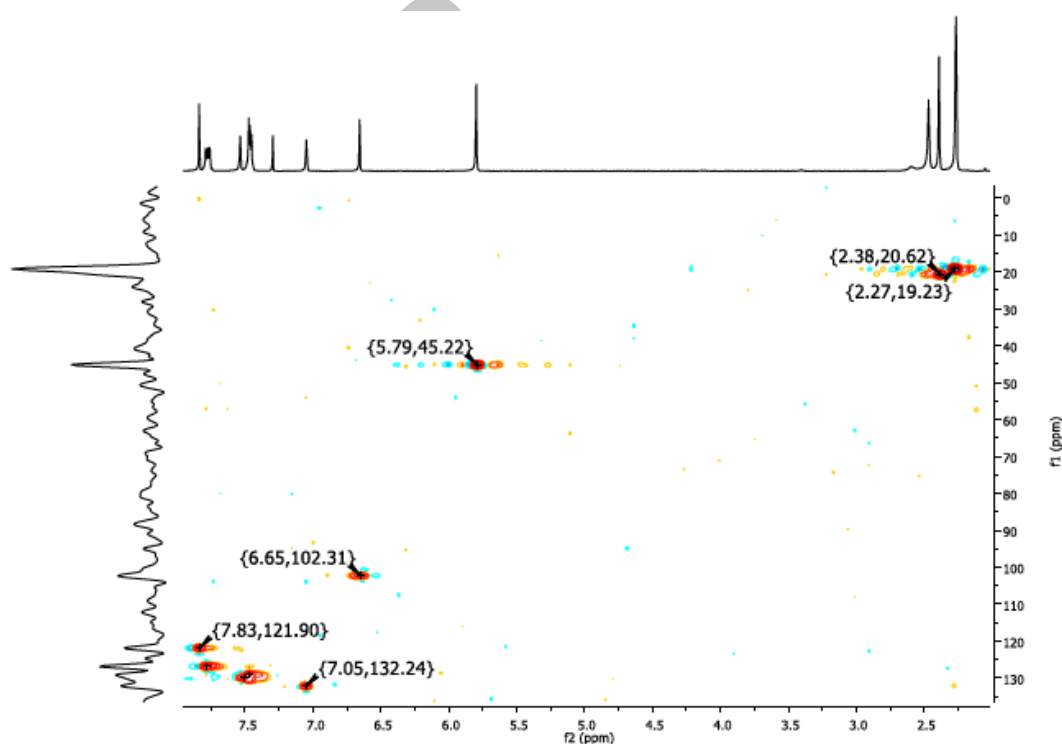


Fig. S14. ^1H -NMR spectrum of **compound 13**: 5-((4-(4-methoxy-2-methylphenyl)-1H-1,2,3-triazol-1-yl)methyl)-3-phenylisoxazole (300 MHz, CDCl_3).

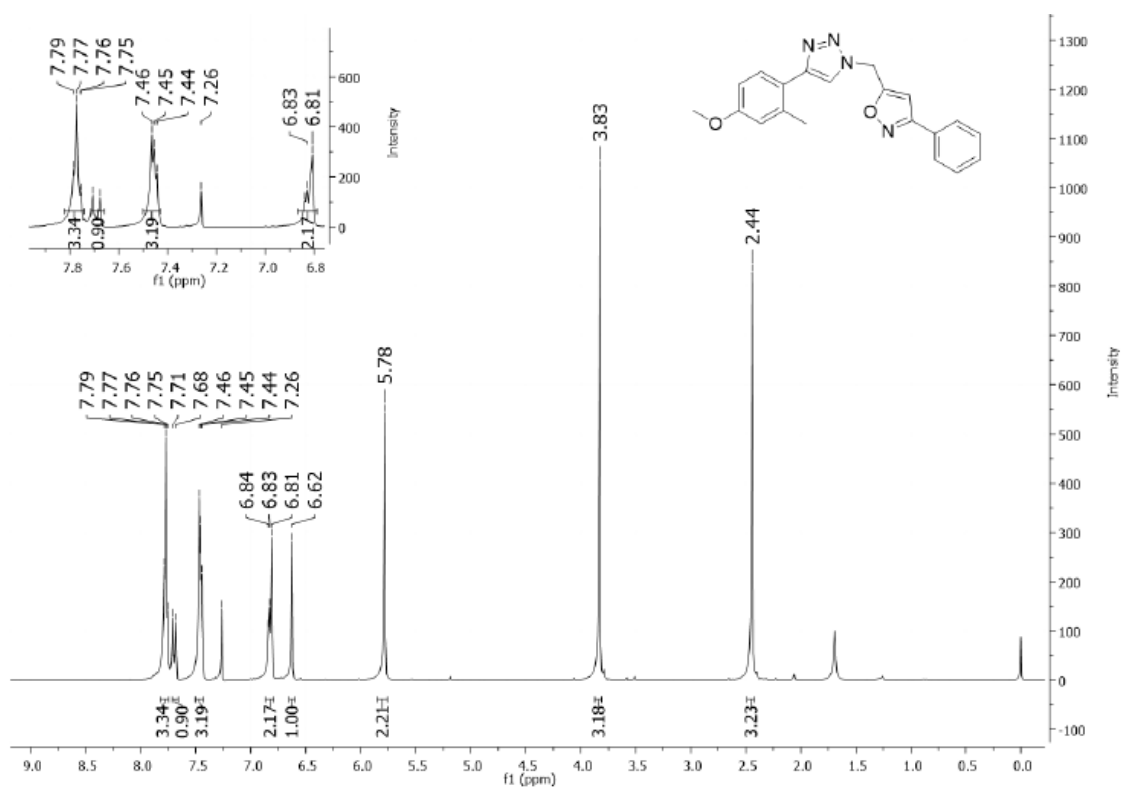


Fig. S15. HSQC spectrum of **compound 13**: 5-((4-(4-methoxy-2-methylphenyl)-1H-1,2,3-triazol-1-yl)methyl)-3-phenylisoxazole (^1H : 300 MHz, ^{13}C : 75 MHz, CDCl_3).

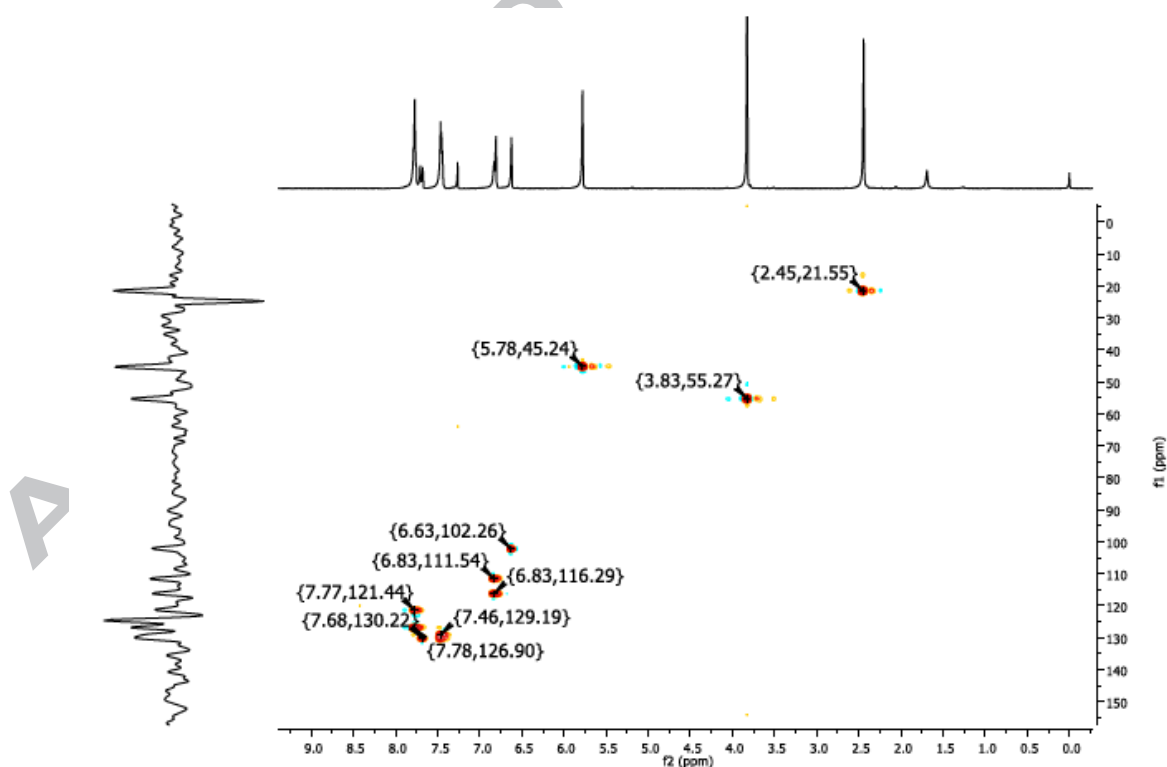


Fig. S16. ^1H -NMR spectrum of **compound 14**: 5-((4-(2,5-dimethylphenyl)-1H-1,2,3-triazol-1-yl)methyl)-3-phenylisoxazole (300 MHz, CDCl_3).

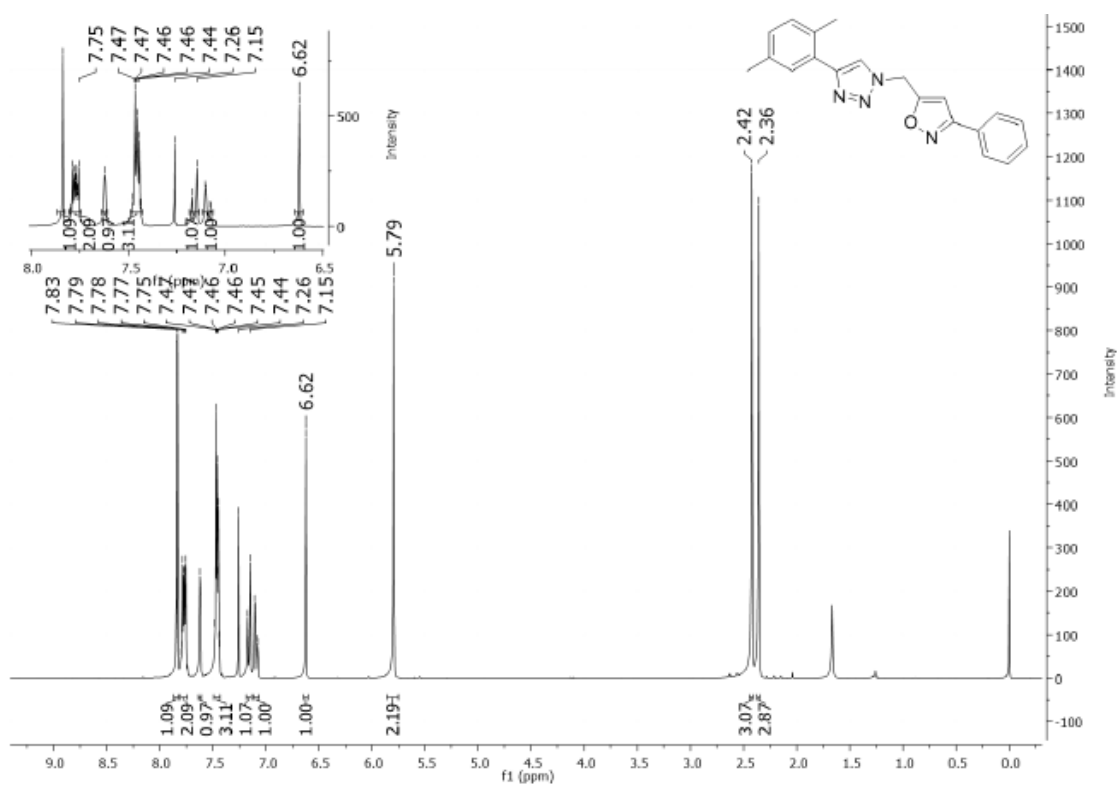


Fig. S17. HSQC spectrum of **compound 14**: 5-((4-(2,5-dimethylphenyl)-1H-1,2,3-triazol-1-yl)methyl)-3-phenylisoxazole (^1H : 300 MHz, ^{13}C : 75 MHz, CDCl_3).

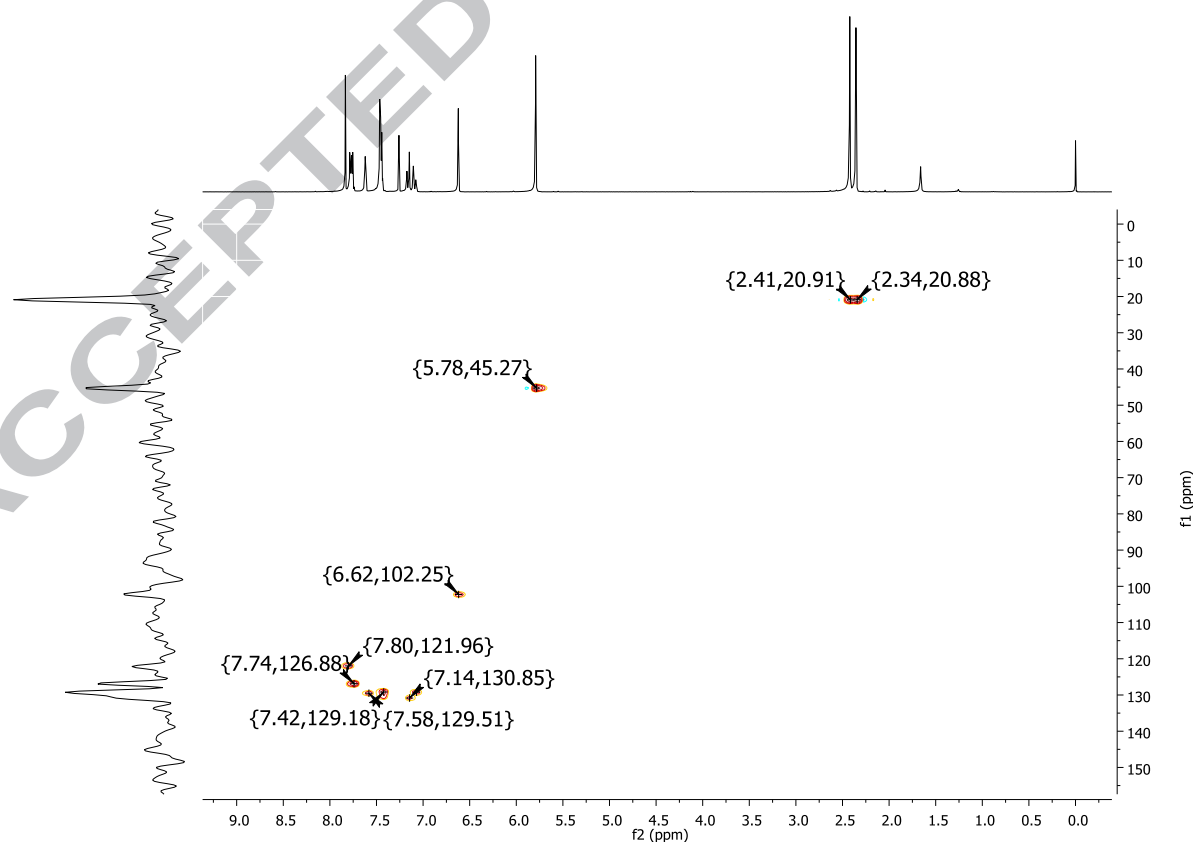


Fig. S18. ^1H -NMR spectrum of **compound 15**: 5-((4-(6-methoxynaphthalen-2-yl)-1H-1,2,3-triazol-1-yl)methyl)-3-phenylisoxazole (300 MHz, CDCl_3).

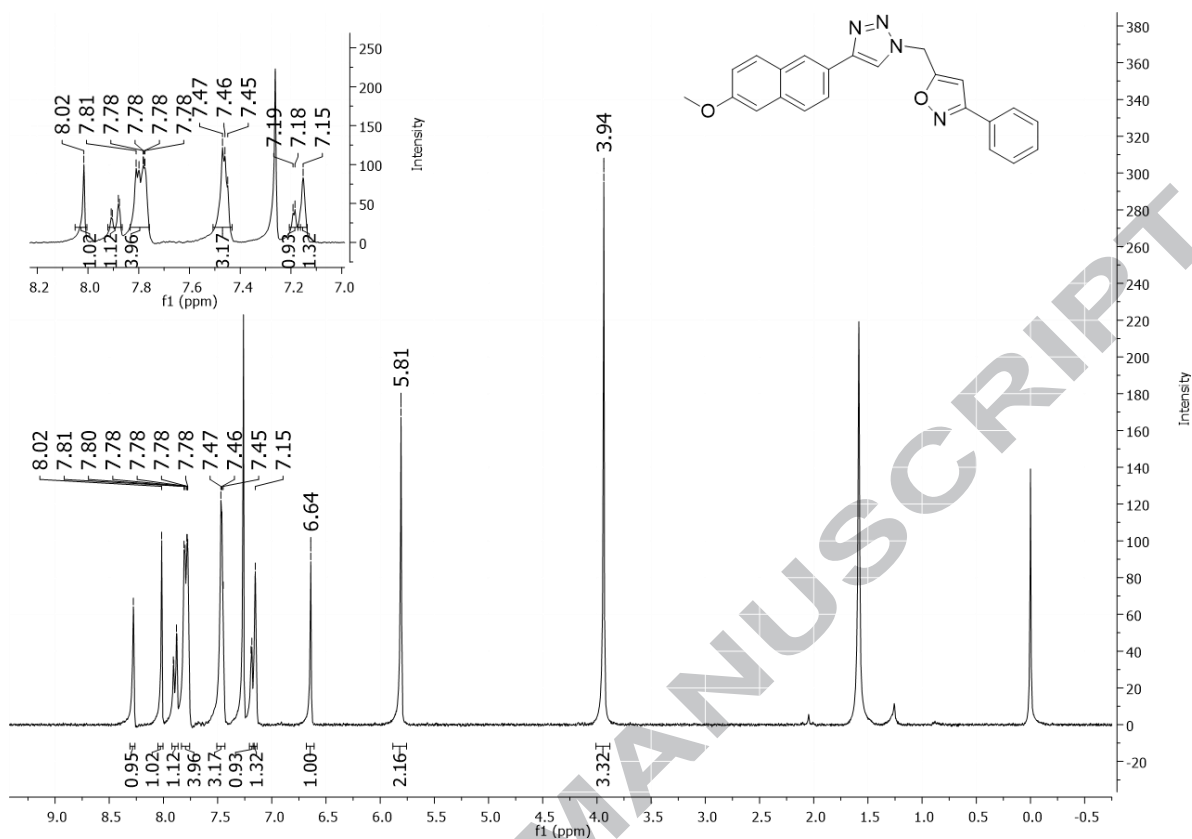


Fig. S19. HSQC spectrum of **compound 15**: 5-((4-(6-methoxynaphthalen-2-yl)-1H-1,2,3-triazol-1-yl)methyl)-3-phenylisoxazole (^1H : 300 MHz, ^{13}C : 75 MHz, CDCl_3).

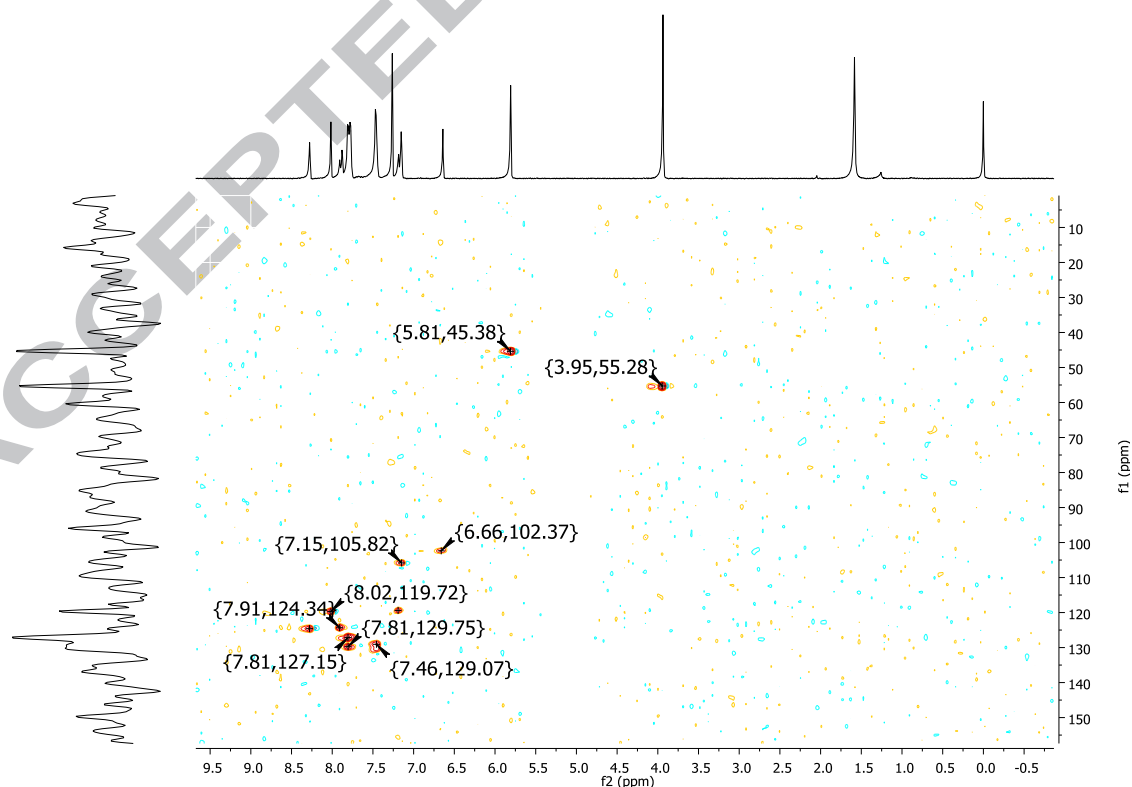


Fig. S20. ^1H -NMR spectrum of **compound 16**: 5-((4-(4-nitrophenyl)-1H-1,2,3-triazol-1-yl)methyl)-3-phenylisoxazole (300 MHz, CDCl_3).

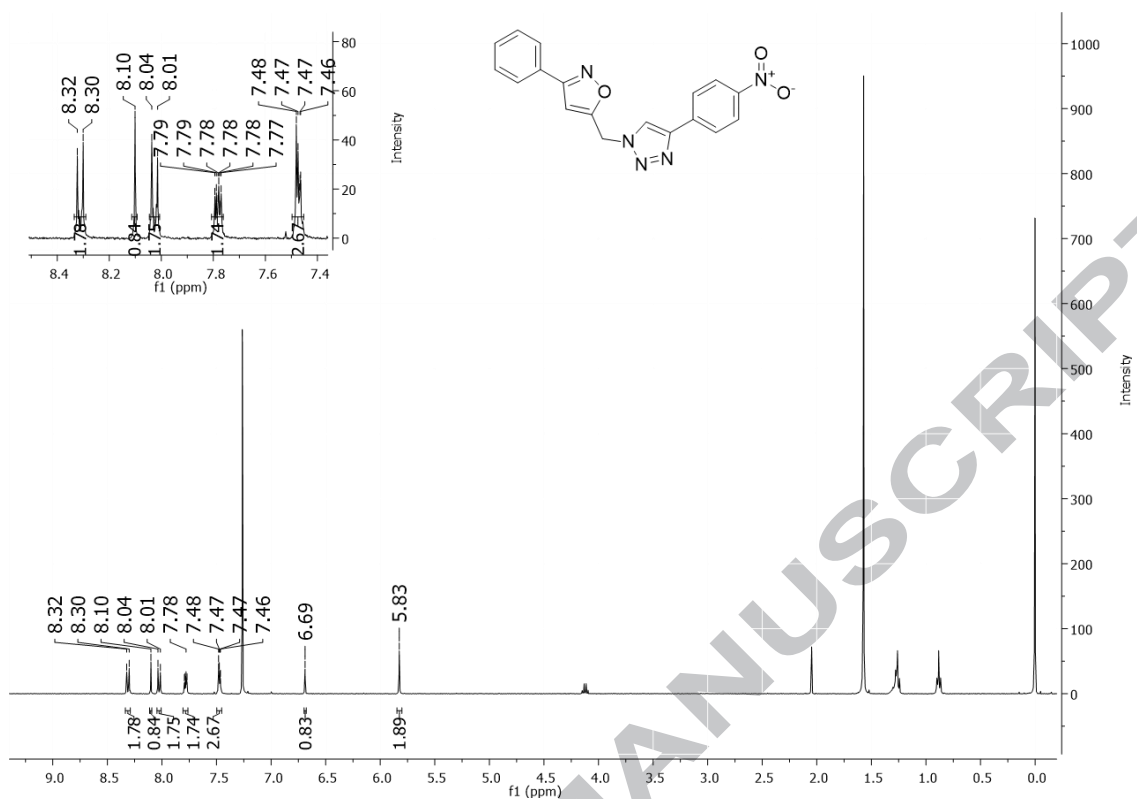


Fig. S21. HSQC spectrum of **compound 16**: 5-((4-(4-nitrophenyl)-1H-1,2,3-triazol-1-yl)methyl)-3-phenylisoxazole (^1H : 300 MHz, ^{13}C : 75 MHz, CDCl_3).

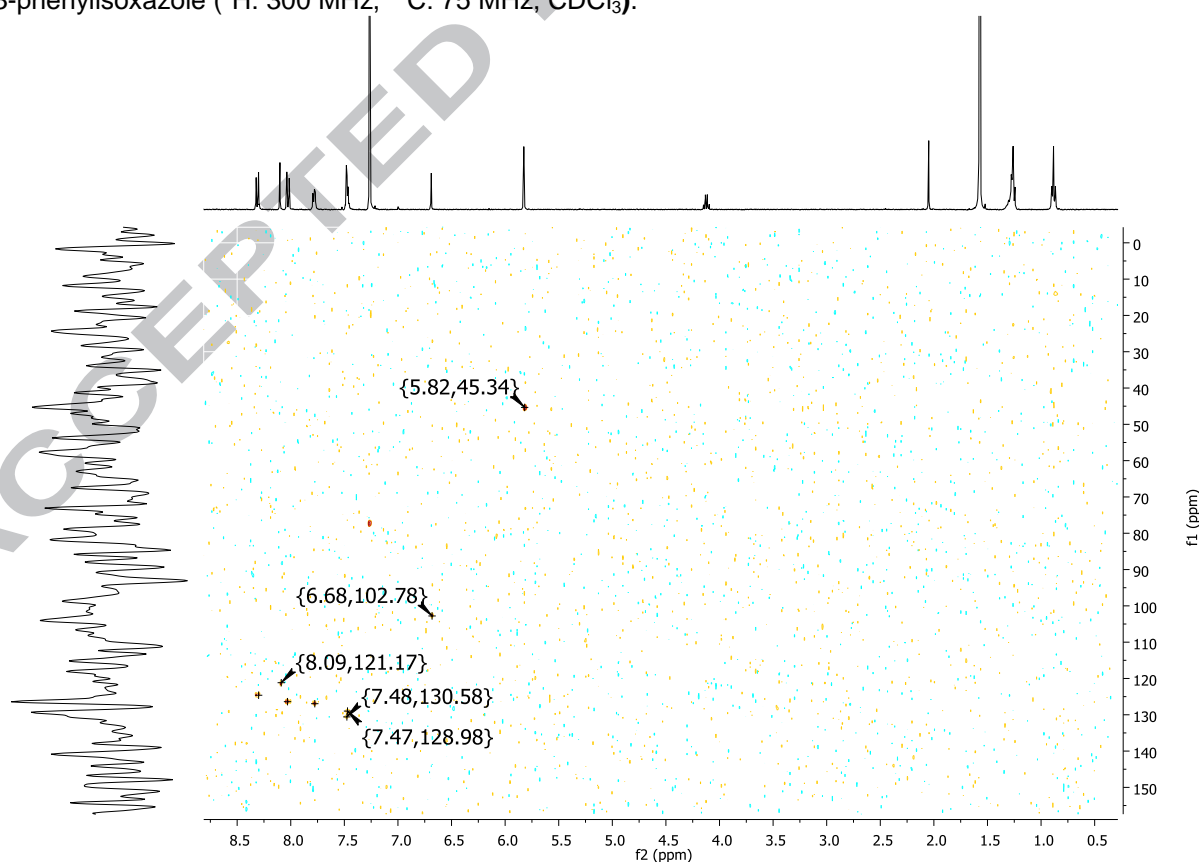


Fig. S22. ^1H -NMR spectrum of **compound 17**: 3-phenyl-5-((4-(4-(trifluoromethoxy)phenyl)-1H-1,2,3-triazol-1-yl)methyl)isoxazole (300 MHz, CDCl_3).

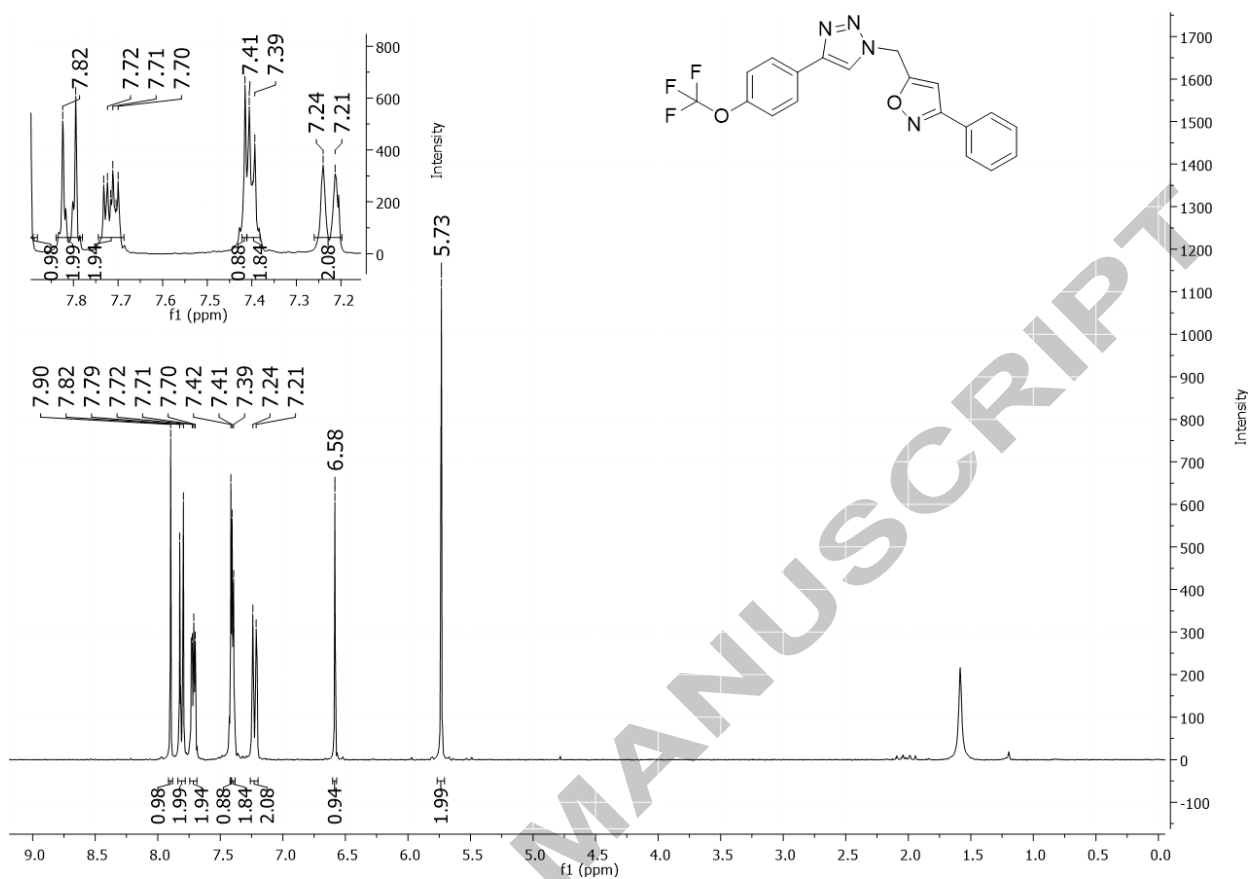


Fig. S23. ^{13}C -NMR spectrum of **compound 17**: 3-phenyl-5-((4-(4-(trifluoromethoxy)phenyl)-1H-1,2,3-triazol-1-yl)methyl)isoxazole (75 MHz, CDCl_3).

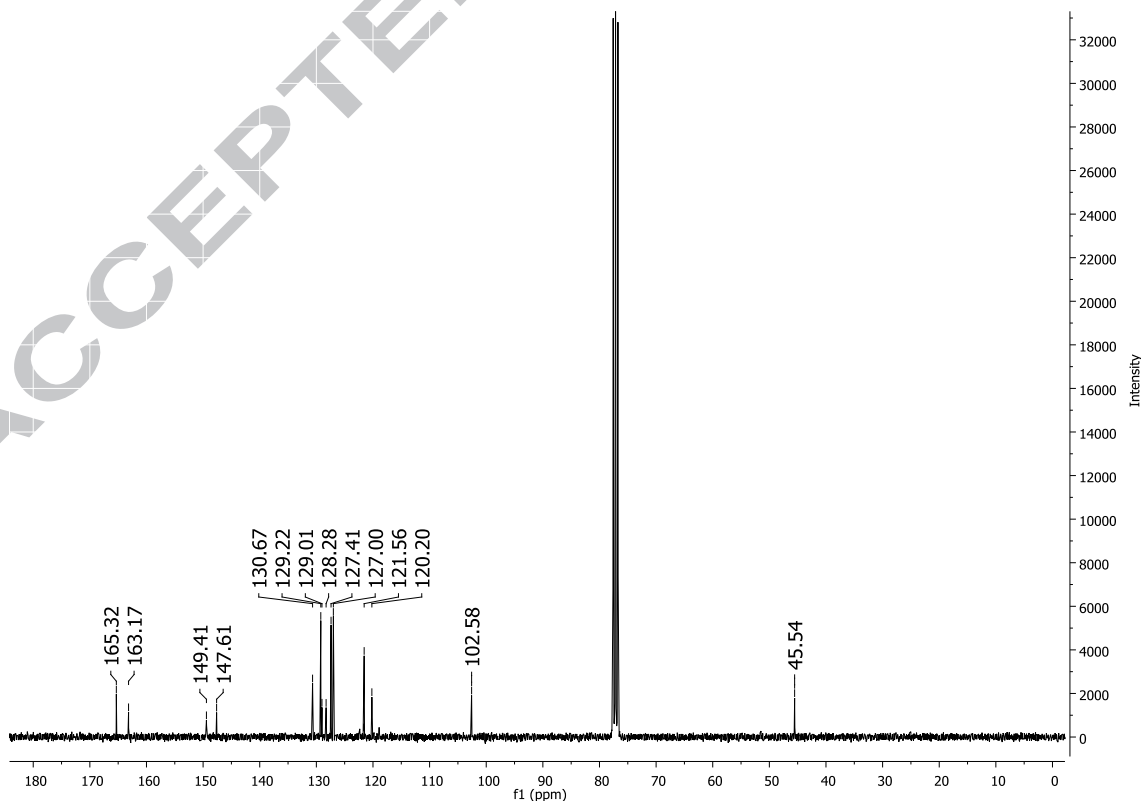


Fig. S24. $^1\text{H-NMR}$ spectrum of **compound 18**: 5-((4-(4-fluorophenyl)-1H-1,2,3-triazol-1-yl)methyl)-3-phenylisoxazole (300 MHz, CDCl_3).

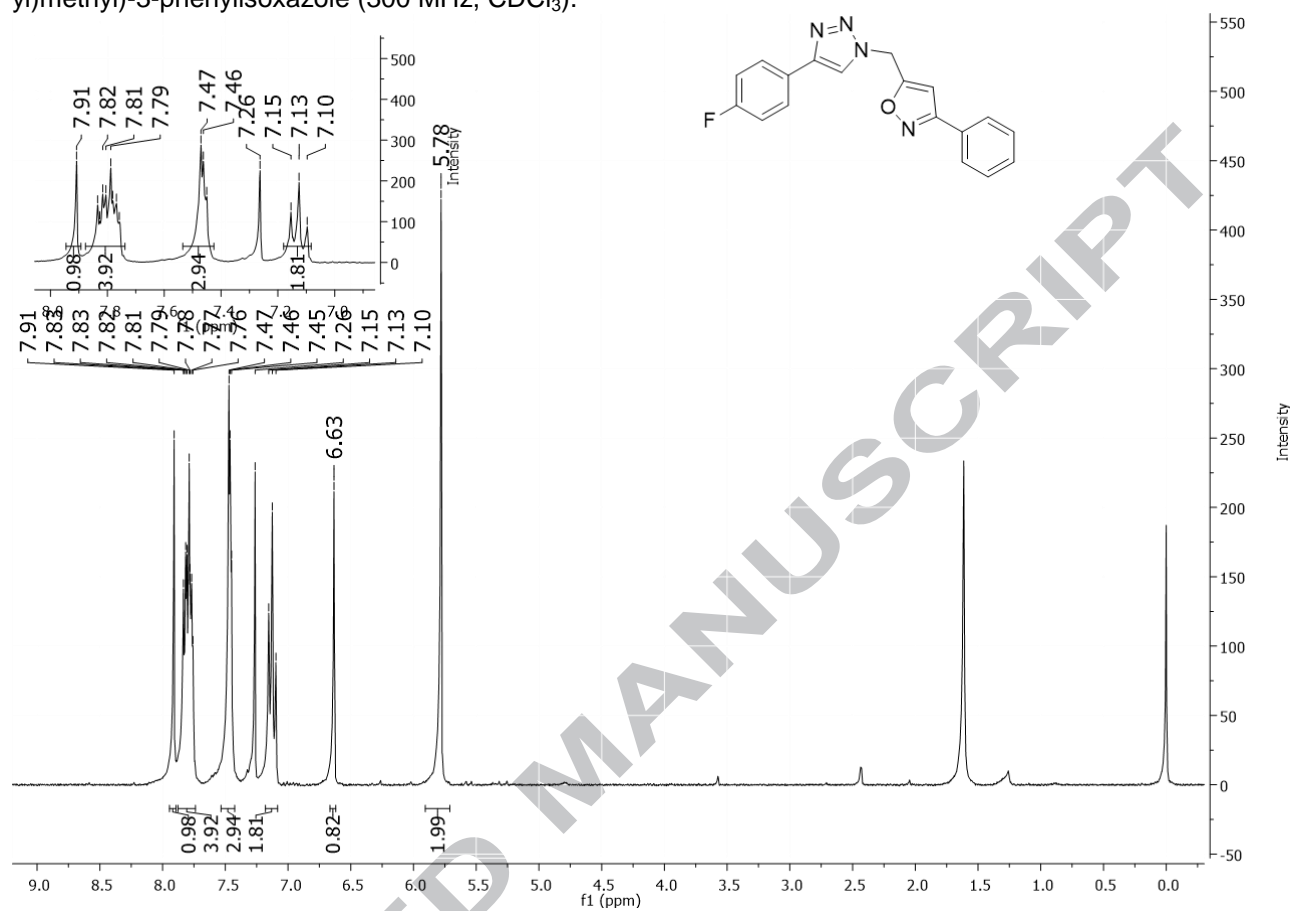


Fig. S25. $^{13}\text{C-NMR}$ spectrum of **compound 18**: 5-((4-(4-fluorophenyl)-1H-1,2,3-triazol-1-yl)methyl)-3-phenylisoxazole (75 MHz, CDCl_3).

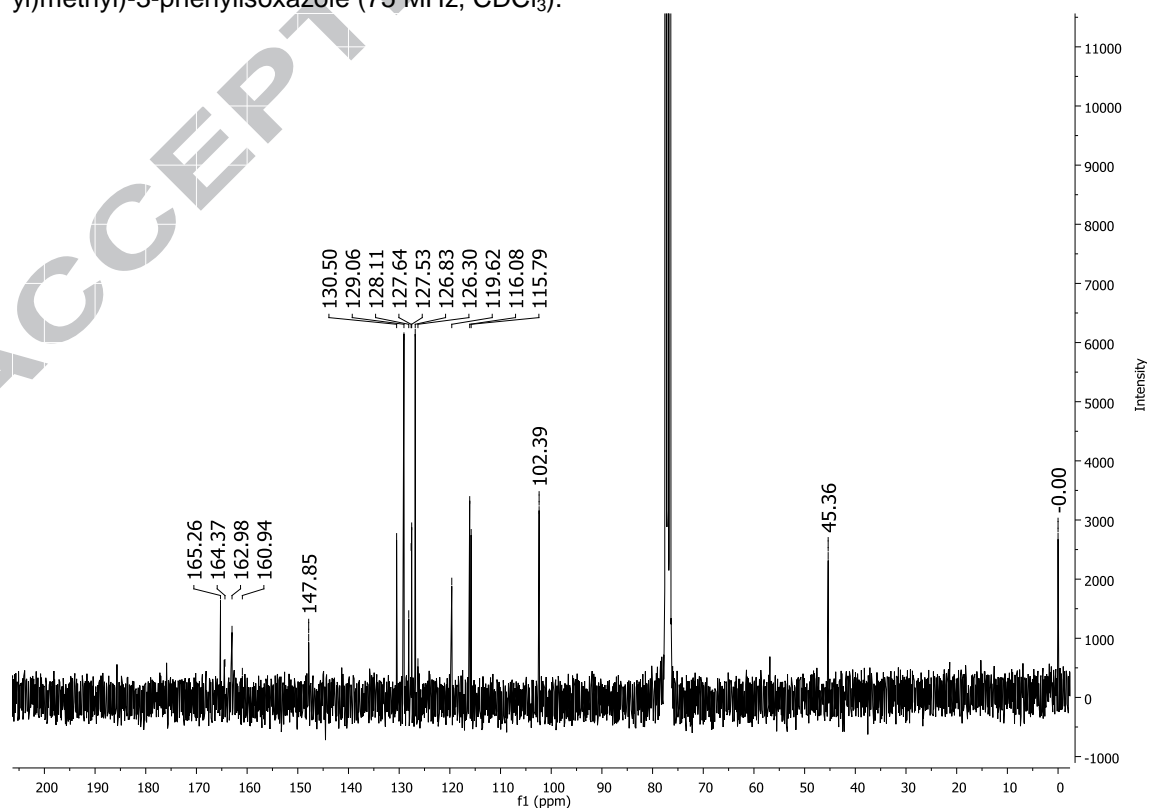


Fig. S26. $^1\text{H-NMR}$ spectrum of **compound 19**: N,N-dimethyl-4-(1-((3-phenylisoxazol-5-yl)methyl)-1H-1,2,3-triazol-4-yl)aniline (300 MHz, CDCl_3).

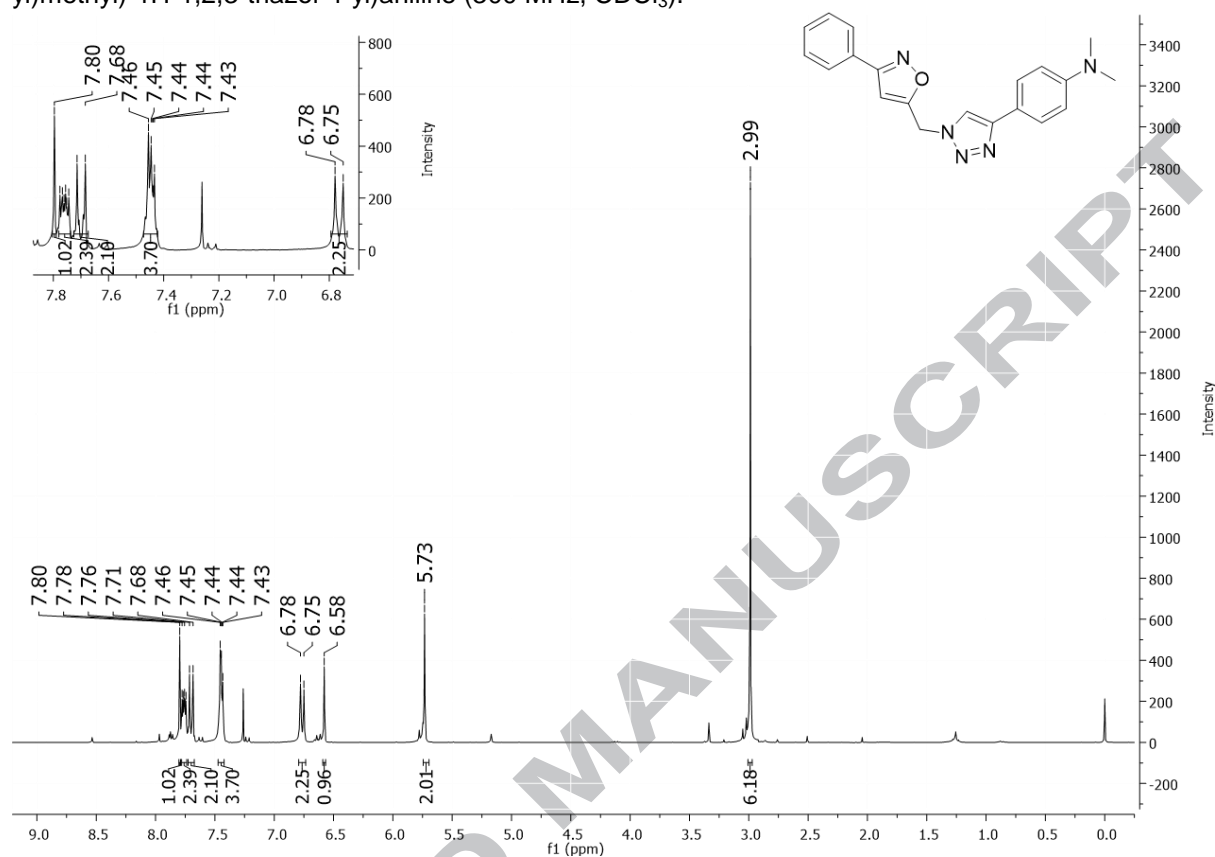


Fig. S27. HSQC spectrum of **compound 19**: N,N-dimethyl-4-(1-((3-phenylisoxazol-5-yl)methyl)-1H-1,2,3-triazol-4-yl)aniline (^1H : 300 MHz, ^{13}C : 75 MHz, CDCl_3).

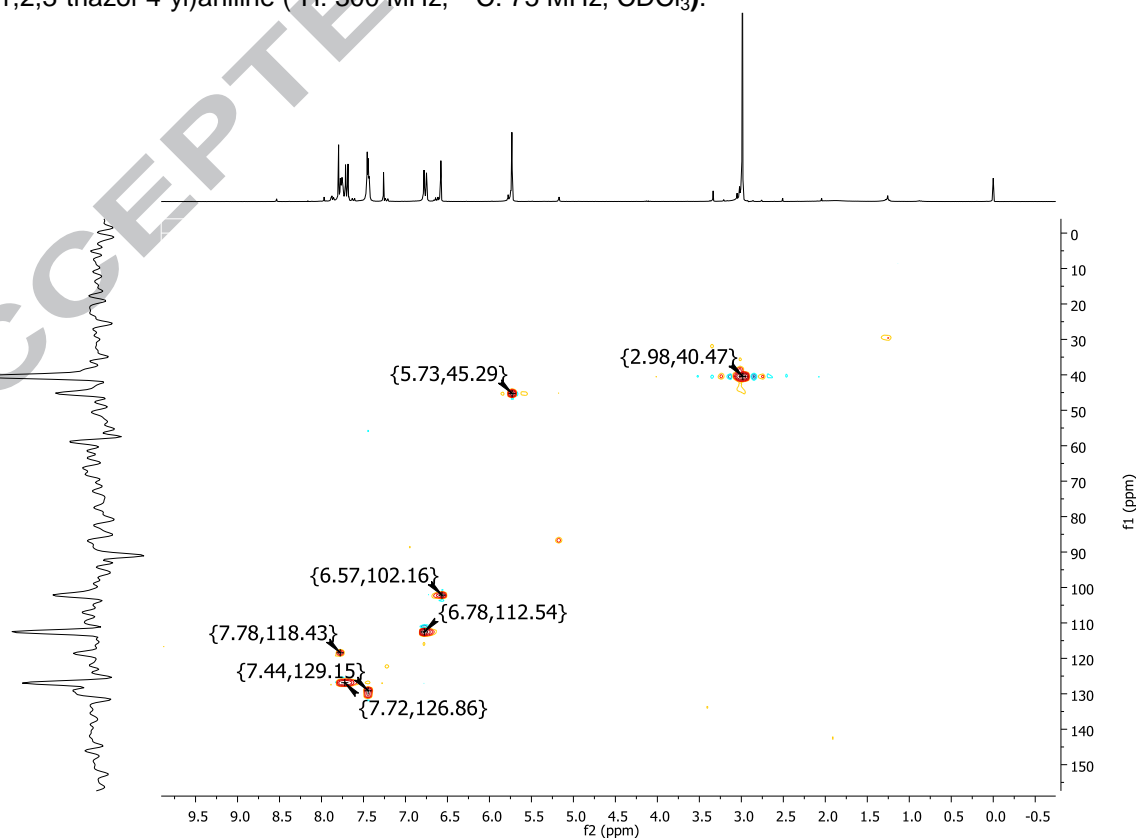


Fig. S28. $^1\text{H-NMR}$ spectrum of **compound 20**: 4-(1-((3-phenylisoxazol-5-yl)methyl)-1H-1,2,3-triazol-4-yl)aniline (300 MHz, CDCl_3).

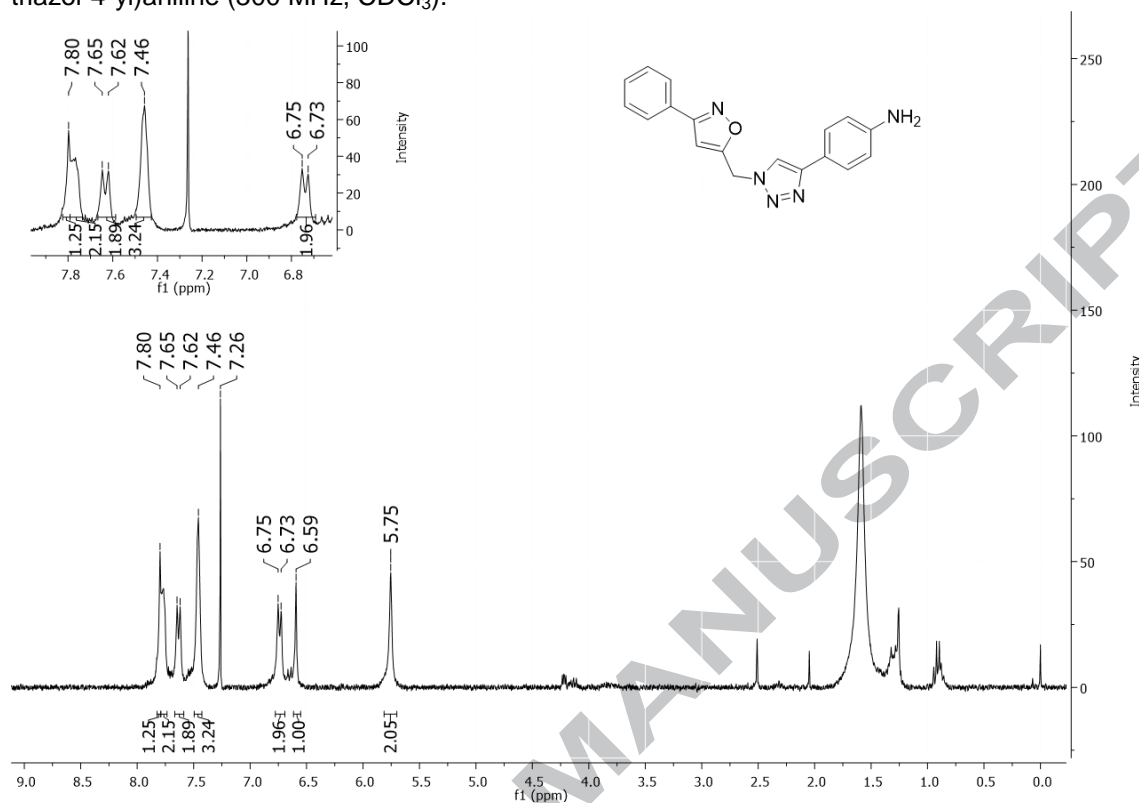


Fig. S29. $^{13}\text{C-NMR}$ spectrum of **compound 20**: 4-(1-((3-phenylisoxazol-5-yl)methyl)-1H-1,2,3-triazol-4-yl)aniline (125 MHz, MeOD-d_4).

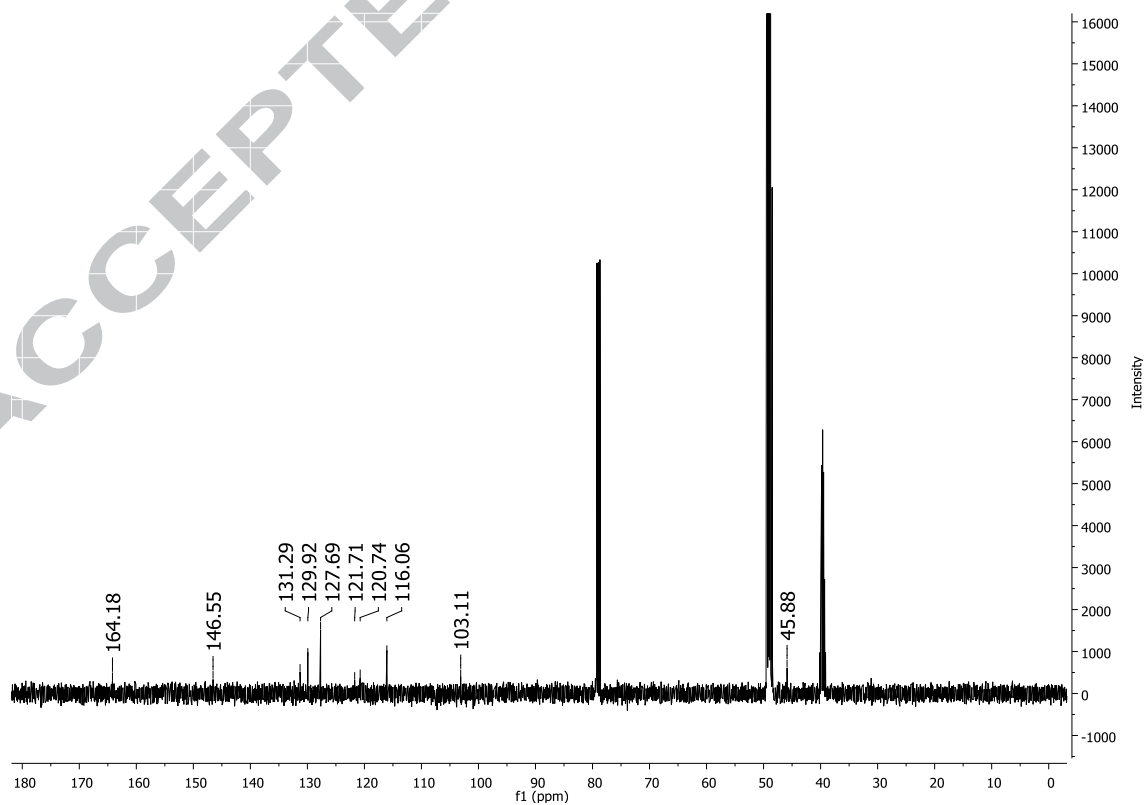


Fig. S30. $^1\text{H-NMR}$ spectrum of **compound 21**: (4-(1-((3-phenylisoxazol-5-yl)methyl)-1H-1,2,3-triazol-4-yl)phenyl)methanol (400 MHz, $\text{MeOD} - d_4$).

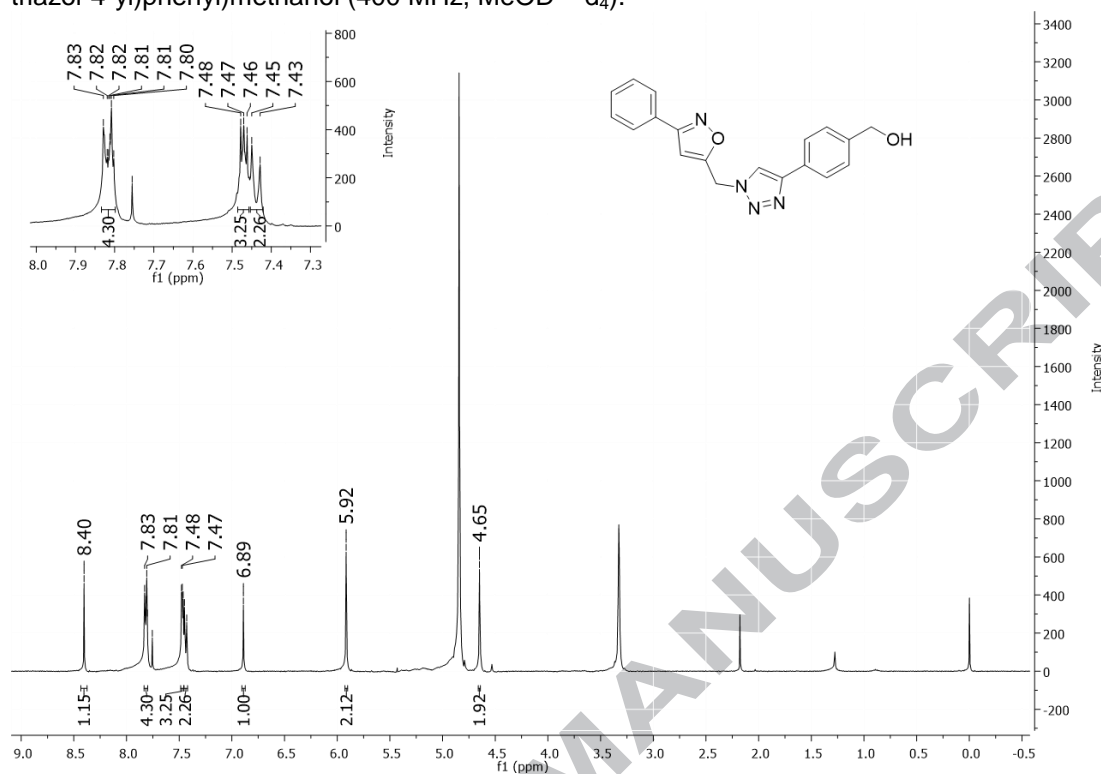


Fig. S31. $^{13}\text{C-NMR}$ spectrum of **compound 21**: (4-(1-((3-phenylisoxazol-5-yl)methyl)-1H-1,2,3-triazol-4-yl)phenyl)methanol (100 MHz, $\text{MeOD} - d_4$).

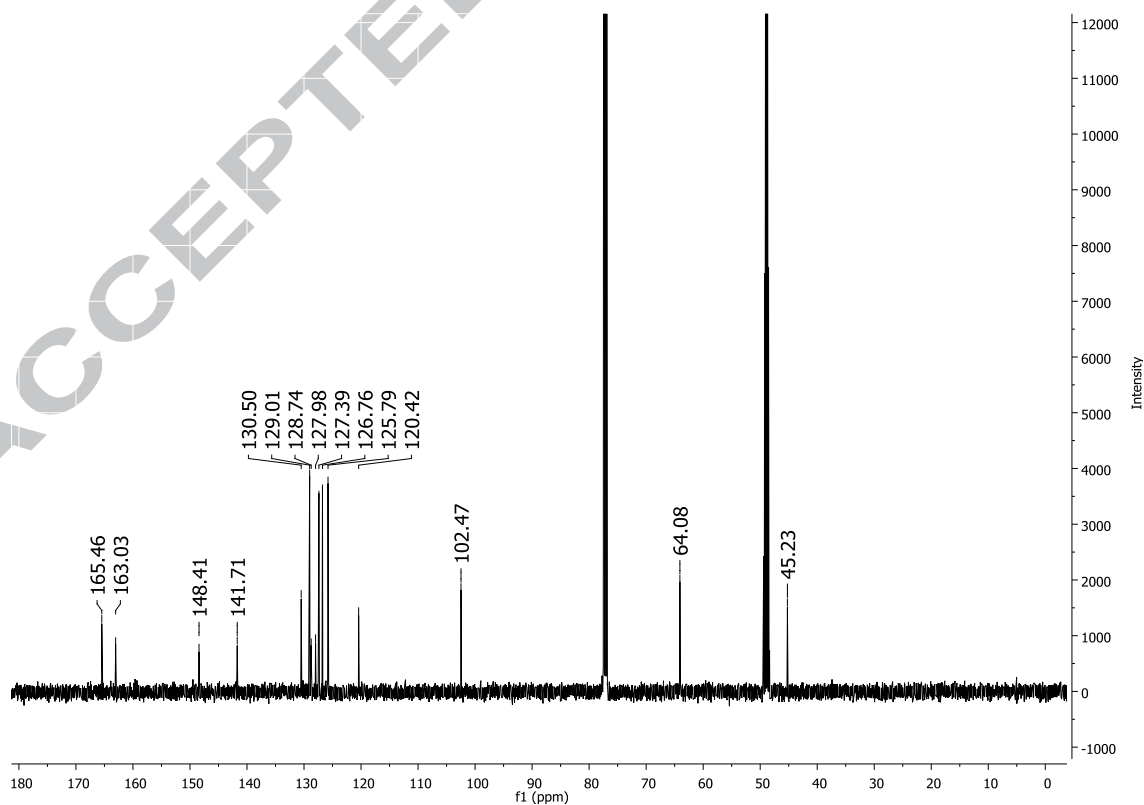


Fig. S32. $^1\text{H-NMR}$ spectrum of **compound 22**: 5-((4-(4-pentylphenyl)-1H-1,2,3-triazol-1-yl)methyl)-3-phenylisoxazole (300 MHz, CDCl_3).

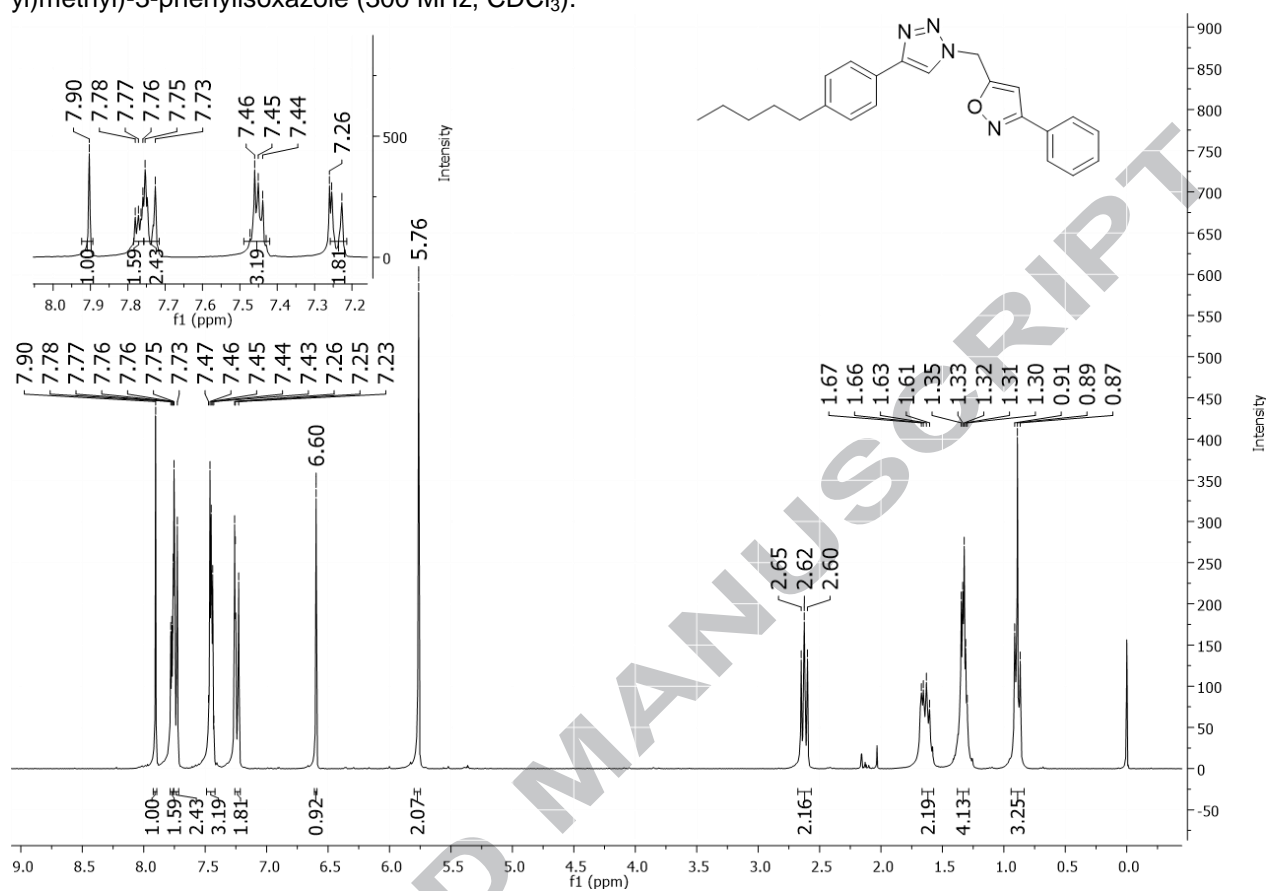


Fig. S33. HSQC spectrum of **compound 22**: 5-((4-(4-pentylphenyl)-1H-1,2,3-triazol-1-yl)methyl)-3-phenylisoxazole (^1H : 400 MHz, ^{13}C : 75 MHz, CDCl_3).

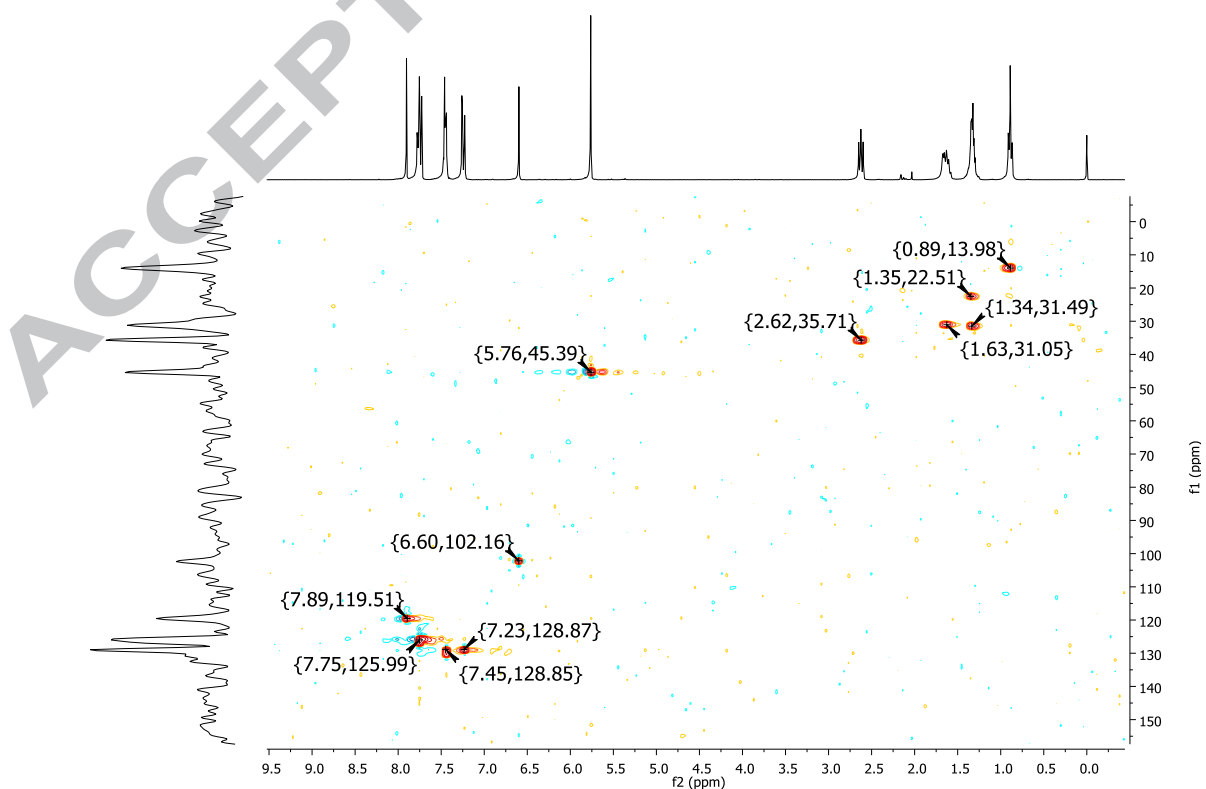


Fig. S34. $^1\text{H-NMR}$ spectrum of **compound 23**: 3-(4-methoxyphenyl)-5-((4-(2,4,5-trimethylphenyl)-1H-1,2,3-triazol-1-yl)methyl)isoxazole (300 MHz, CDCl_3).

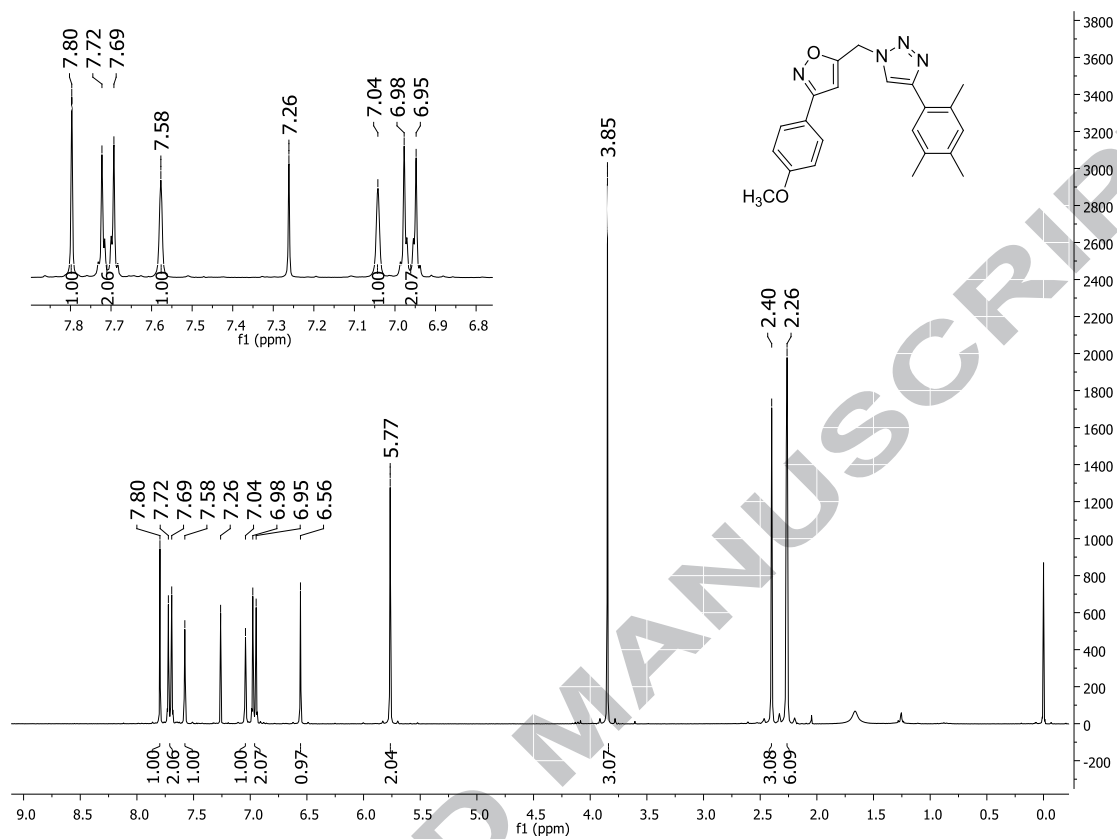


Fig. S35. $^{13}\text{C-NMR}$ spectrum of **compound 23**: 3-(4-methoxyphenyl)-5-((4-(2,4,5-trimethylphenyl)-1H-1,2,3-triazol-1-yl)methyl)isoxazole (100 MHz, CDCl_3).

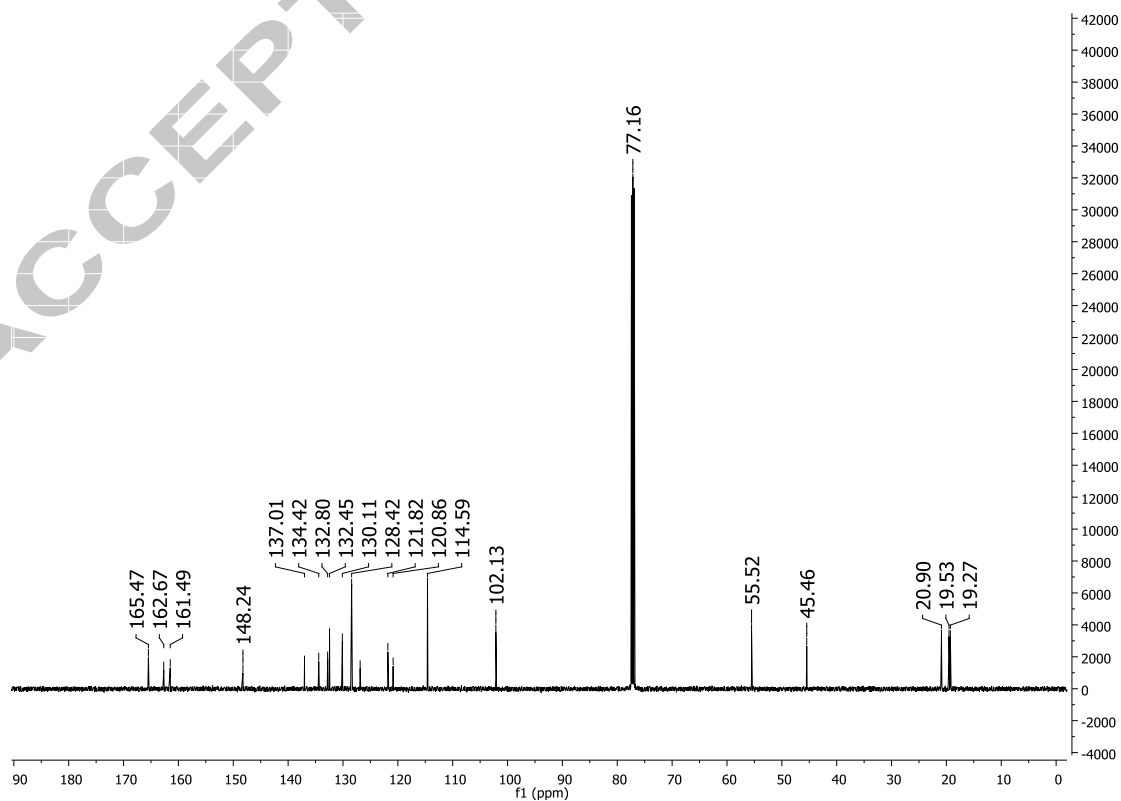


Fig. S36. $^1\text{H-NMR}$ spectrum of **compound 24**: 5-((4-(3,5-dimethoxyphenyl)-1H-1,2,3-triazol-1-yl)methyl)-3-(4-methoxyphenyl)isoxazole (300 MHz, CDCl_3).

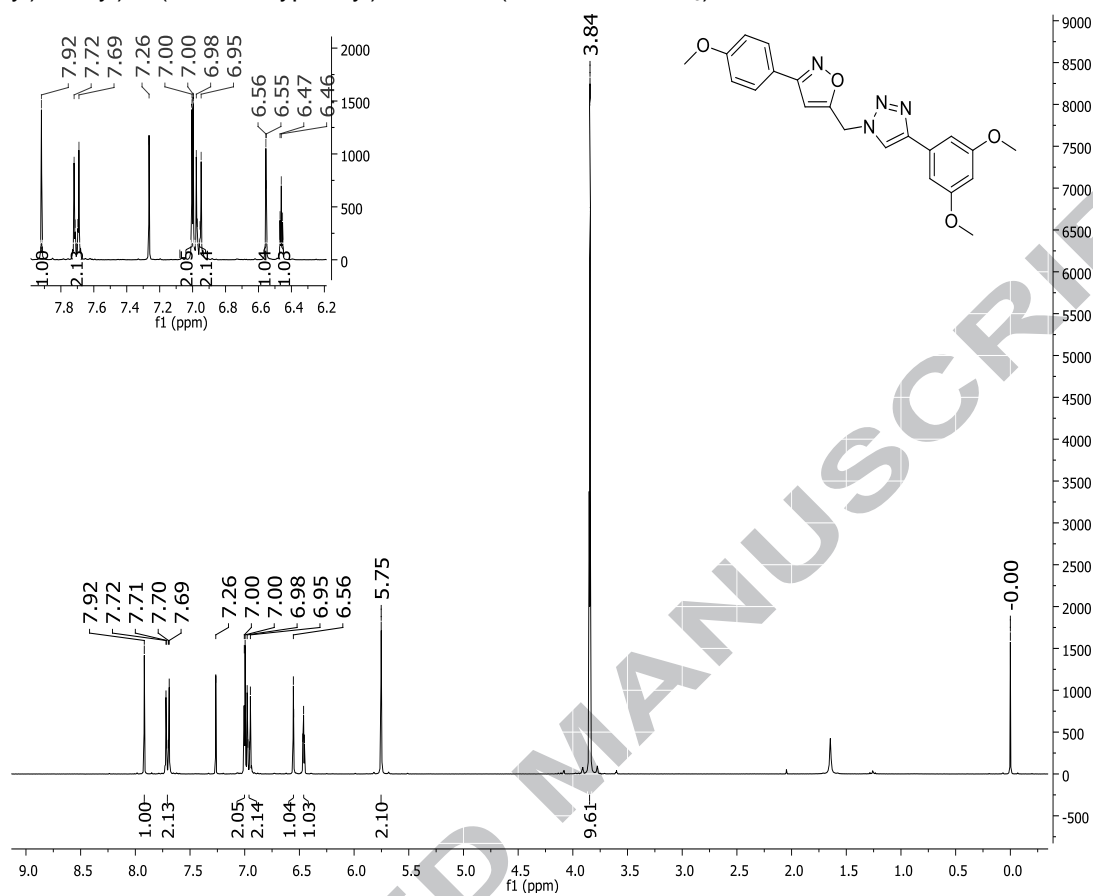


Fig. S37. $^{13}\text{C-NMR}$ spectrum of **compound 24**: 5-((4-(3,5-dimethoxyphenyl)-1H-1,2,3-triazol-1-yl)methyl)-3-(4-methoxyphenyl)isoxazole (100 MHz, CDCl_3).

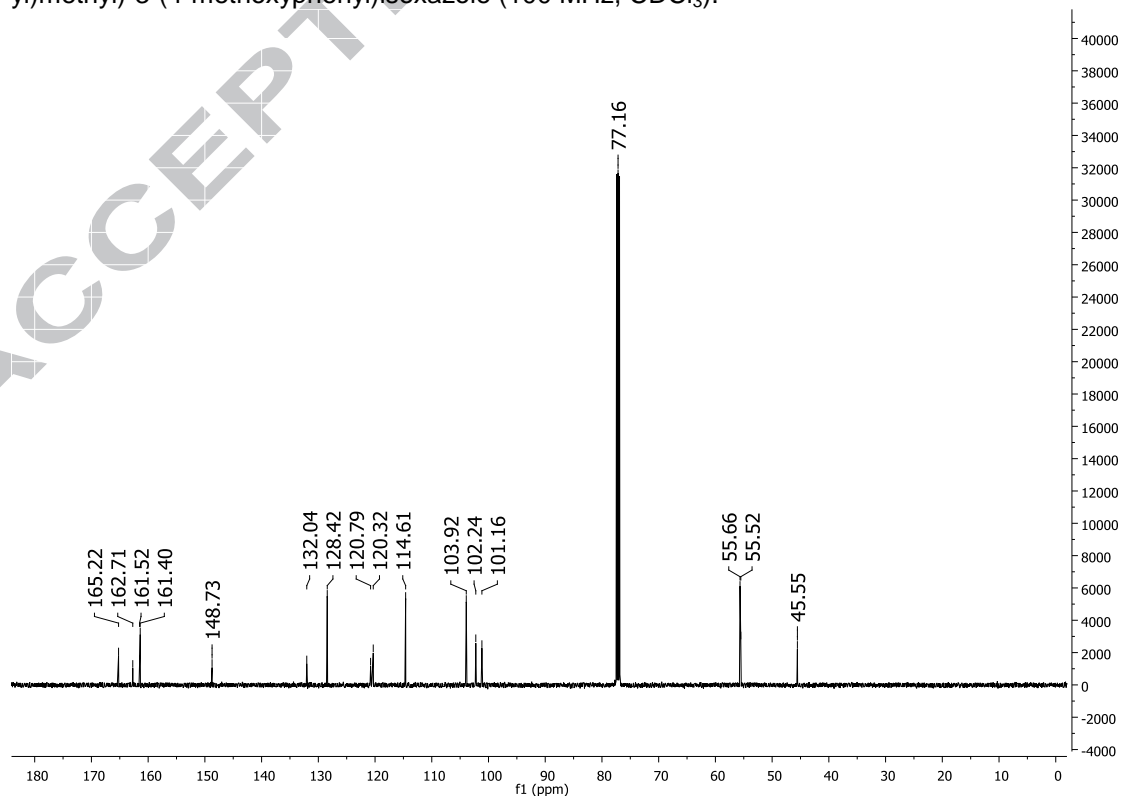


Fig. S38. $^1\text{H-NMR}$ spectrum of **compound 25**: 3-(3,4-dimethoxyphenyl)-5-((4-(2,4,5-trimethylphenyl)-1H-1,2,3-triazol-1-yl)methyl)isoxazole (400 MHz, CDCl_3).

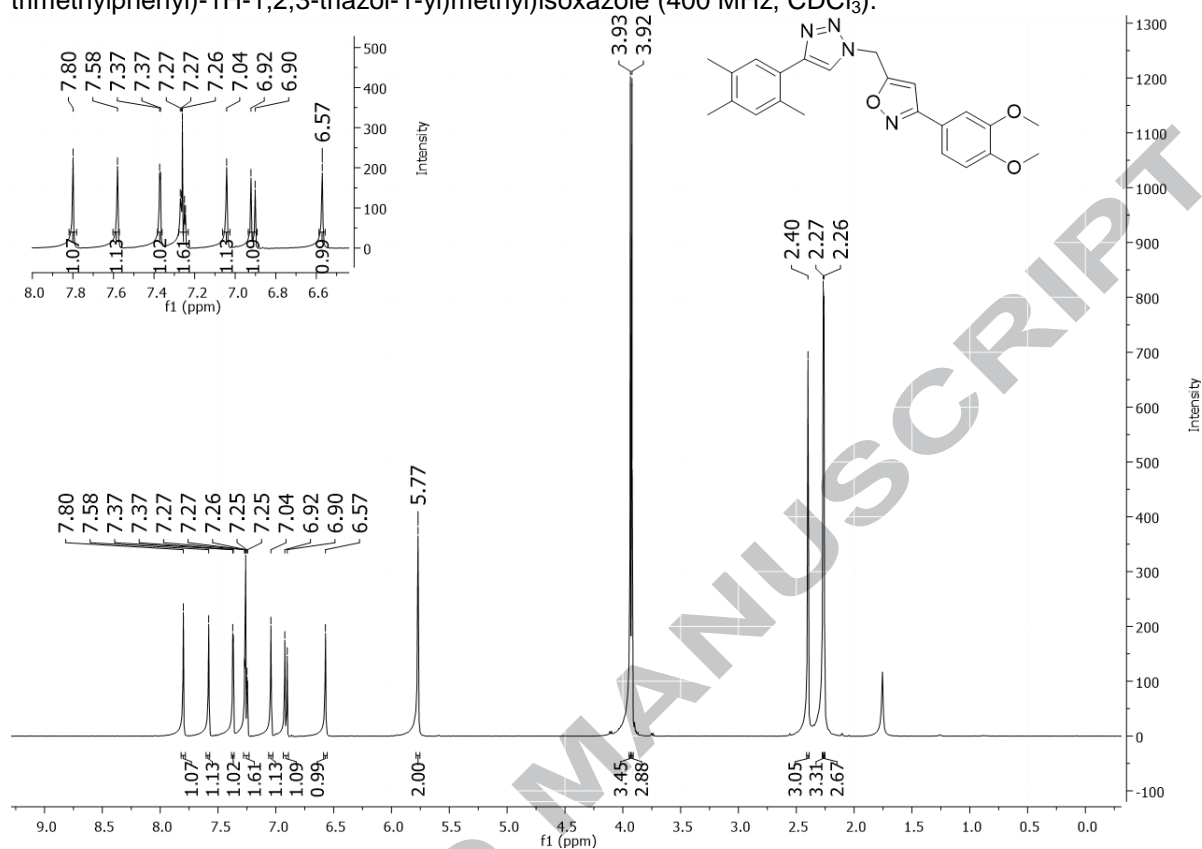


Fig. S39. $^{13}\text{C-NMR}$ spectrum of **compound 25**: 3-(3,4-dimethoxyphenyl)-5-((4-(2,4,5-trimethylphenyl)-1H-1,2,3-triazol-1-yl)methyl)isoxazole (100 MHz, CDCl_3).

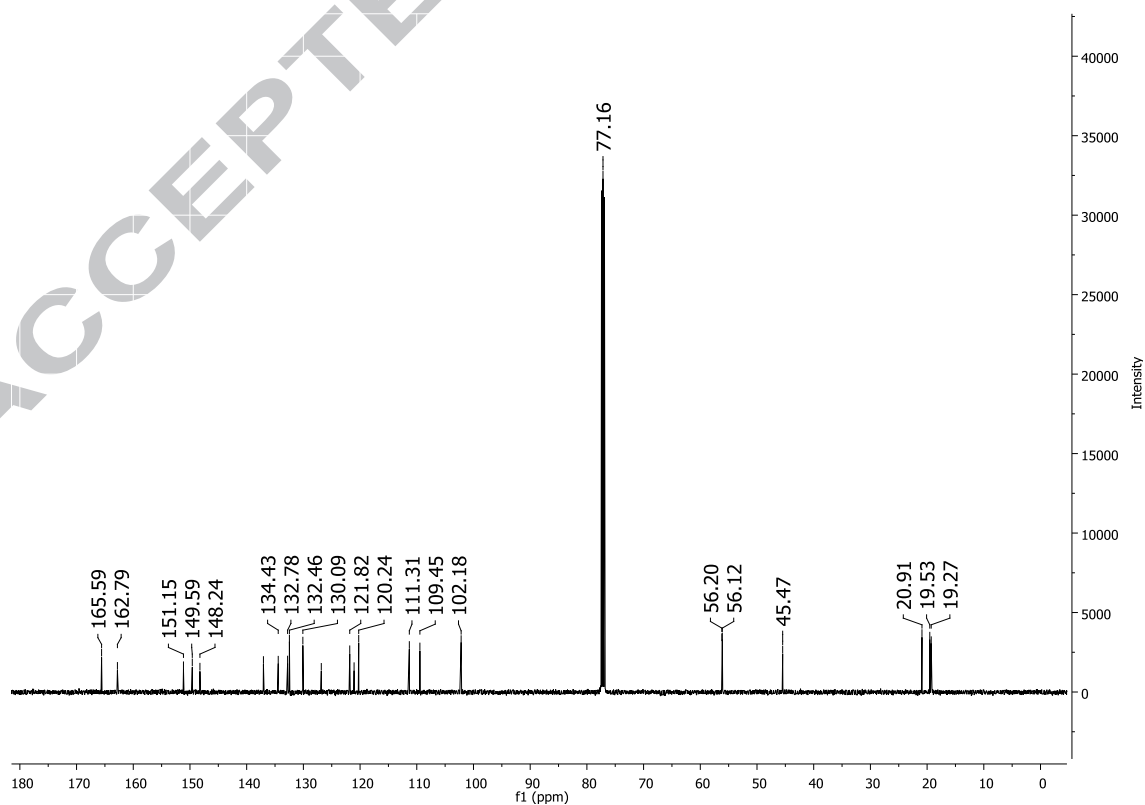


Fig. S40. $^1\text{H-NMR}$ spectrum of **compound 26**: 3-(3,4-dimethoxyphenyl)-5-((4-(3,5-dimethoxyphenyl)-1H-1,2,3-triazol-1-yl)methyl)isoxazole (400 MHz, CDCl_3).

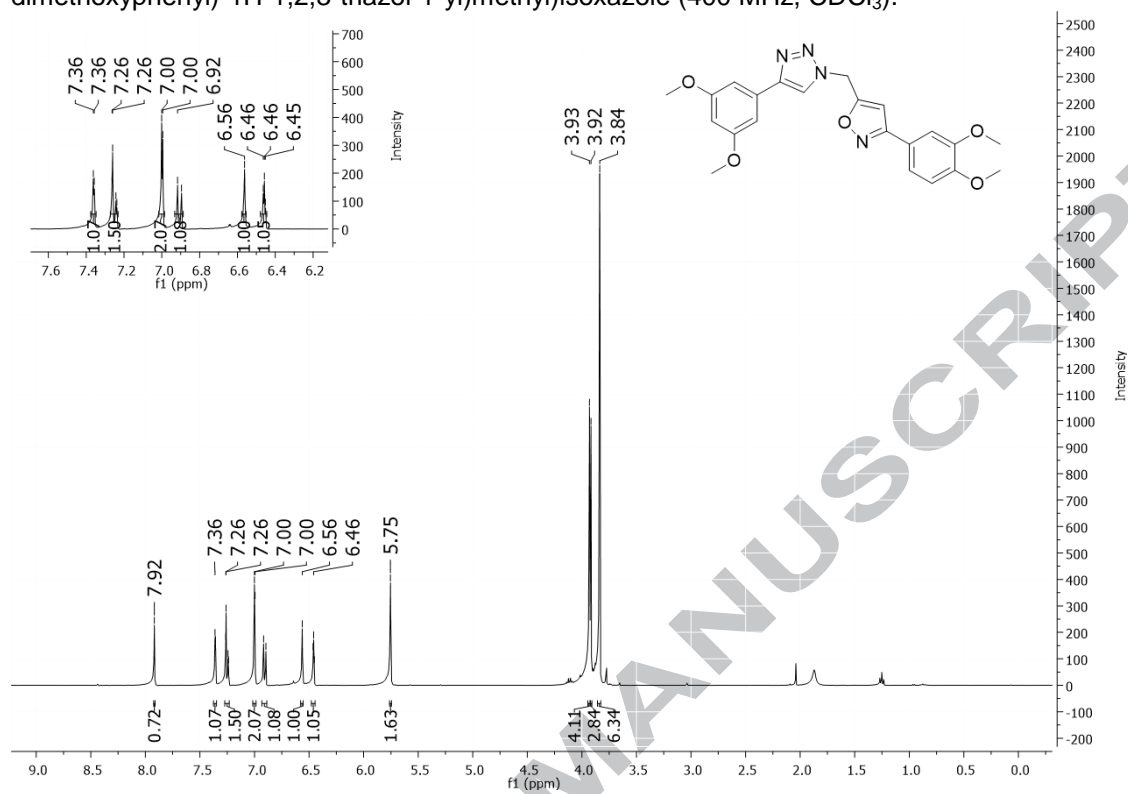


Fig. S41. $^{13}\text{C-NMR}$ spectrum of **compound 26**: 3-(3,4-dimethoxyphenyl)-5-((4-(3,5-dimethoxyphenyl)-1H-1,2,3-triazol-1-yl)methyl)isoxazole (100 MHz, CDCl_3).

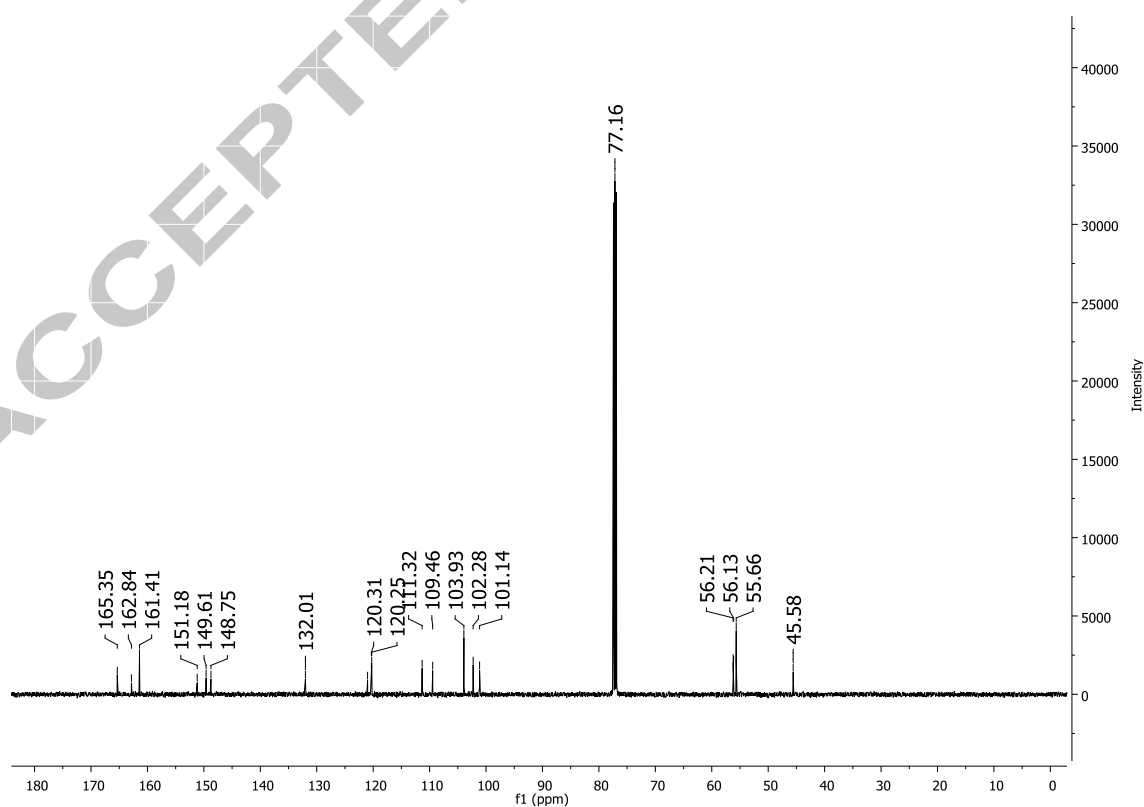


Fig. S42. $^1\text{H-NMR}$ spectrum of **compound 27**: 3-(benzo[d][1,3]dioxol-5-yl)-5-((4-(2,4,5-trimethylphenyl)-1H-1,2,3-triazol-1-yl)methyl)isoxazole (400 MHz, CDCl_3).

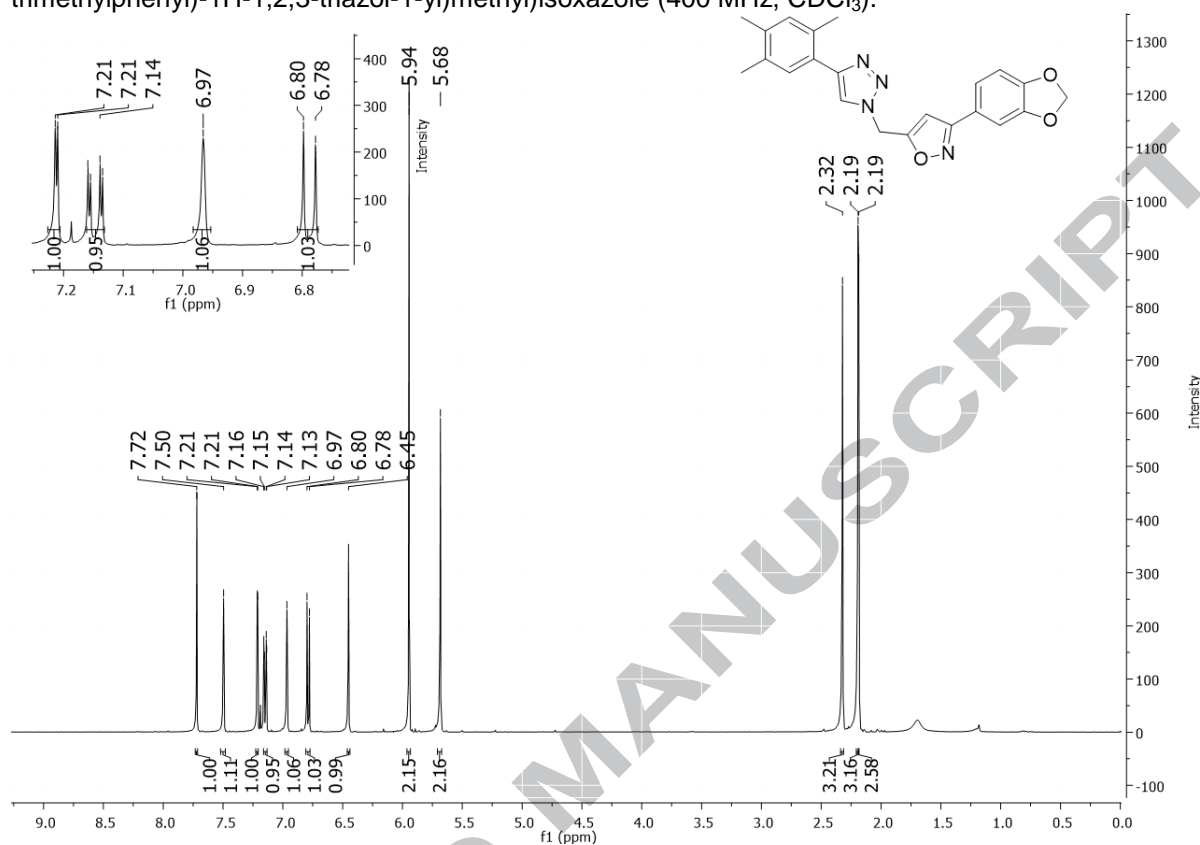


Fig. S43. $^{13}\text{C-NMR}$ spectrum of **compound 27**: 3-(benzo[d][1,3]dioxol-5-yl)-5-((4-(2,4,5-trimethylphenyl)-1H-1,2,3-triazol-1-yl)methyl)isoxazole (100 MHz, CDCl_3).

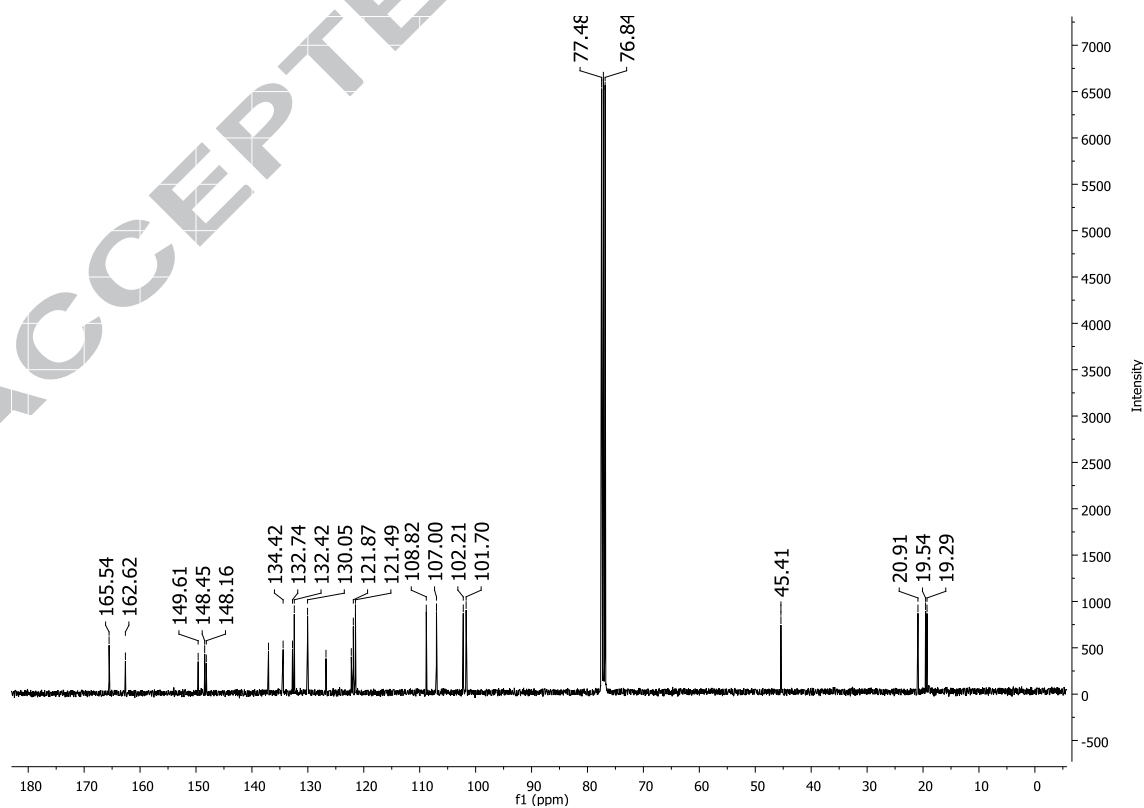


Fig. S44. $^1\text{H-NMR}$ spectrum of **compound 28**: 3-(benzo[d][1,3]dioxol-5-yl)-5-((4-(3,5-dimethoxyphenyl)-1H-1,2,3-triazol-1-yl)methyl)isoxazole (500 MHz, DMSO-d_6).

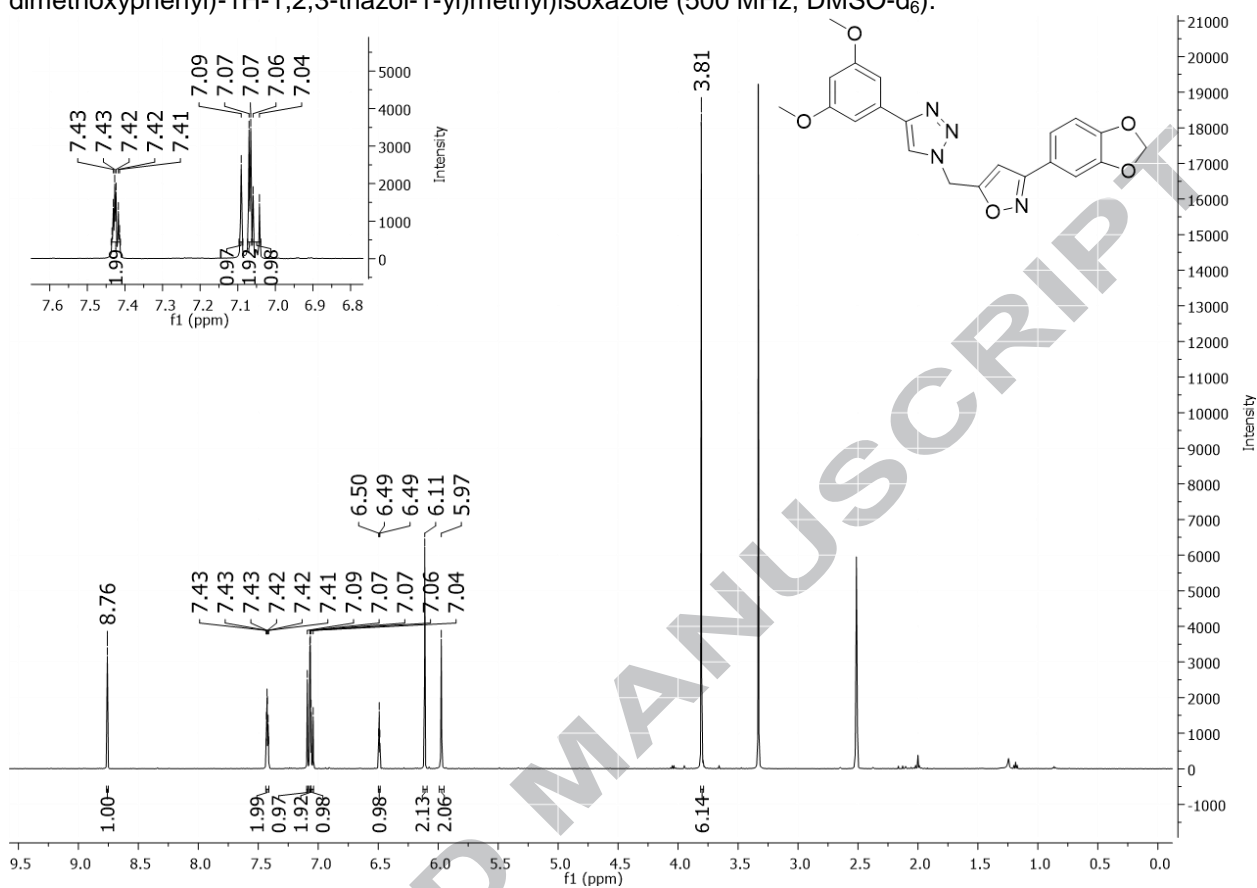


Fig. S45. $^{13}\text{C-NMR}$ spectrum of **compound 28**: 3-(benzo[d][1,3]dioxol-5-yl)-5-((4-(3,5-dimethoxyphenyl)-1H-1,2,3-triazol-1-yl)methyl)isoxazole (125 MHz, DMSO-d_6).

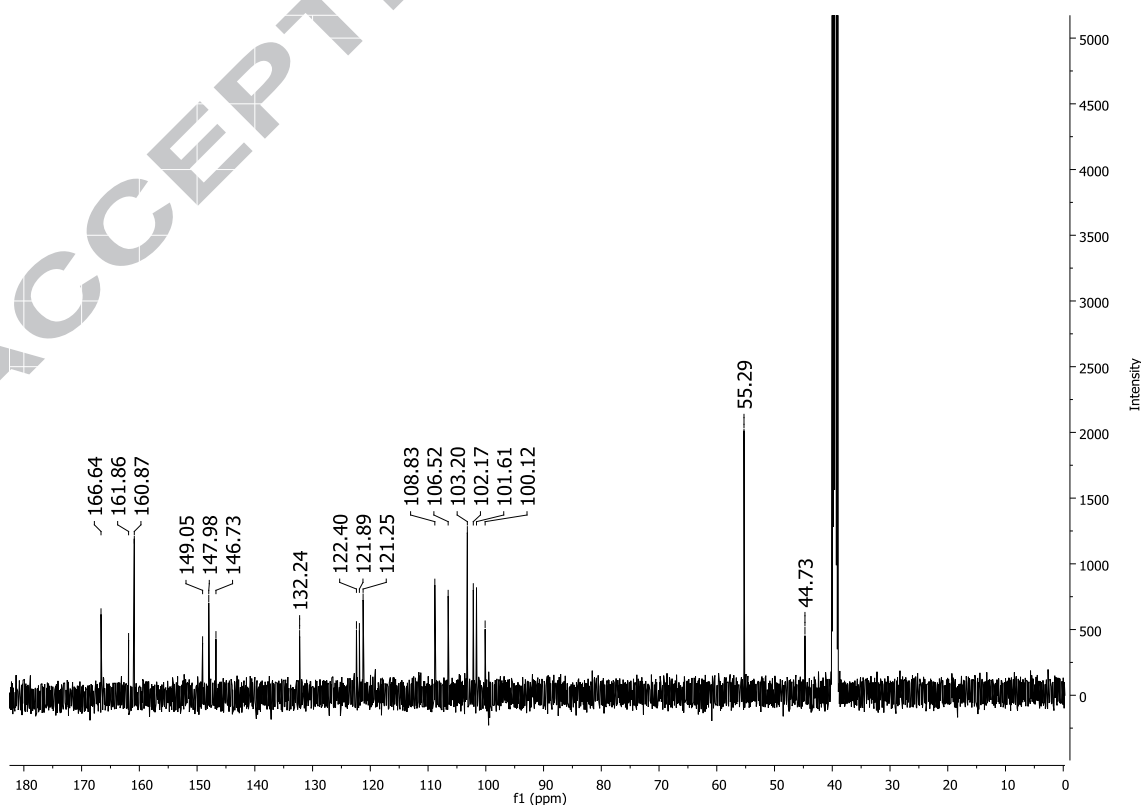


Fig. S46. $^1\text{H-NMR}$ spectrum of **compound 29**: 3-(3,4-dimethoxyphenyl)-5-((4-(4-methoxyphenyl)-1H-1,2,3-triazol-1-yl)methyl)isoxazole (400 MHz, CDCl_3).

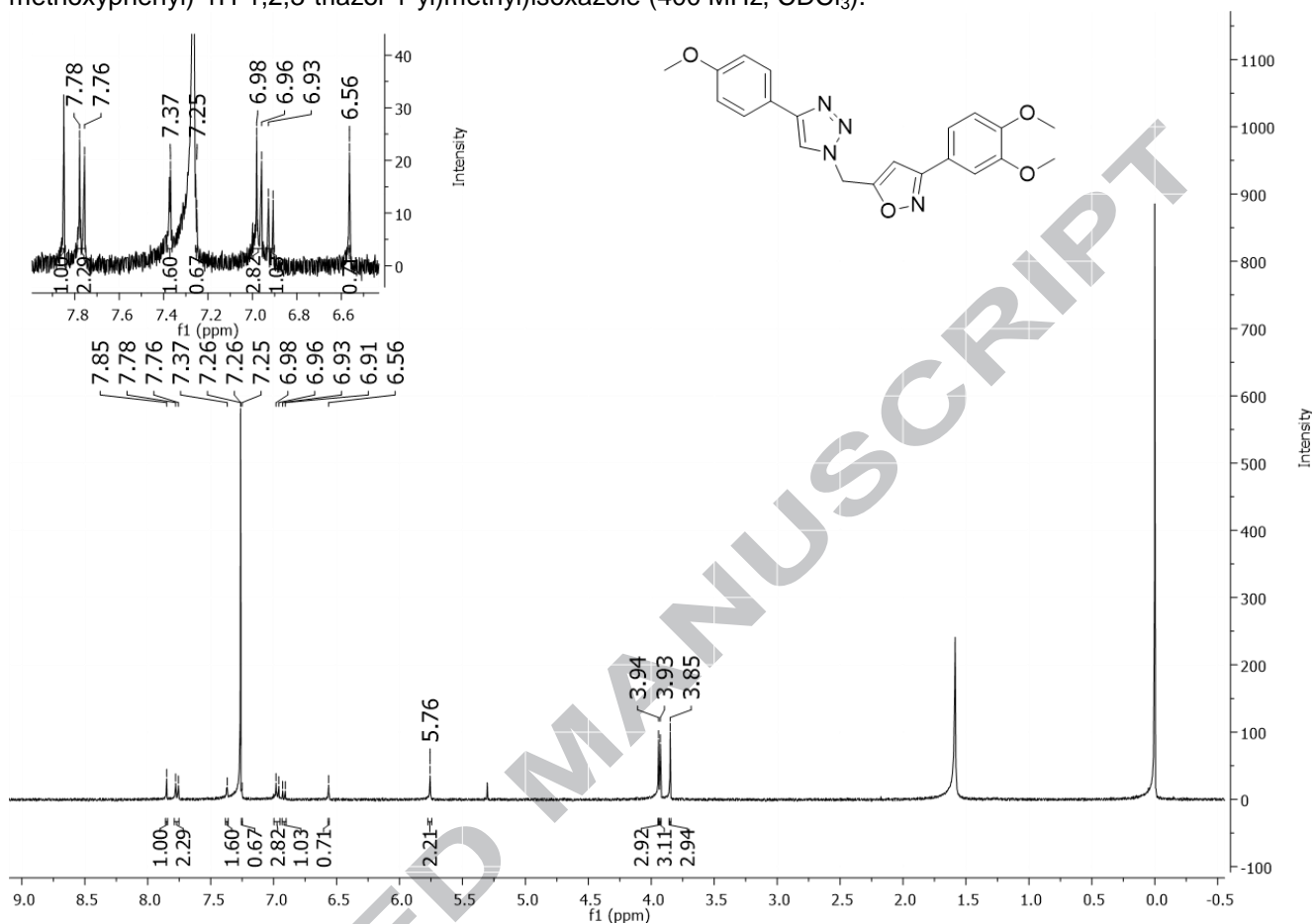


Fig. S47. $^{13}\text{C-NMR}$ spectrum of **compound 29**: 3-(3,4-dimethoxyphenyl)-5-((4-(4-methoxyphenyl)-1H-1,2,3-triazol-1-yl)methyl)isoxazole (100 MHz, CDCl_3).

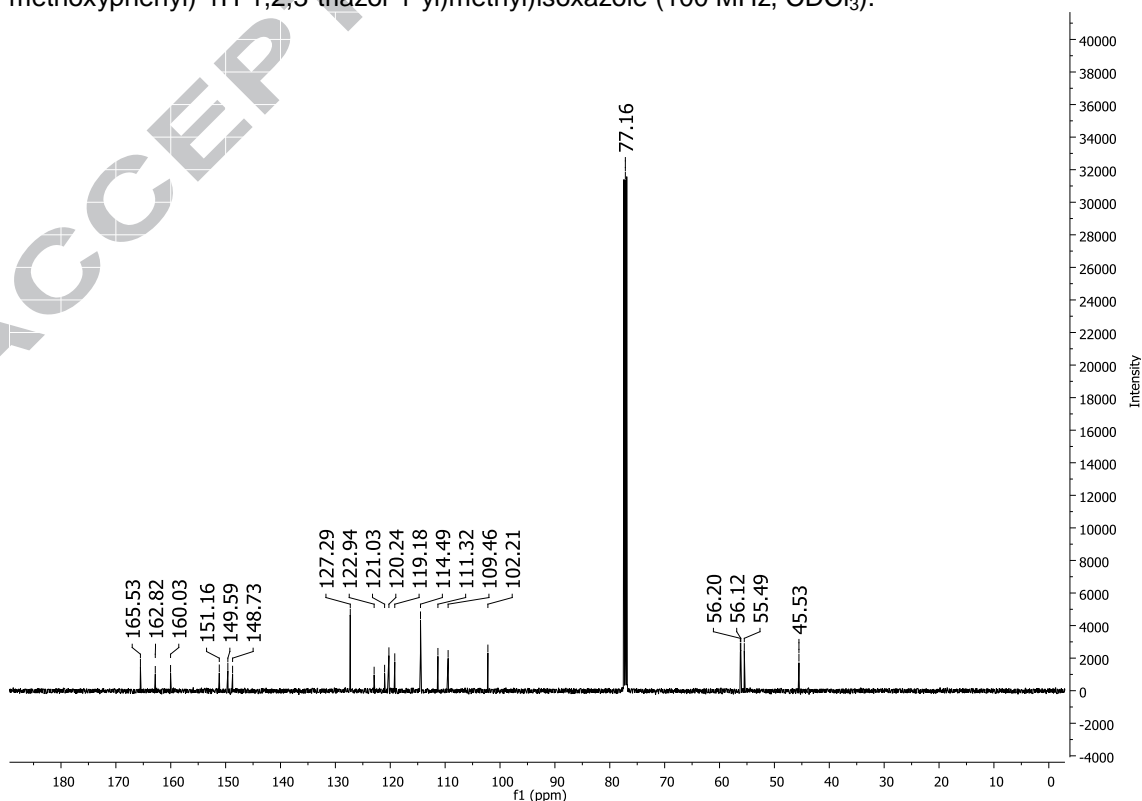


Fig. S48. $^1\text{H-NMR}$ spectrum of **compound 30**: 3-(3,4-dimethoxyphenyl)-5-((4-(4-(trifluoromethoxy)phenyl)-1H-1,2,3-triazol-1-yl)methyl)isoxazole (400 MHz, CDCl_3).

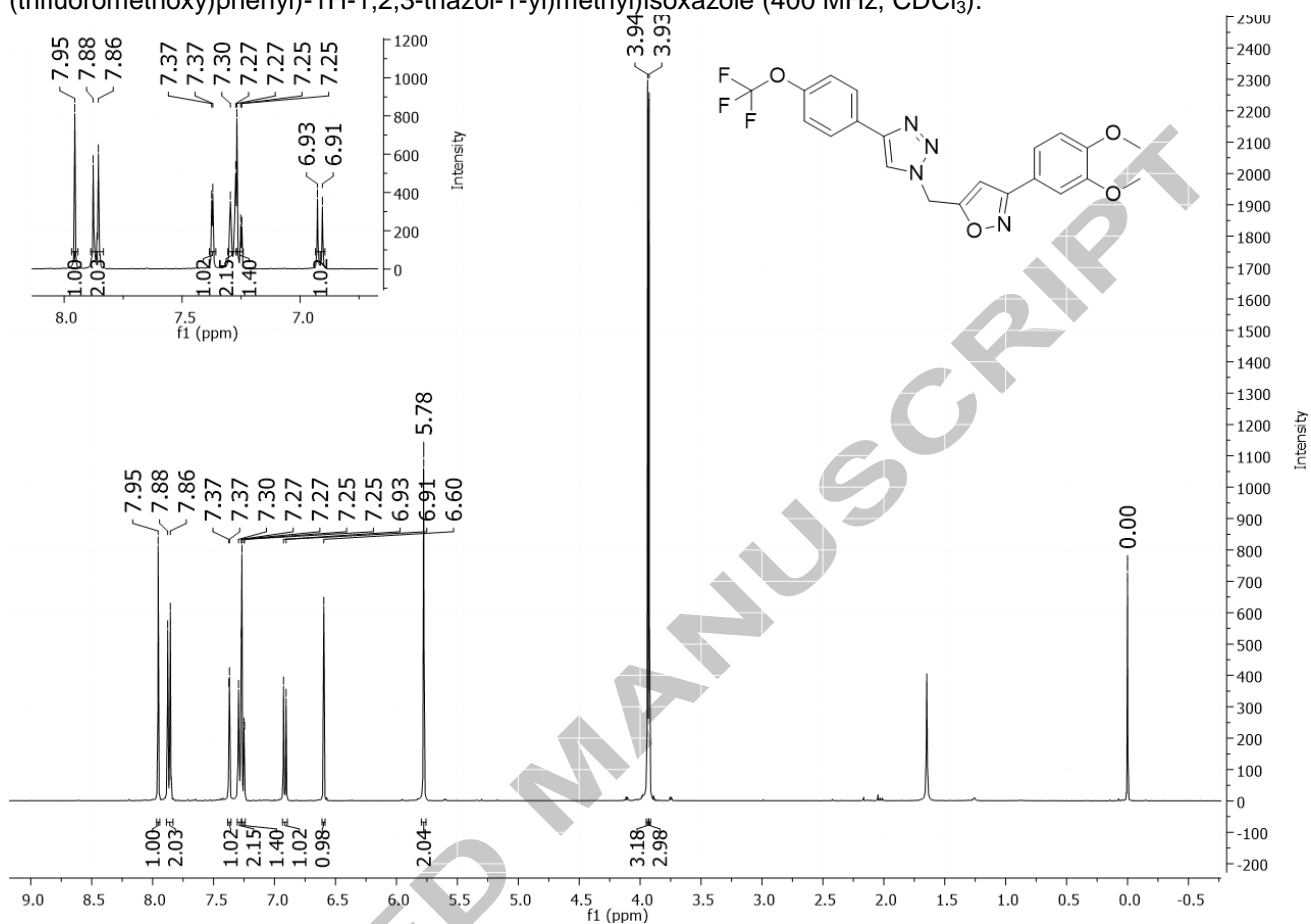


Fig. S49. $^{13}\text{C-NMR}$ spectrum of **compound 30**: 3-(3,4-dimethoxyphenyl)-5-((4-(4-(trifluoromethoxy)phenyl)-1H-1,2,3-triazol-1-yl)methyl)isoxazole (100 MHz, CDCl_3).

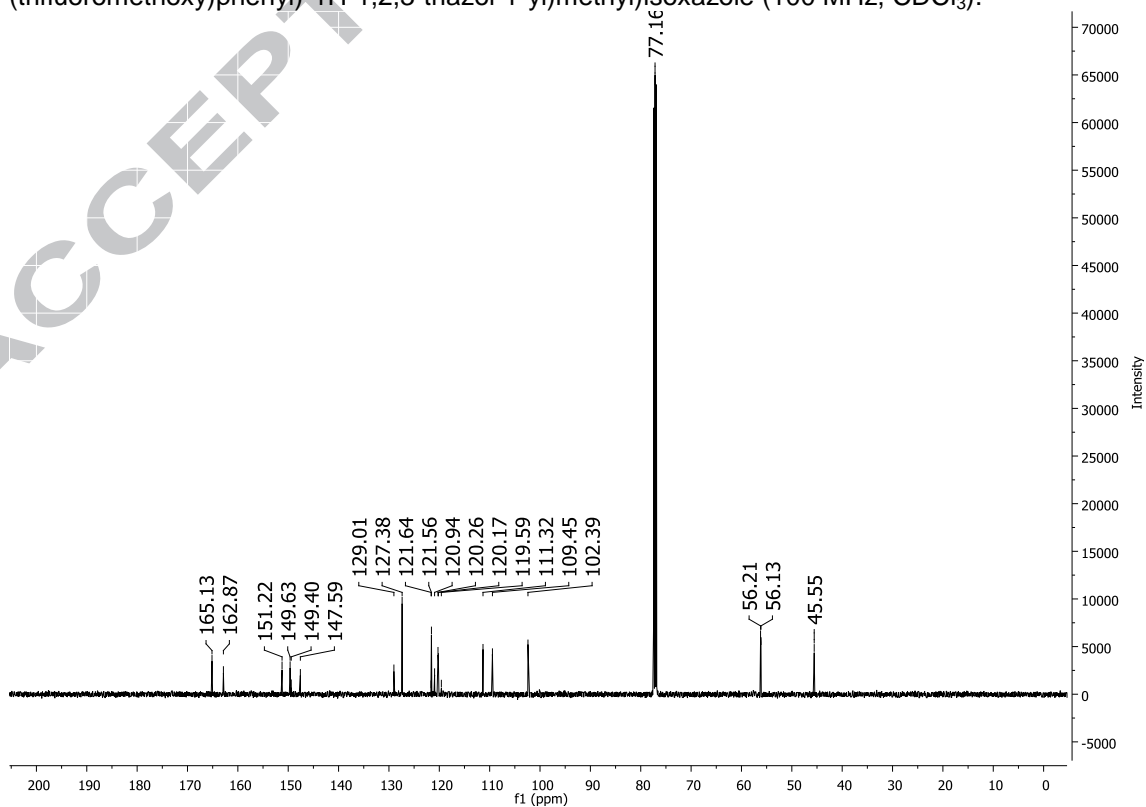


Fig. S50. $^1\text{H-NMR}$ spectrum of **compound 31**: 3-(3,4-dimethoxyphenyl)-5-((4-(4-pentylphenyl)-1H-1,2,3-triazol-1-yl)methyl)isoxazole (300 MHz, CDCl_3).

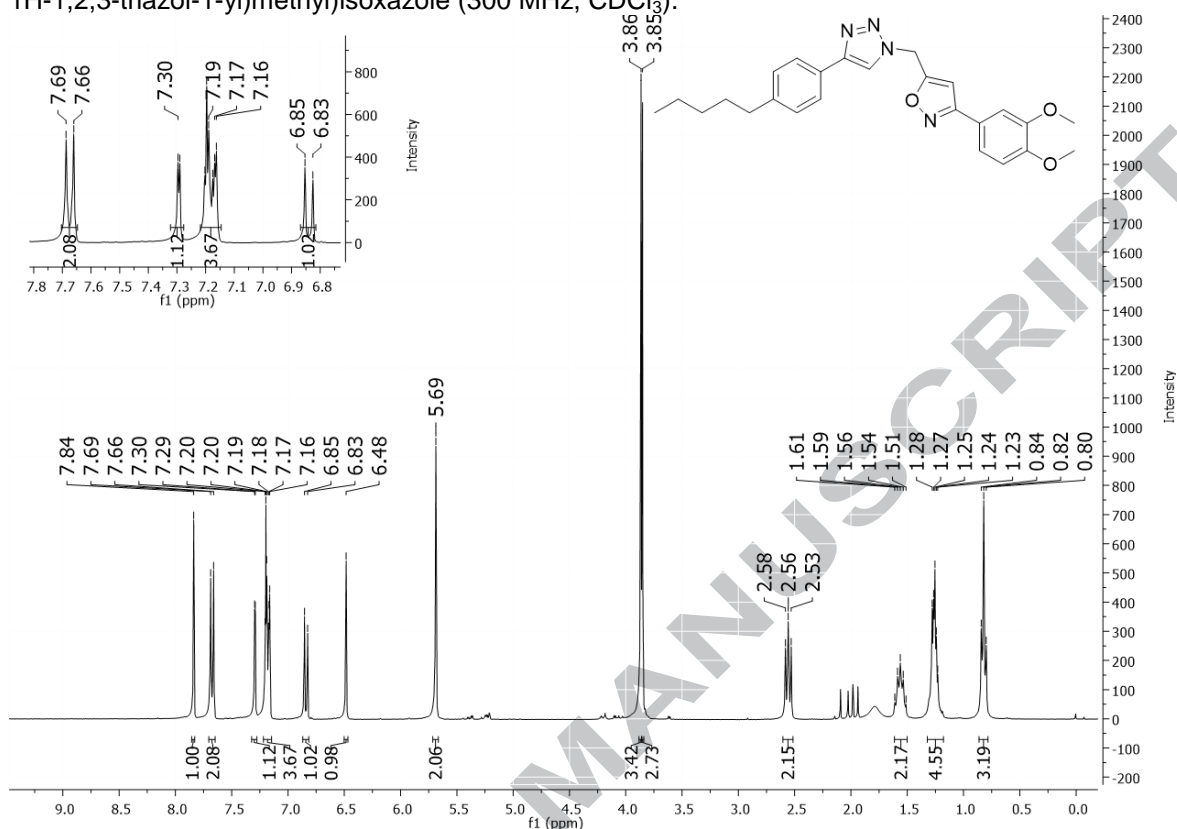


Fig. S51. $^{13}\text{C-NMR}$ spectrum of **compound 31**: 3-(3,4-dimethoxyphenyl)-5-((4-(4-pentylphenyl)-1H-1,2,3-triazol-1-yl)methyl)isoxazole (100 MHz, CDCl_3).

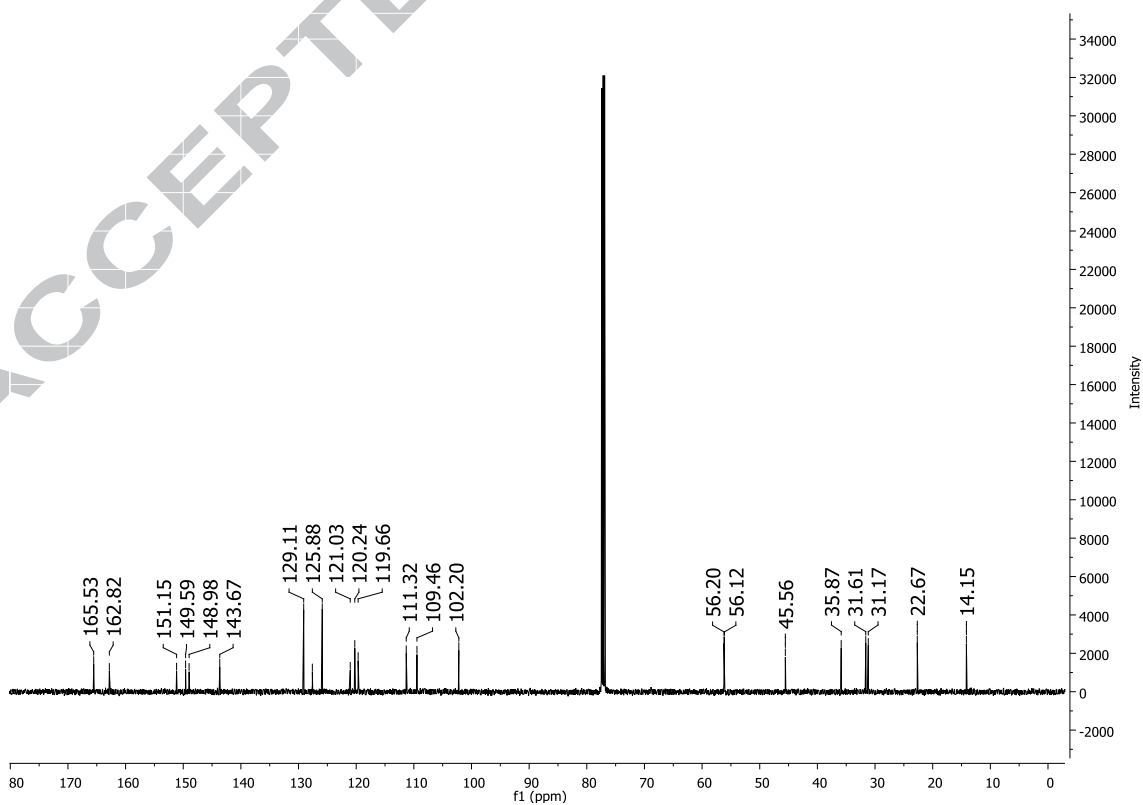


Fig. S56. $^1\text{H-NMR}$ spectrum of **compound 32**: 4-(1-((3-(3,4-dimethoxyphenyl)isoxazol-5-yl)methyl)-1H-1,2,3-triazol-4-yl)aniline (300 MHz, CDCl_3).

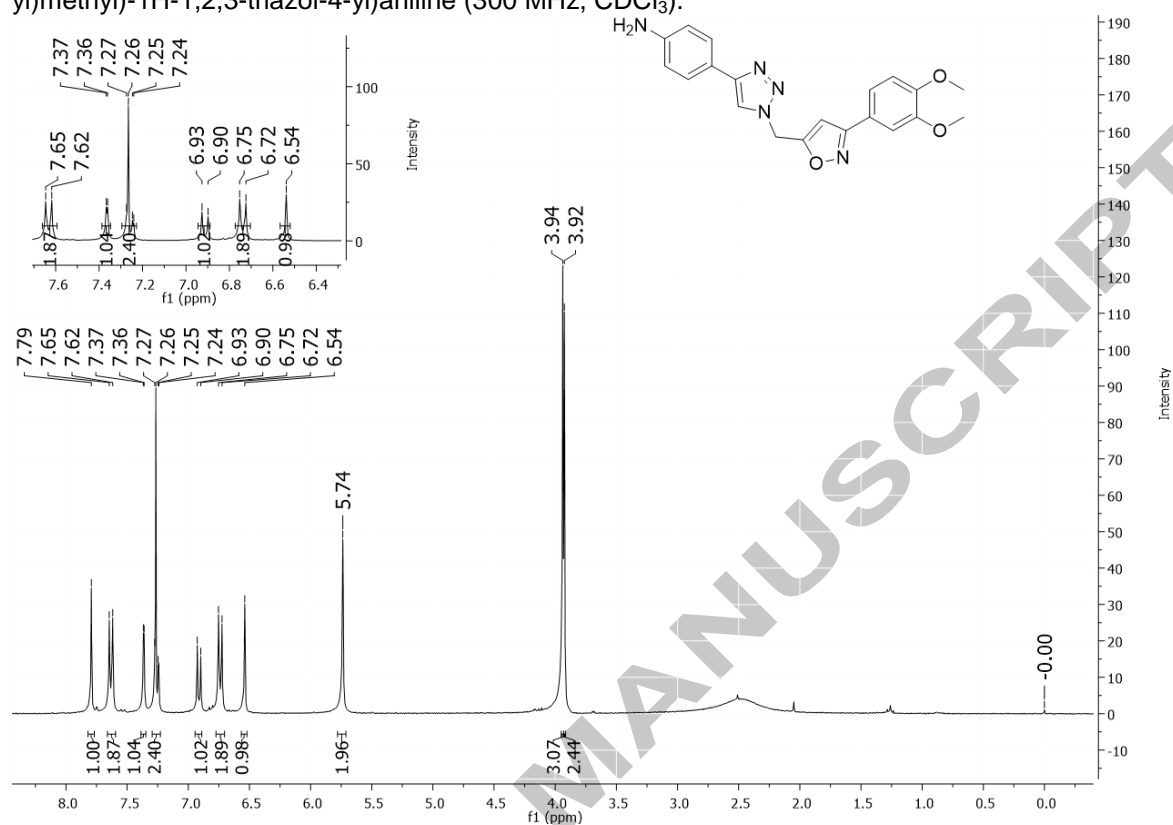


Fig. S57. $^{13}\text{C-NMR}$ spectrum of **compound 32**: 4-(1-((3-(3,4-dimethoxyphenyl)isoxazol-5-yl)methyl)-1H-1,2,3-triazol-4-yl)aniline (100 MHz, CDCl_3).

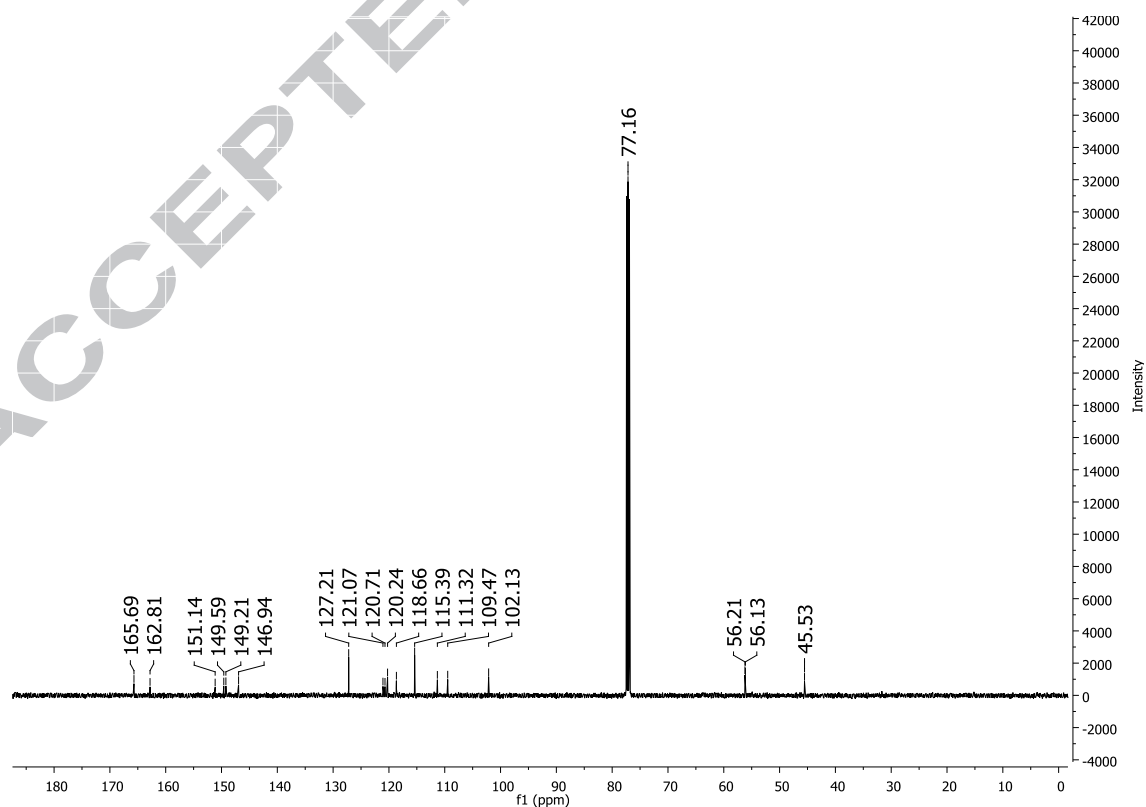


Fig. S58. $^1\text{H-NMR}$ spectrum of **compound 33**: (4-(1-((3-(3,4-dimethoxyphenyl)isoxazol-5-yl)methyl)-1H-1,2,3-triazol-4-yl)phenyl)methanol (400 MHz, CDCl_3).

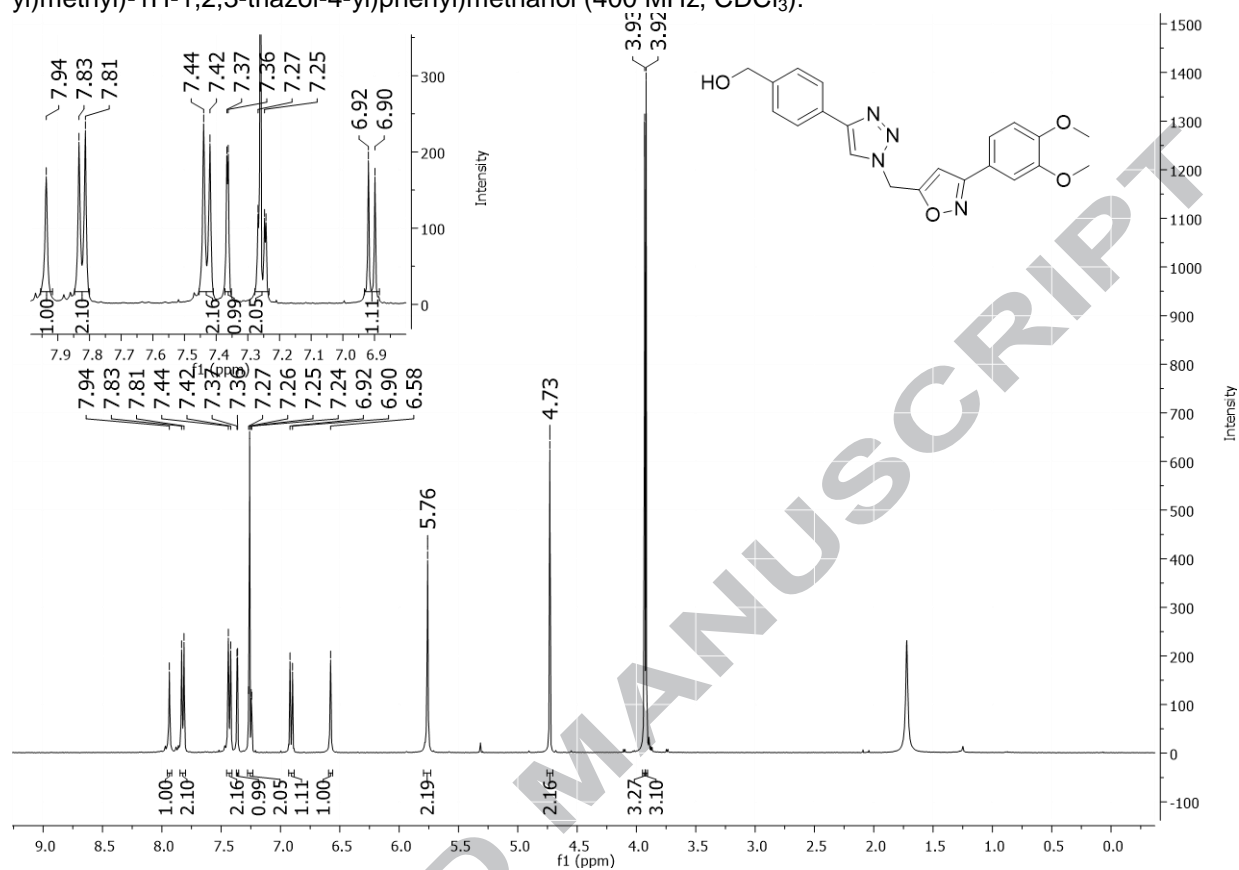


Fig. S59. $^{13}\text{C-NMR}$ spectrum of **compound 33**: (4-(1-((3-(3,4-dimethoxyphenyl)isoxazol-5-yl)methyl)-1H-1,2,3-triazol-4-yl)phenyl)methanol (100 MHz, CDCl_3).

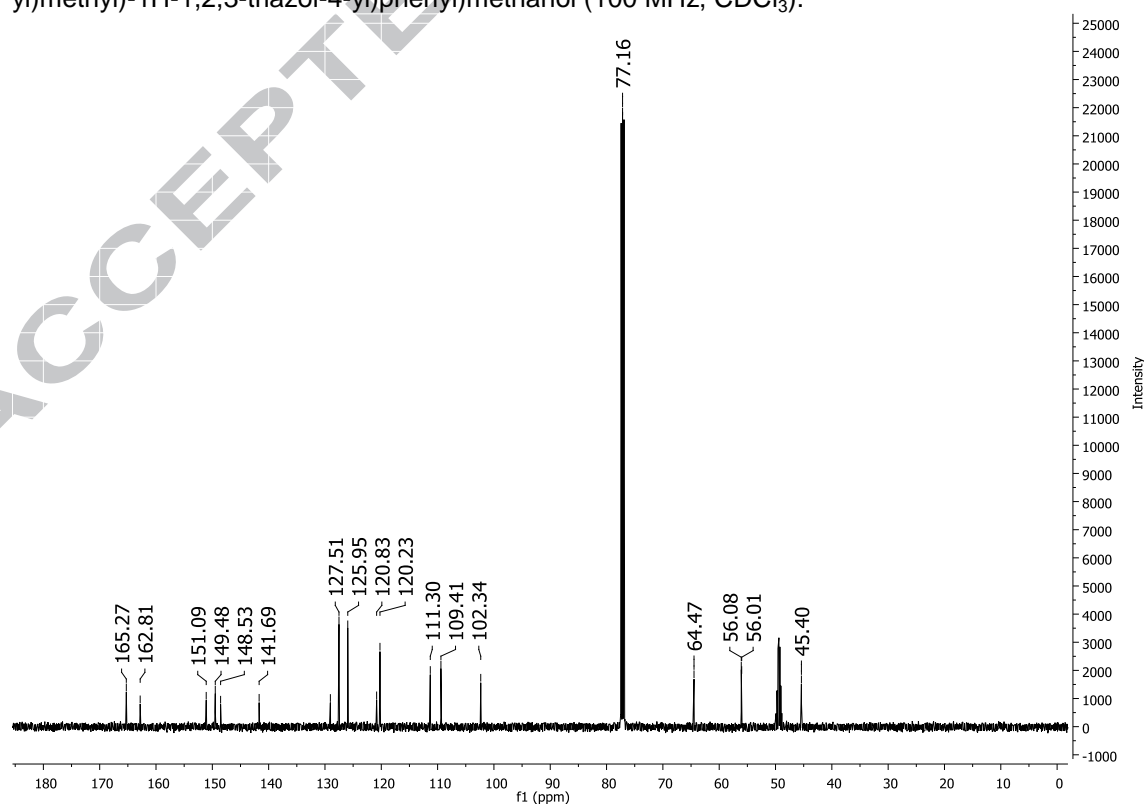


Fig. S60. $^1\text{H-NMR}$ spectrum of **compound 34**: 3-(3,4-dimethoxyphenyl)-5-((4-phenyl-1H-1,2,3-triazol-1-yl)methyl)isoxazole (400 MHz, CDCl_3).

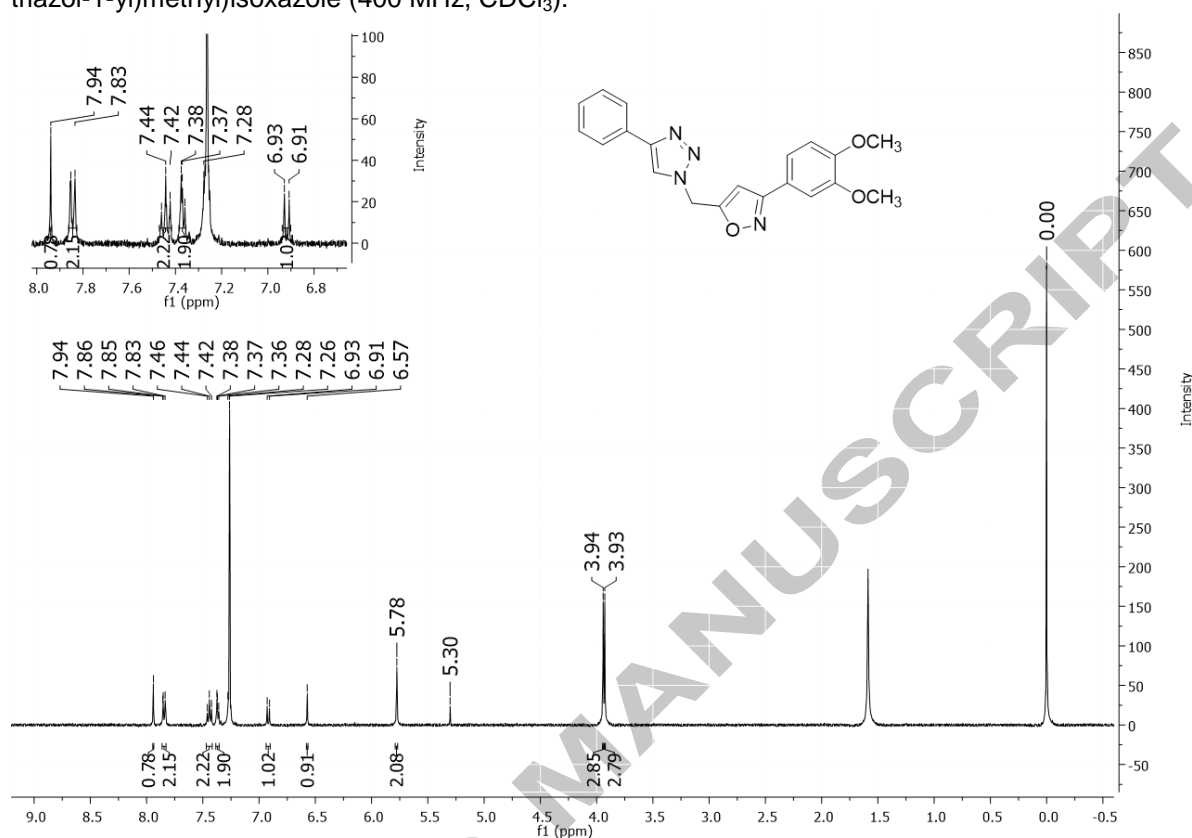


Fig. S61. $^{13}\text{C-NMR}$ spectrum of **compound 34**: 3-(3,4-dimethoxyphenyl)-5-((4-phenyl-1H-1,2,3-triazol-1-yl)methyl)isoxazole (100 MHz, CDCl_3).

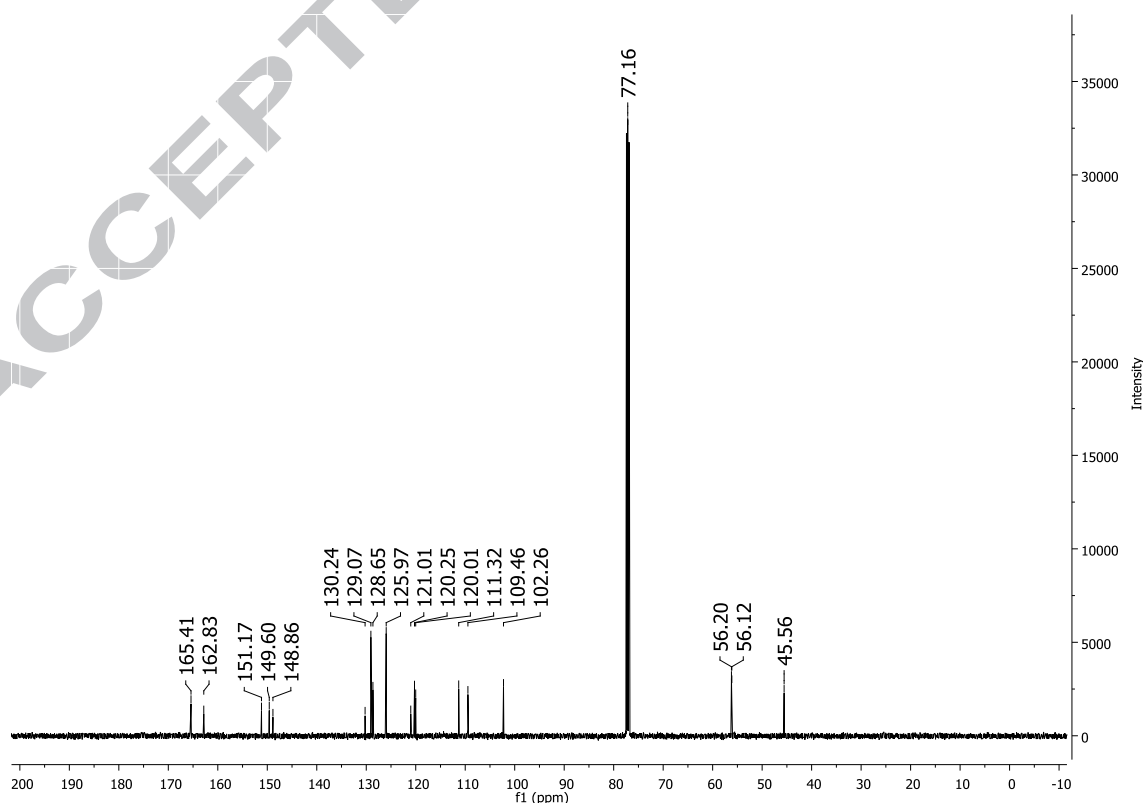


Fig. S62. $^1\text{H-NMR}$ spectrum of **compound 35**: 3-(3,4-dimethoxyphenyl)-5-((4-(p-tolyl)-1H-1,2,3-triazol-1-yl)methyl)isoxazole (400 MHz, CDCl_3).

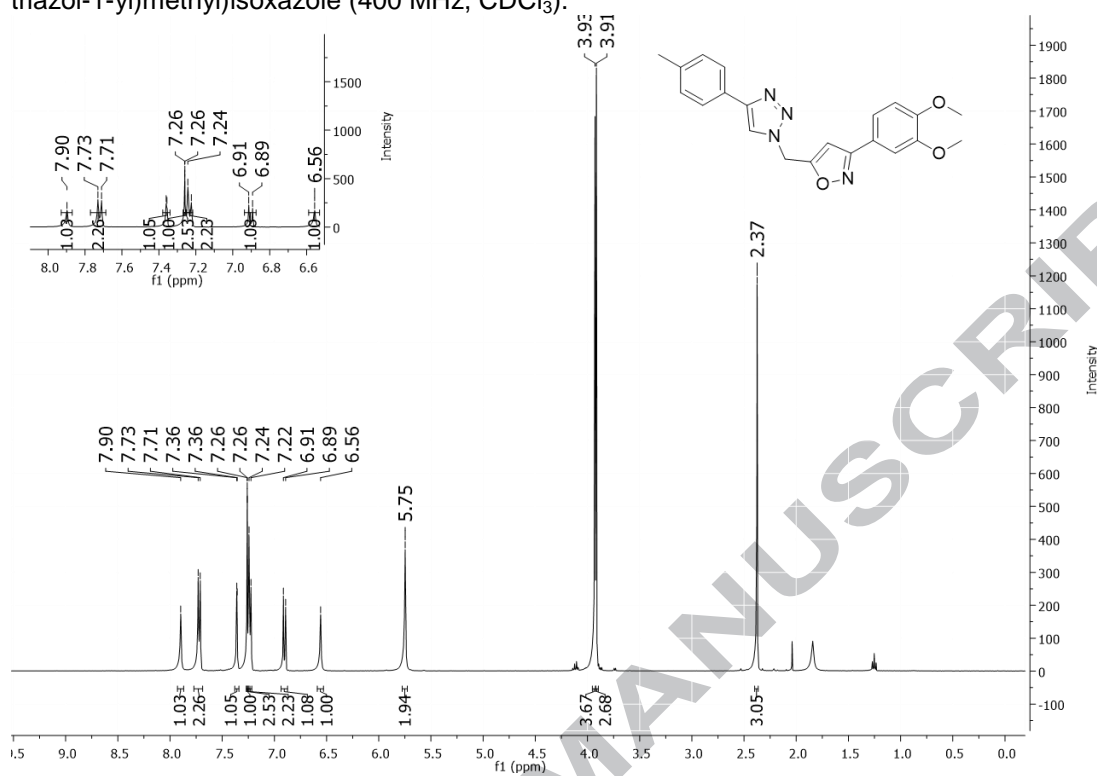


Fig. S63. $^{13}\text{C-NMR}$ spectrum of **compound 35**: 3-(3,4-dimethoxyphenyl)-5-((4-(p-tolyl)-1H-1,2,3-triazol-1-yl)methyl)isoxazole (100 MHz, CDCl_3).

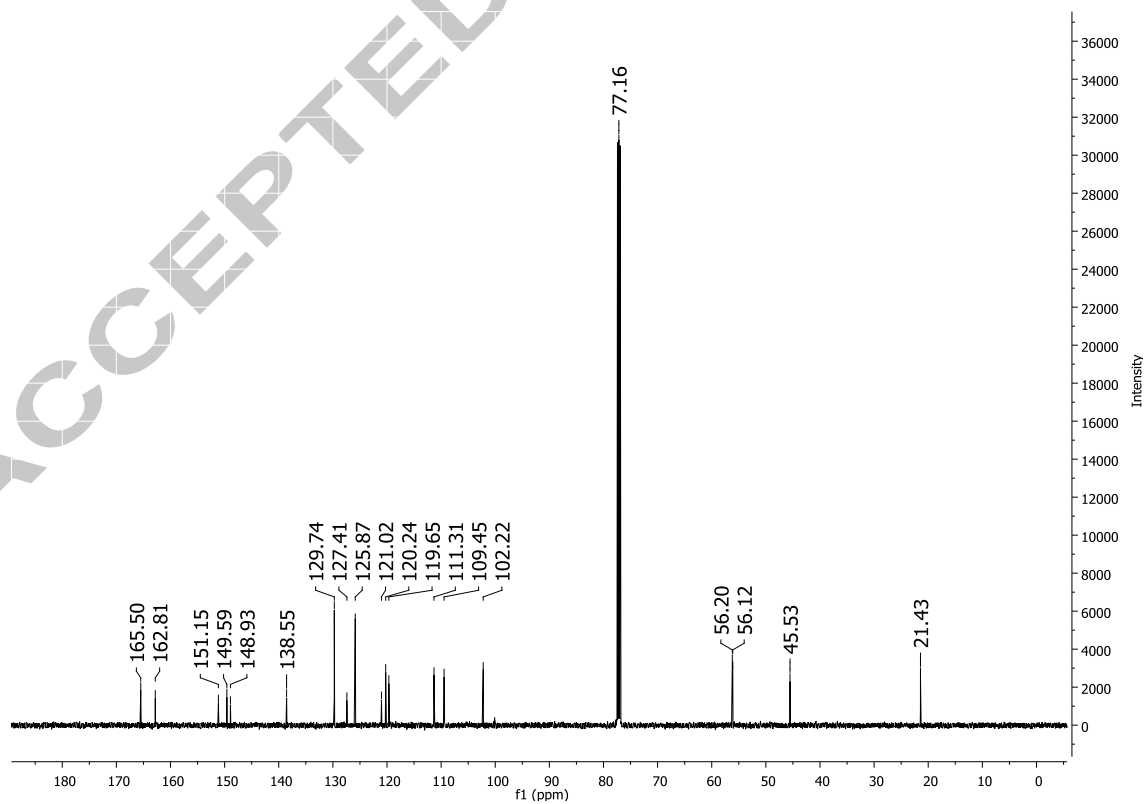


Fig. S64. $^1\text{H-NMR}$ spectrum of **compound 36**: 3-(3,4-dimethoxyphenyl)-5-((4-(2-methoxyphenyl)-1H-1,2,3-triazol-1-yl)methyl)isoxazole (400 MHz, CDCl_3).

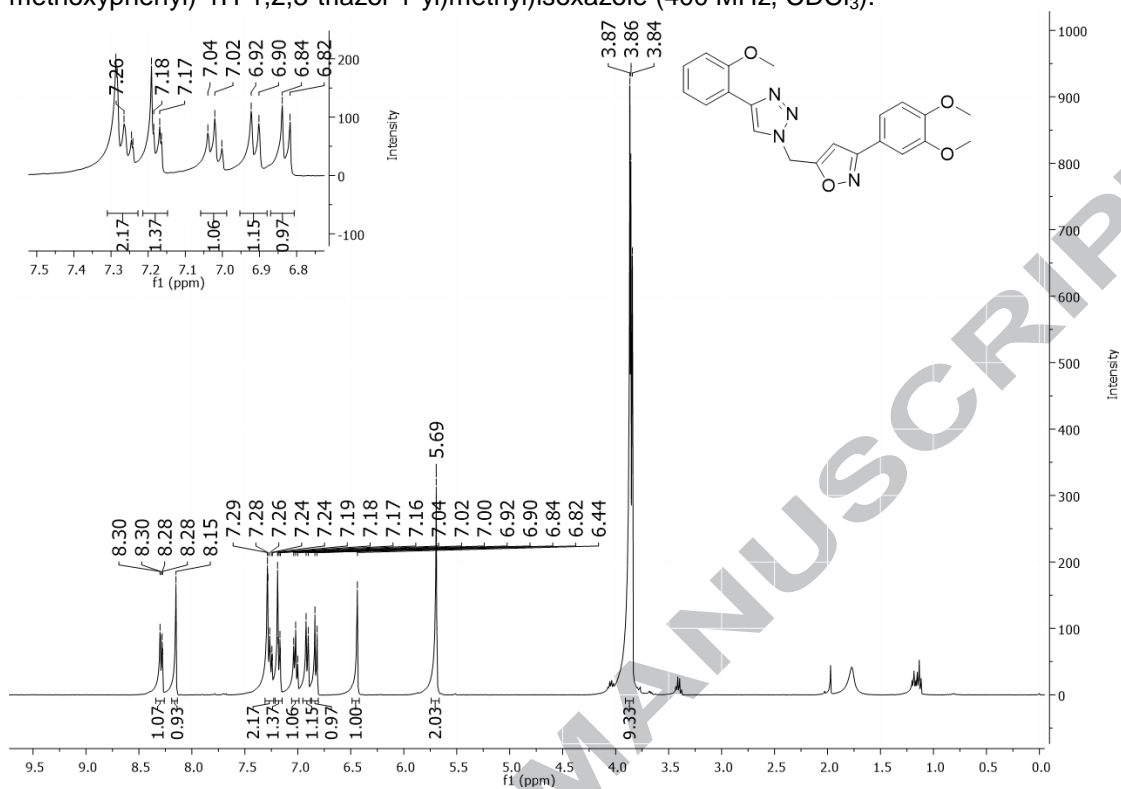


Fig. S65. $^{13}\text{C-NMR}$ spectrum of **compound 36**: 3-(3,4-dimethoxyphenyl)-5-((4-(2-methoxyphenyl)-1H-1,2,3-triazol-1-yl)methyl)isoxazole (100 MHz, CDCl_3).

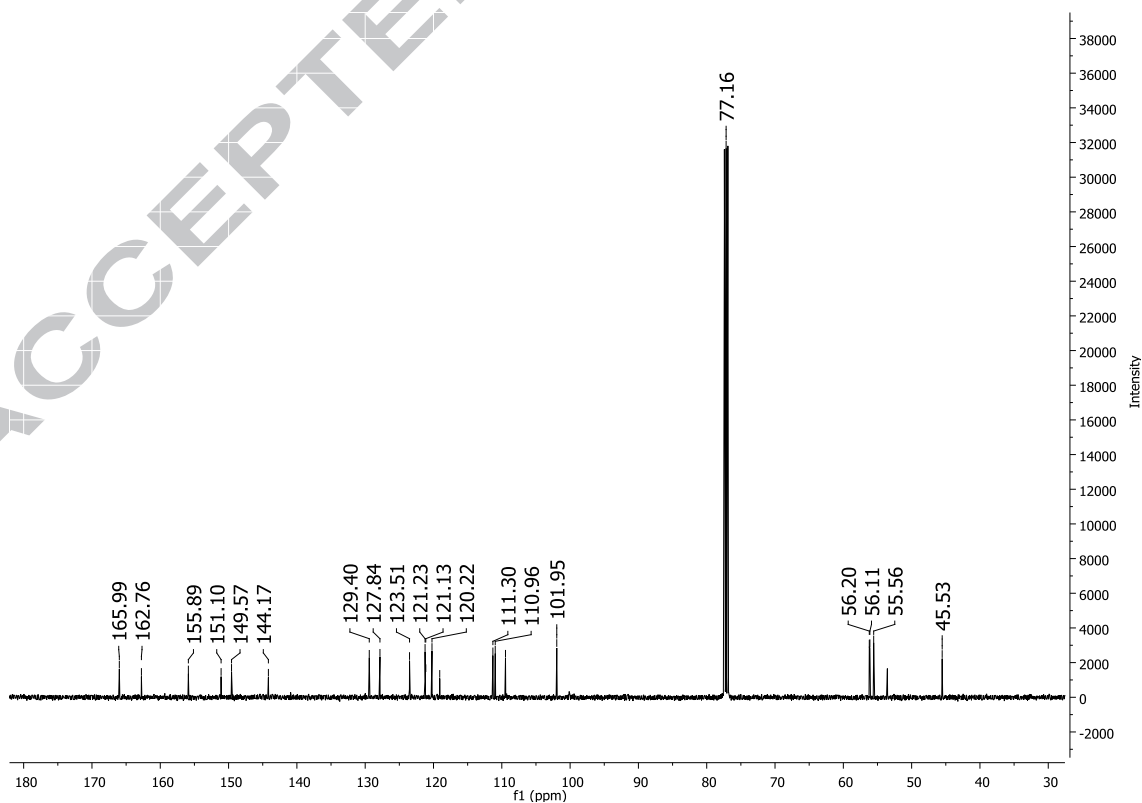


Fig. S66. $^1\text{H-NMR}$ spectrum of **compound 37**: 3-(3,4-dimethoxyphenyl)-5-((4-(4-methoxy-2-methylphenyl)-1H-1,2,3-triazol-1-yl)methyl)isoxazole (400 MHz, CDCl_3).

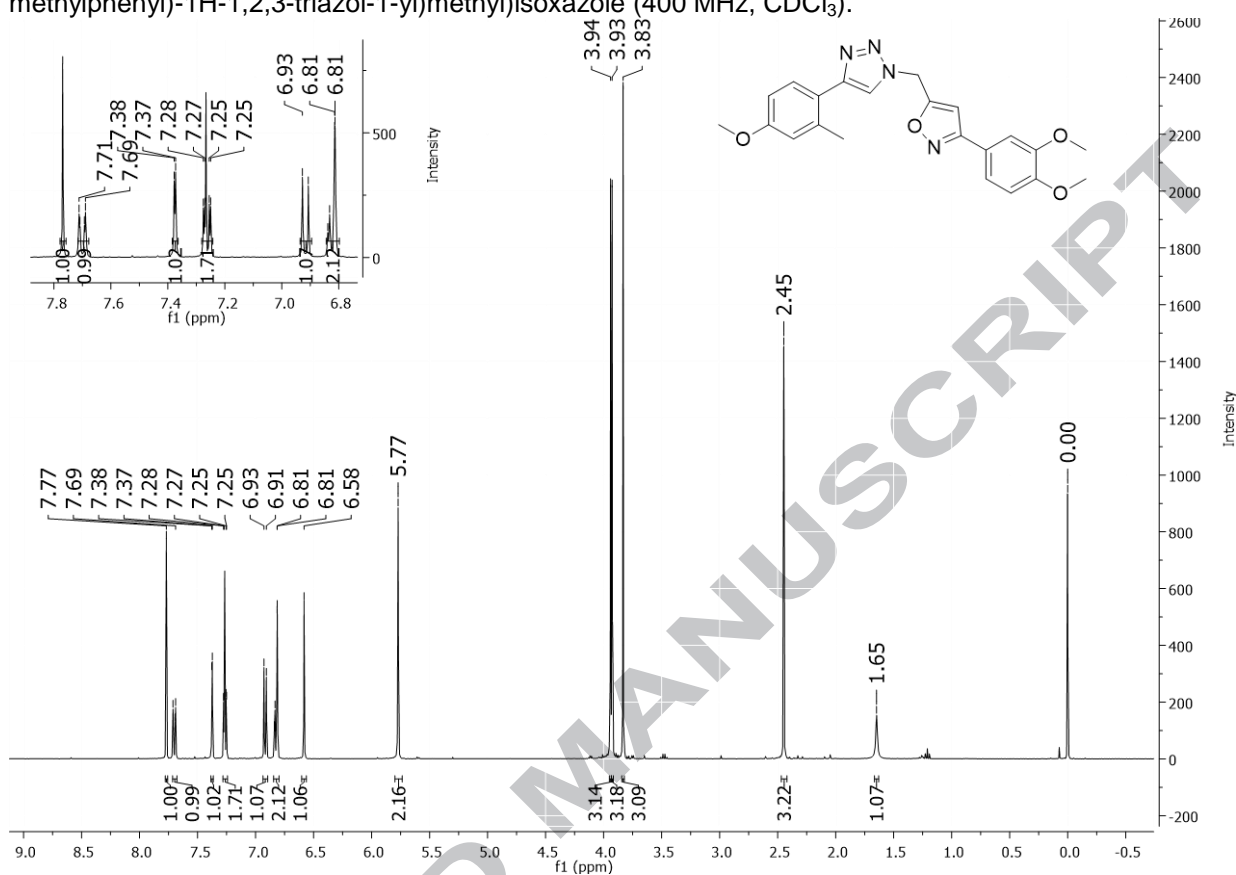


Fig. S67. $^{13}\text{C-NMR}$ spectrum of **compound 37**: 3-(3,4-dimethoxyphenyl)-5-((4-(4-methoxy-2-methylphenyl)-1H-1,2,3-triazol-1-yl)methyl)isoxazole (100 MHz, CDCl_3).

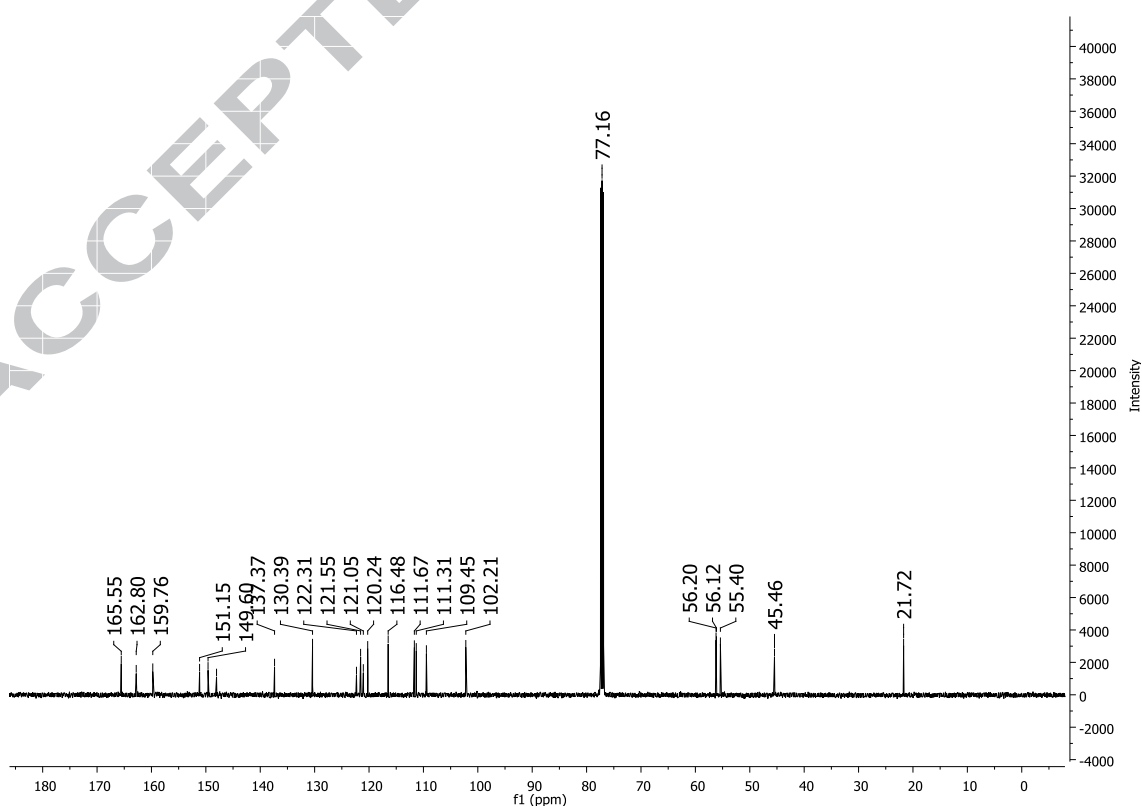


Fig. S68. $^1\text{H-NMR}$ spectrum of **compound 38**: 3-(3,4-dimethoxyphenyl)-5-((4-(2,5-dimethylphenyl)-1H-1,2,3-triazol-1-yl)methyl)isoxazole (300 MHz, CDCl_3).

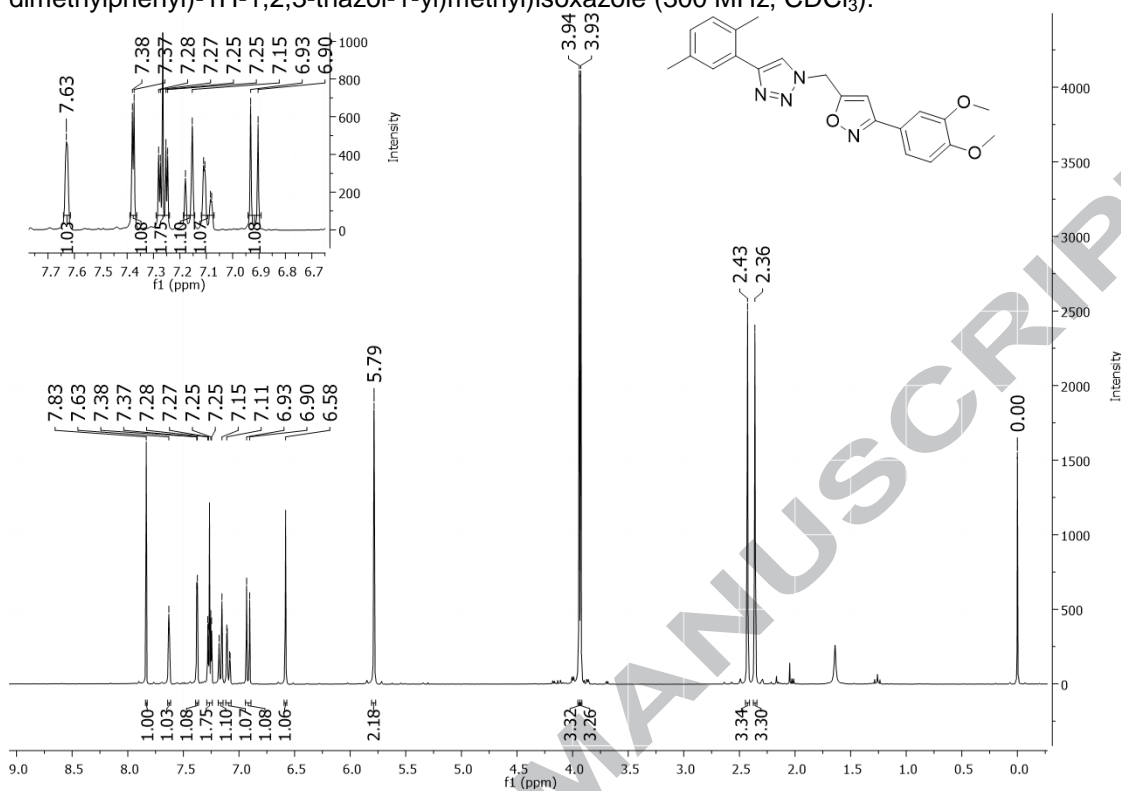


Fig. S69. $^{13}\text{C-NMR}$ spectrum of **compound 38**: 3-(3,4-dimethoxyphenyl)-5-((4-(2,5-dimethylphenyl)-1H-1,2,3-triazol-1-yl)methyl)isoxazole (100 MHz, CDCl_3).

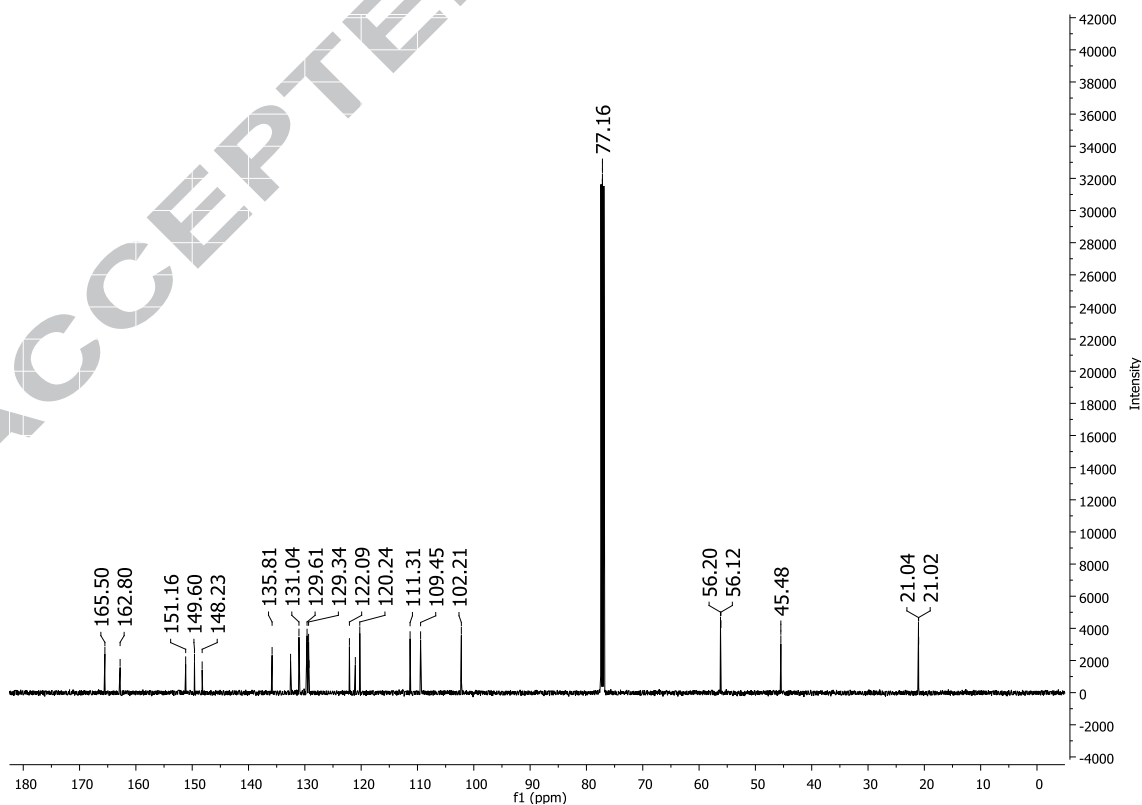


Fig. S70. $^1\text{H-NMR}$ spectrum of **compound 39**: 3-(3,4-dimethoxyphenyl)-5-((4-(4-nitrophenyl)-1H-1,2,3-triazol-1-yl)methyl)isoxazole (300 MHz, CDCl_3).

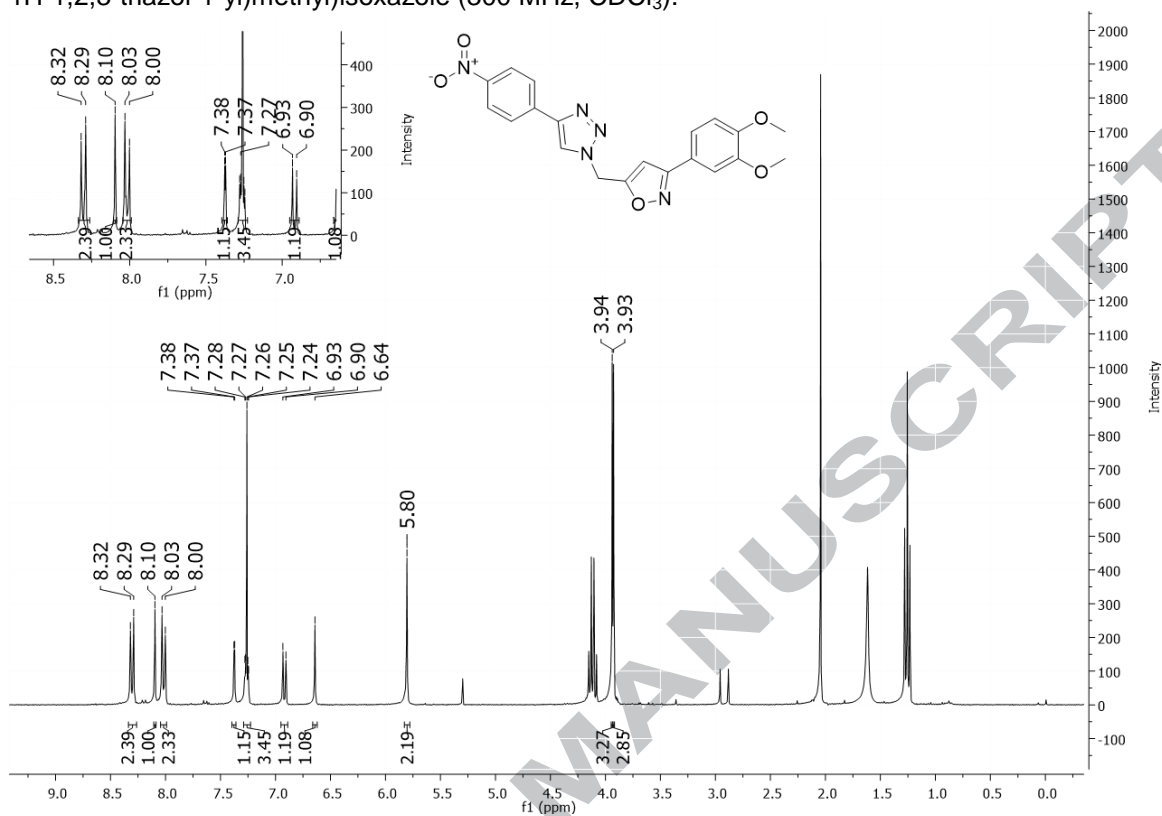


Fig. S71. $^{13}\text{C-NMR}$ spectrum of **compound 39**: 3-(3,4-dimethoxyphenyl)-5-((4-(4-nitrophenyl)-1H-1,2,3-triazol-1-yl)methyl)isoxazole (100 MHz, CDCl_3).

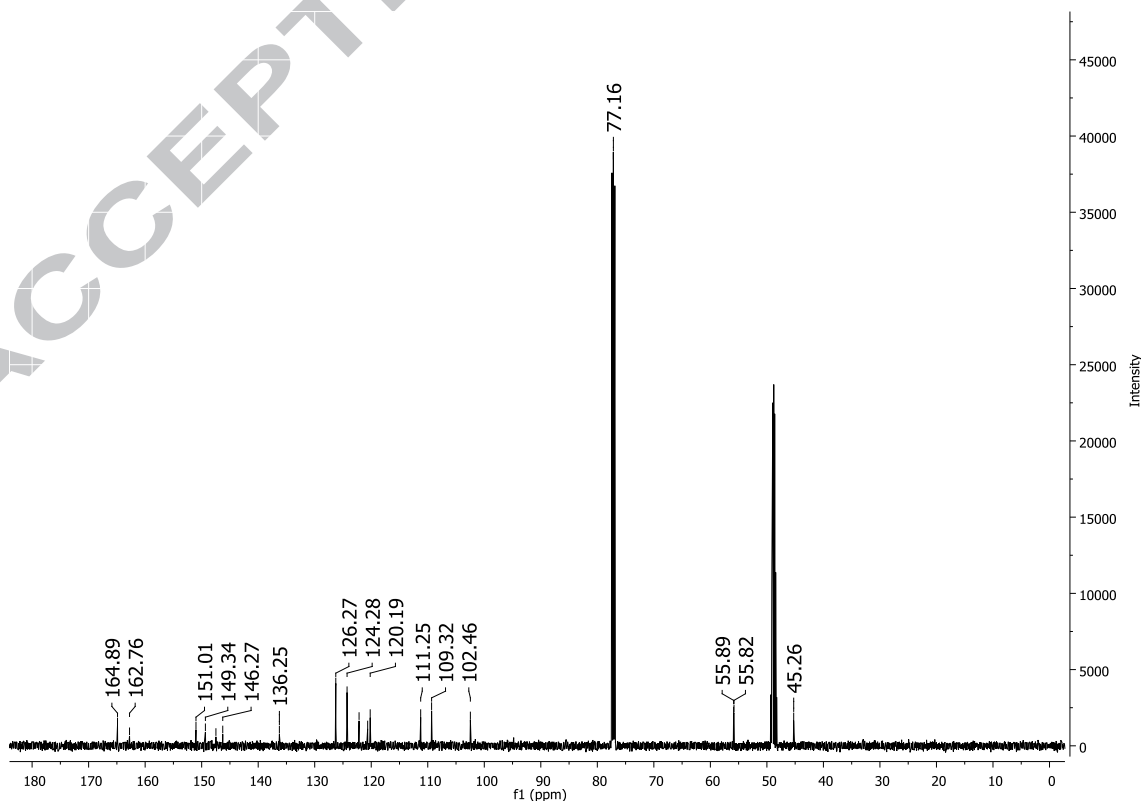


Fig. S72. $^1\text{H-NMR}$ spectrum of **compound 40**: 3-(3,4-dimethoxyphenyl)-5-((4-(4-fluorophenyl)-1H-1,2,3-triazol-1-yl)methyl)isoxazole (300 MHz, CDCl_3).

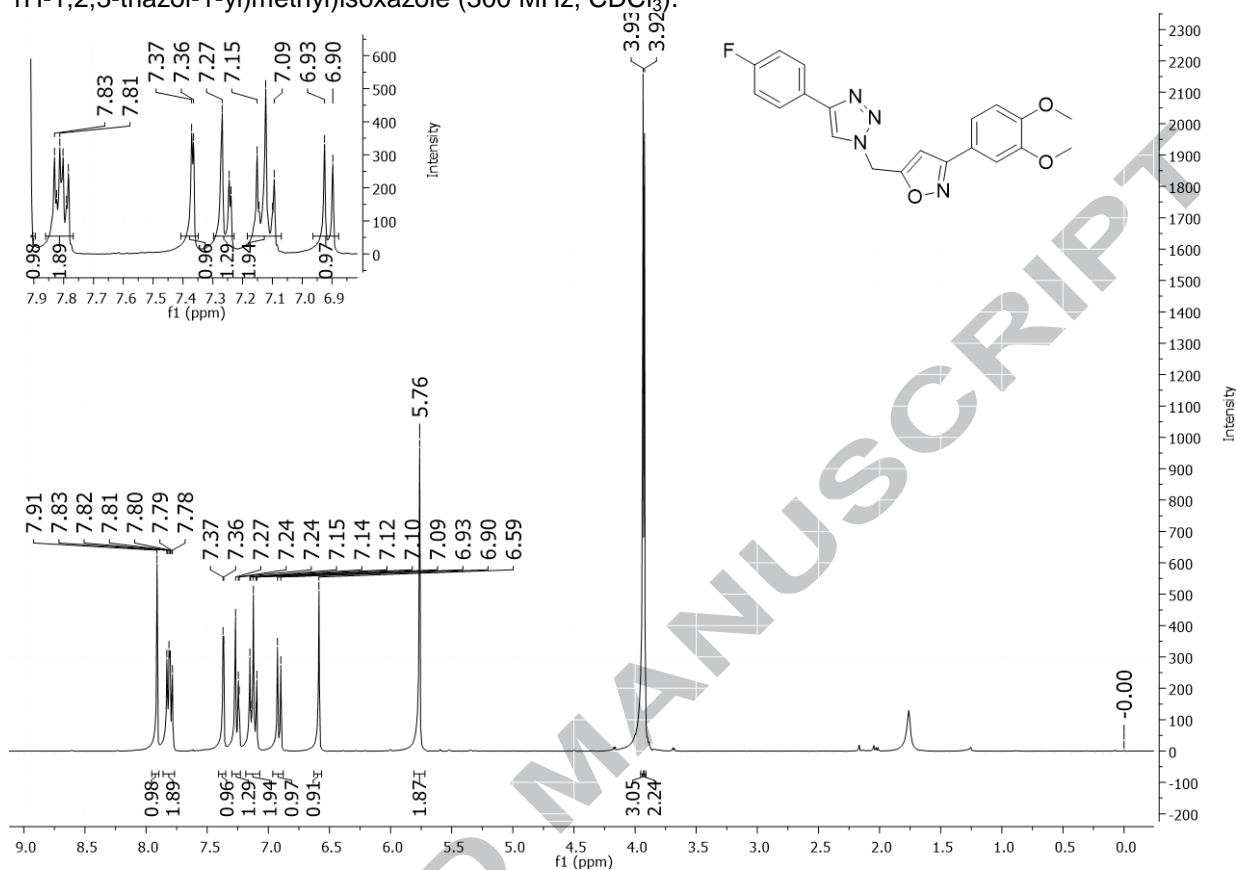


Fig. S73. $^{13}\text{C-NMR}$ spectrum of **compound 40**: 3-(3,4-dimethoxyphenyl)-5-((4-(4-fluorophenyl)-1H-1,2,3-triazol-1-yl)methyl)isoxazole (125 MHz, CDCl_3).

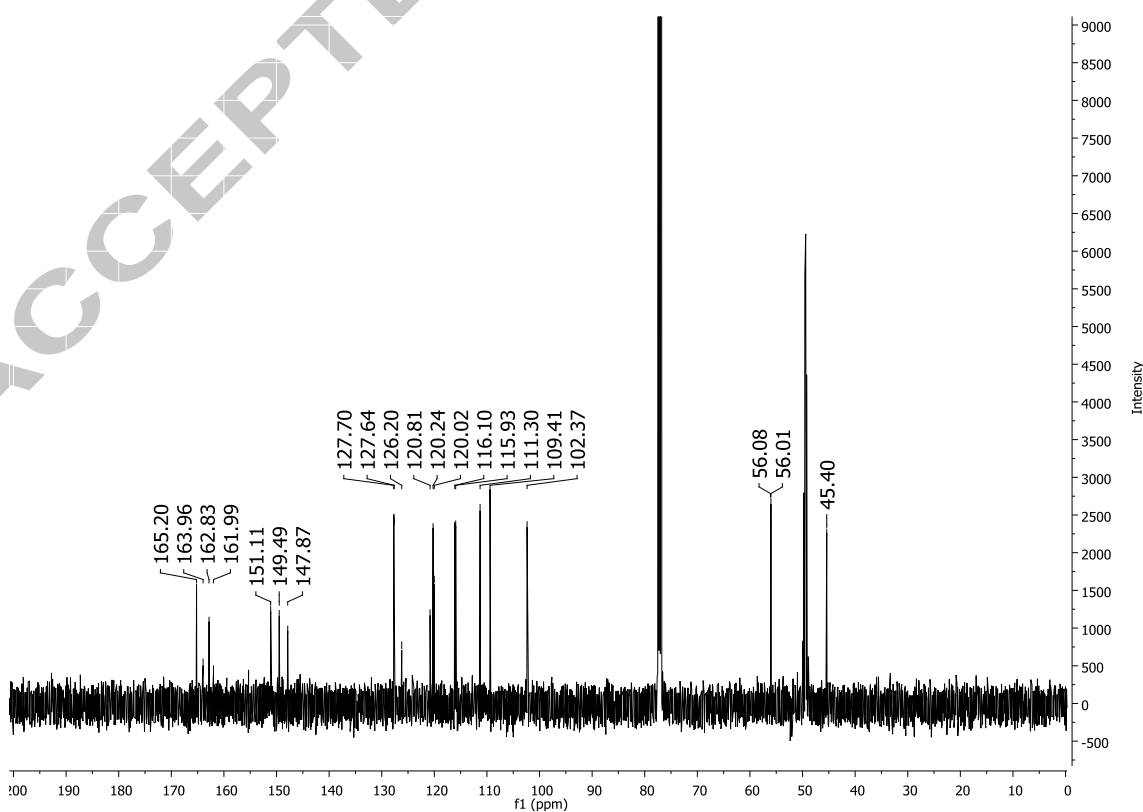


Fig. S74. $^1\text{H-NMR}$ spectrum of **compound 41**: 4-(1-((3-(3,4-dimethoxyphenyl)isoxazol-5-yl)methyl)-1H-1,2,3-triazol-4-yl)-N,N-dimethylaniline (300 MHz, CDCl_3).

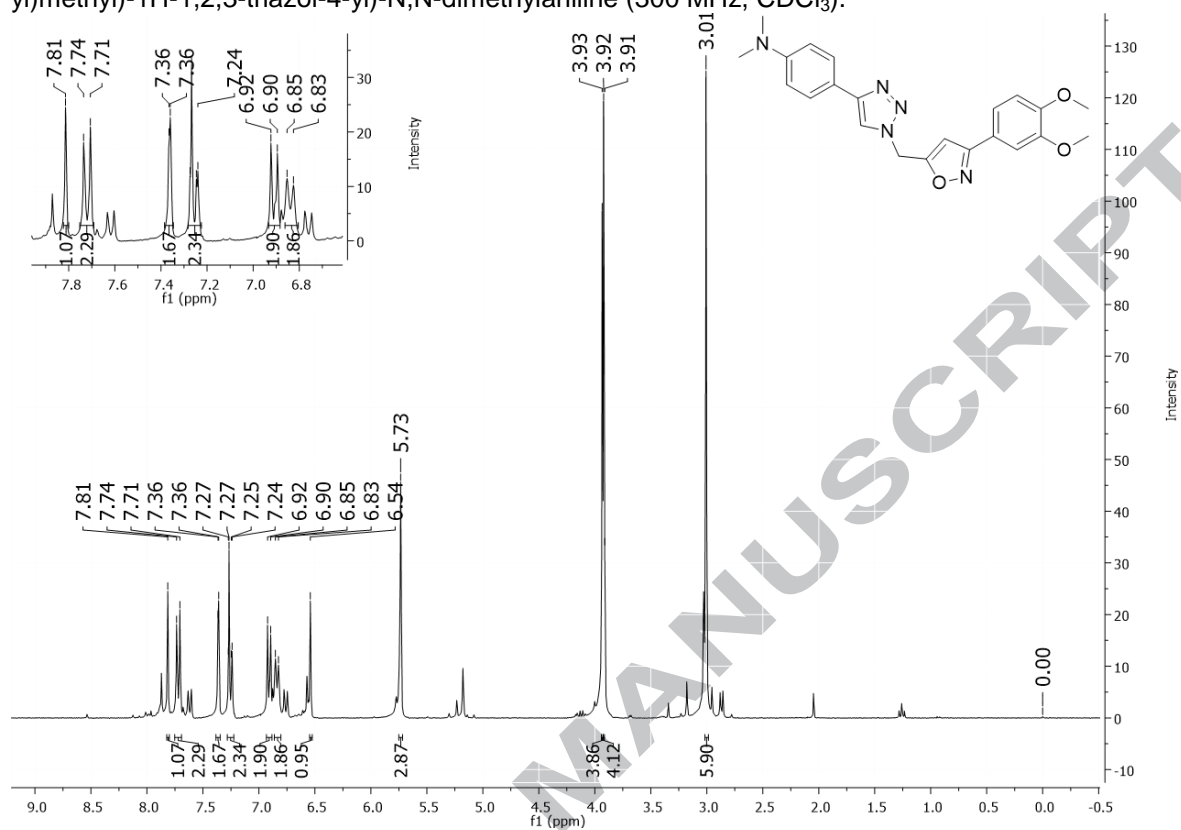


Fig. S75. $^{13}\text{C-NMR}$ spectrum of **compound 41**: 4-(1-((3-(3,4-dimethoxyphenyl)isoxazol-5-yl)methyl)-1H-1,2,3-triazol-4-yl)-N,N-dimethylaniline (100 MHz, CDCl_3).

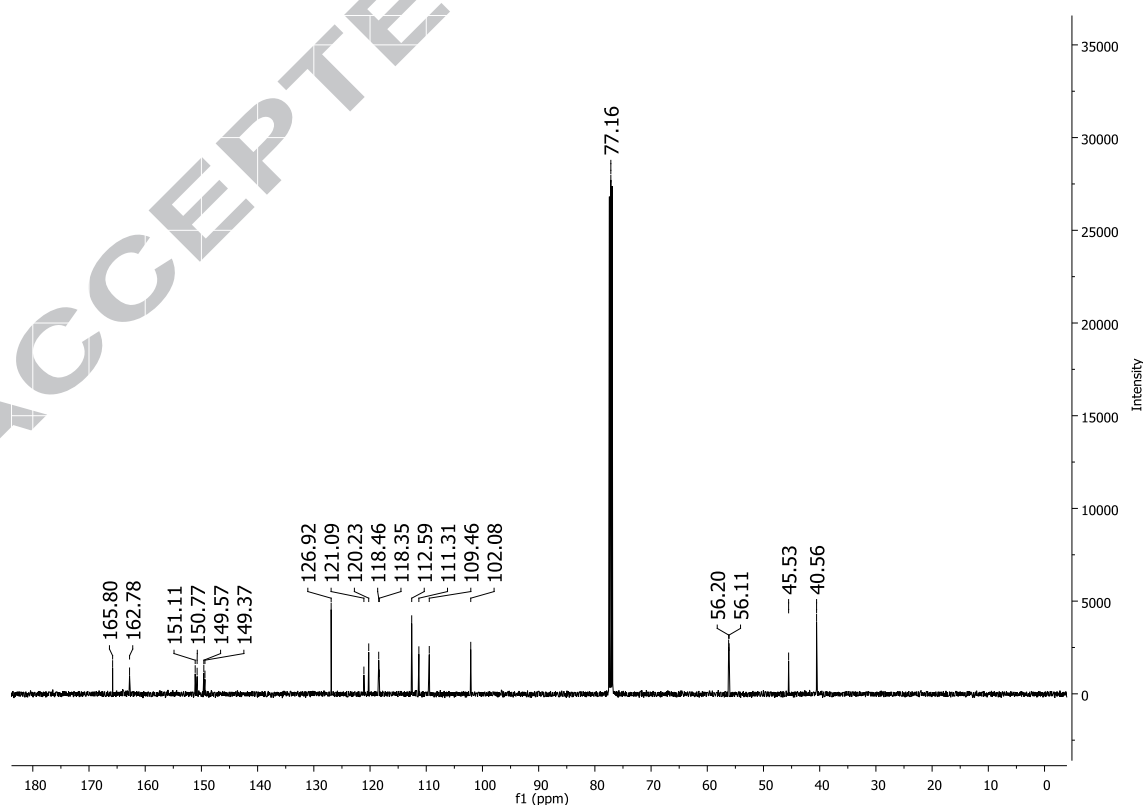


Fig. S76. $^1\text{H-NMR}$ spectrum of **compound 42**: 3-(3,4-dimethoxyphenyl)-5-((4-(6-methoxynaphthalen-2-yl)-1H-1,2,3-triazol-1-yl)methyl)isoxazole (300 MHz, CDCl_3).

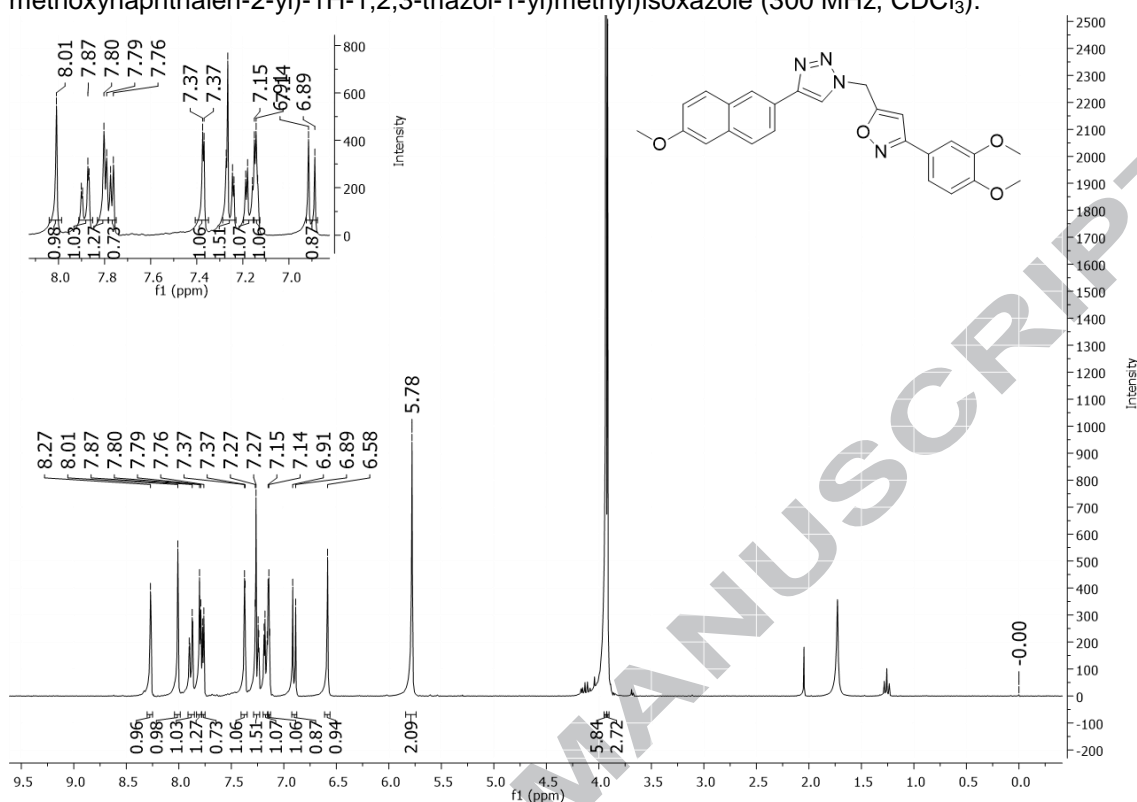


Fig. S77. $^{13}\text{C-NMR}$ spectrum of **compound 42**: 3-(3,4-dimethoxyphenyl)-5-((4-(6-methoxynaphthalen-2-yl)-1H-1,2,3-triazol-1-yl)methyl)isoxazole (100 MHz, CDCl_3).

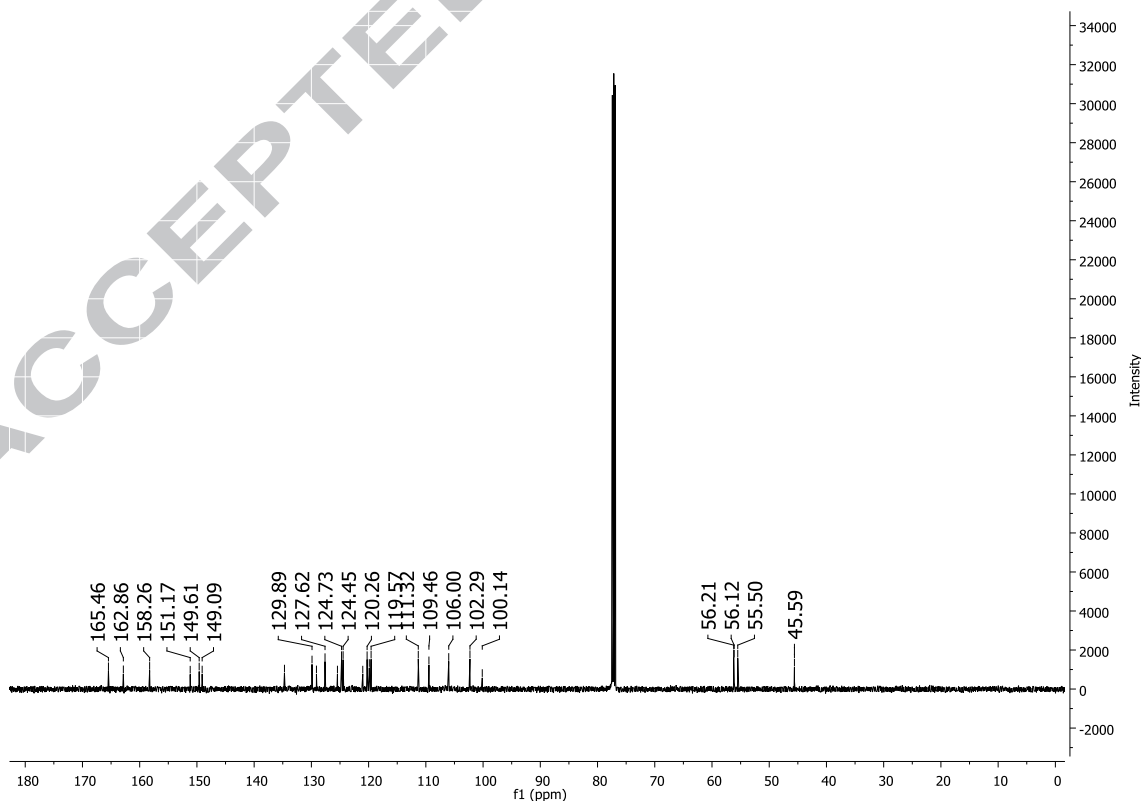


Fig. S78. $^1\text{H-NMR}$ spectrum of **compound 43**: 3-(4-methoxyphenyl)-5-((4-(4-methoxyphenyl)-1H-1,2,3-triazol-1-yl)methyl)isoxazole (400 MHz, CDCl_3).

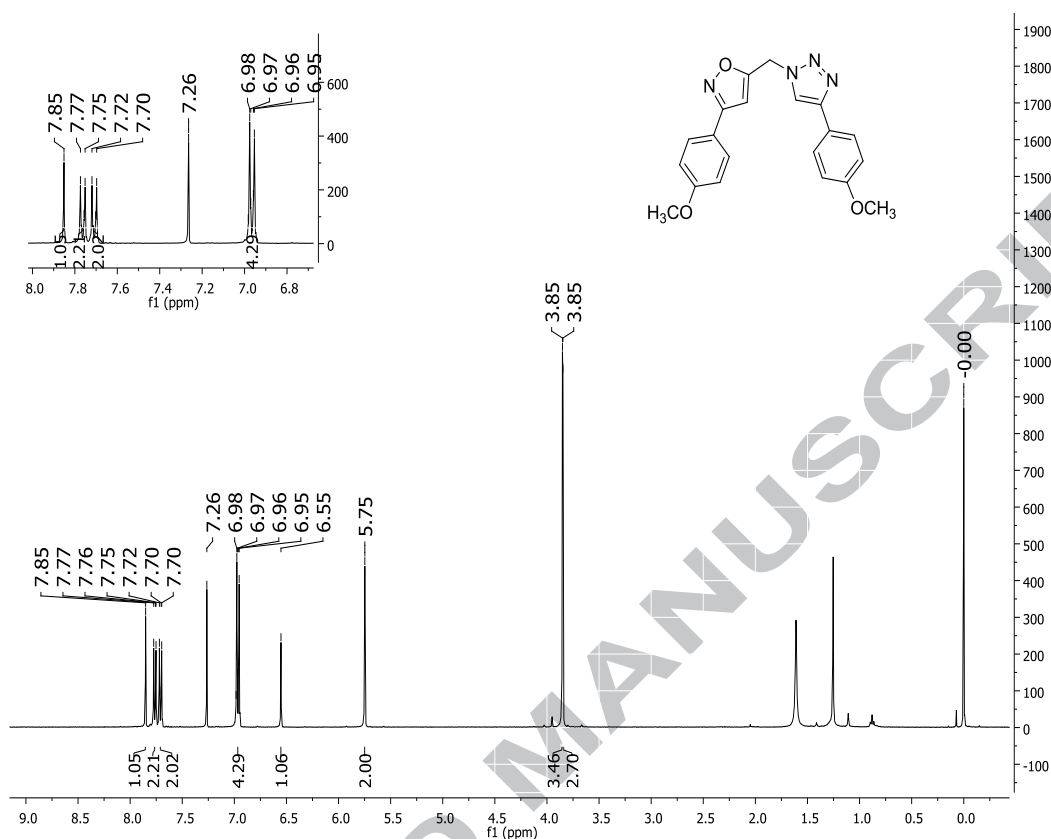


Fig. S79. $^{13}\text{C-NMR}$ spectrum of **compound 43**: 3-(4-methoxyphenyl)-5-((4-(4-methoxyphenyl)-1H-1,2,3-triazol-1-yl)methyl)isoxazole (100 MHz, CDCl_3).

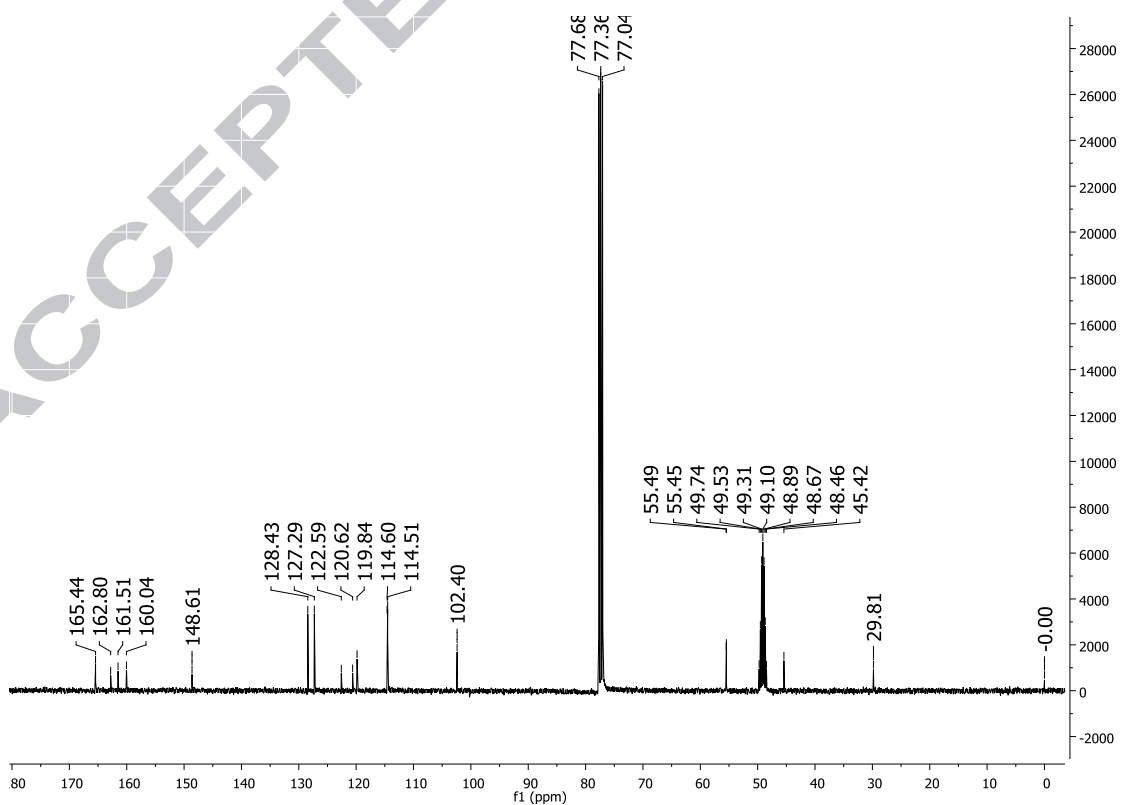


Fig. S80. $^1\text{H-NMR}$ spectrum of **compound 44**: 3-(benzo[d][1,3]dioxol-5-yl)-5-((4-(4-methoxyphenyl)-1H-1,2,3-triazol-1-yl)methyl)isoxazole (400 MHz, CDCl_3).

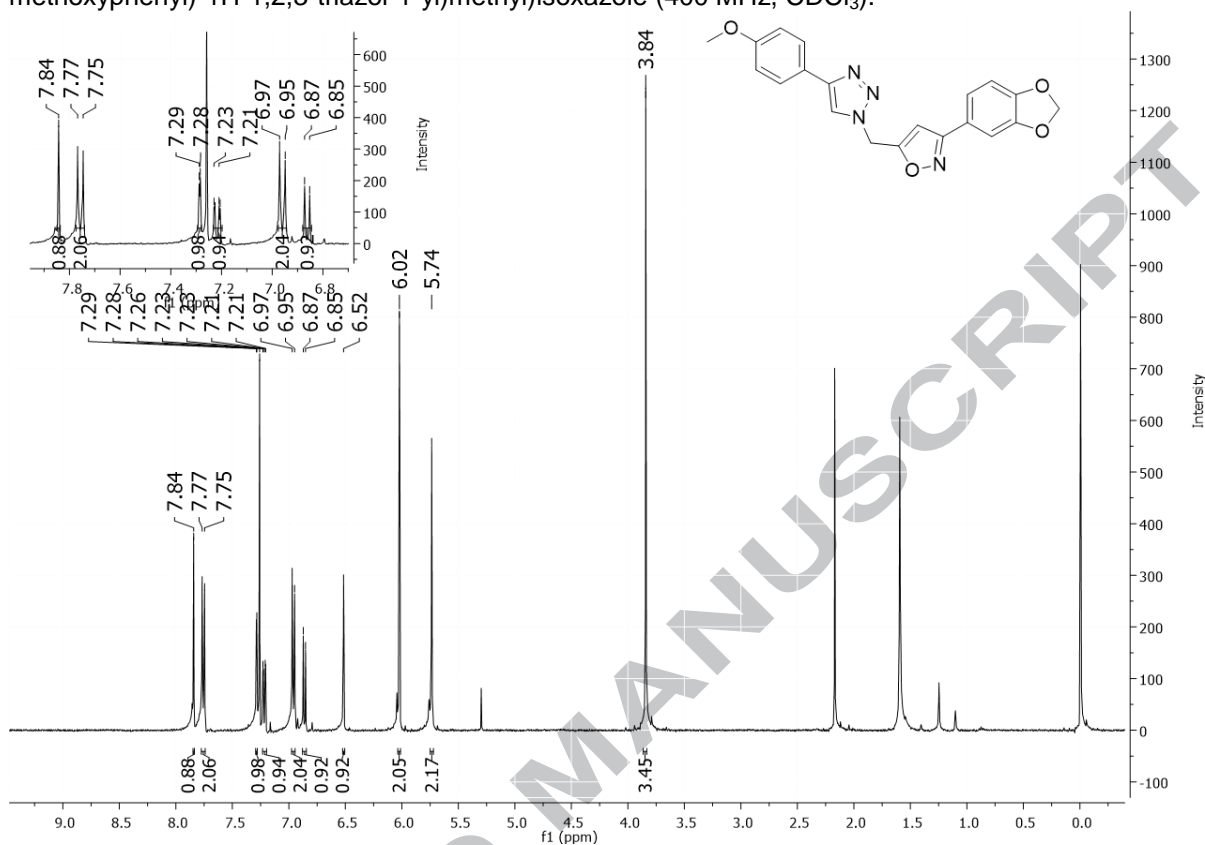


Fig. S81. $^{13}\text{C-NMR}$ spectrum of **compound 44**: 3-(benzo[d][1,3]dioxol-5-yl)-5-((4-(4-methoxyphenyl)-1H-1,2,3-triazol-1-yl)methyl)isoxazole (100 MHz, CDCl_3).

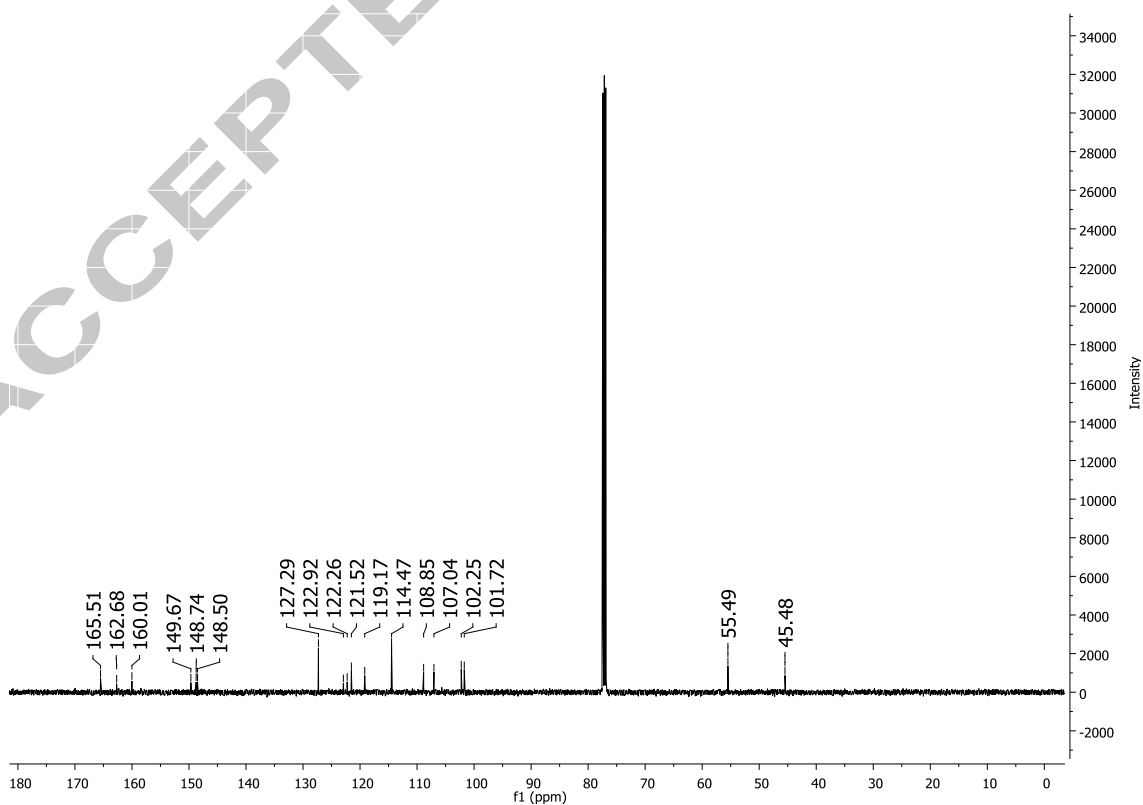


Fig. S82. $^1\text{H-NMR}$ spectrum of **compound 45**: 3-(4-methoxyphenyl)-5-((4-(trifluoromethoxy)phenyl)-1H-1,2,3-triazol-1-yl)methyl)isoxazole (300 MHz, CDCl_3).

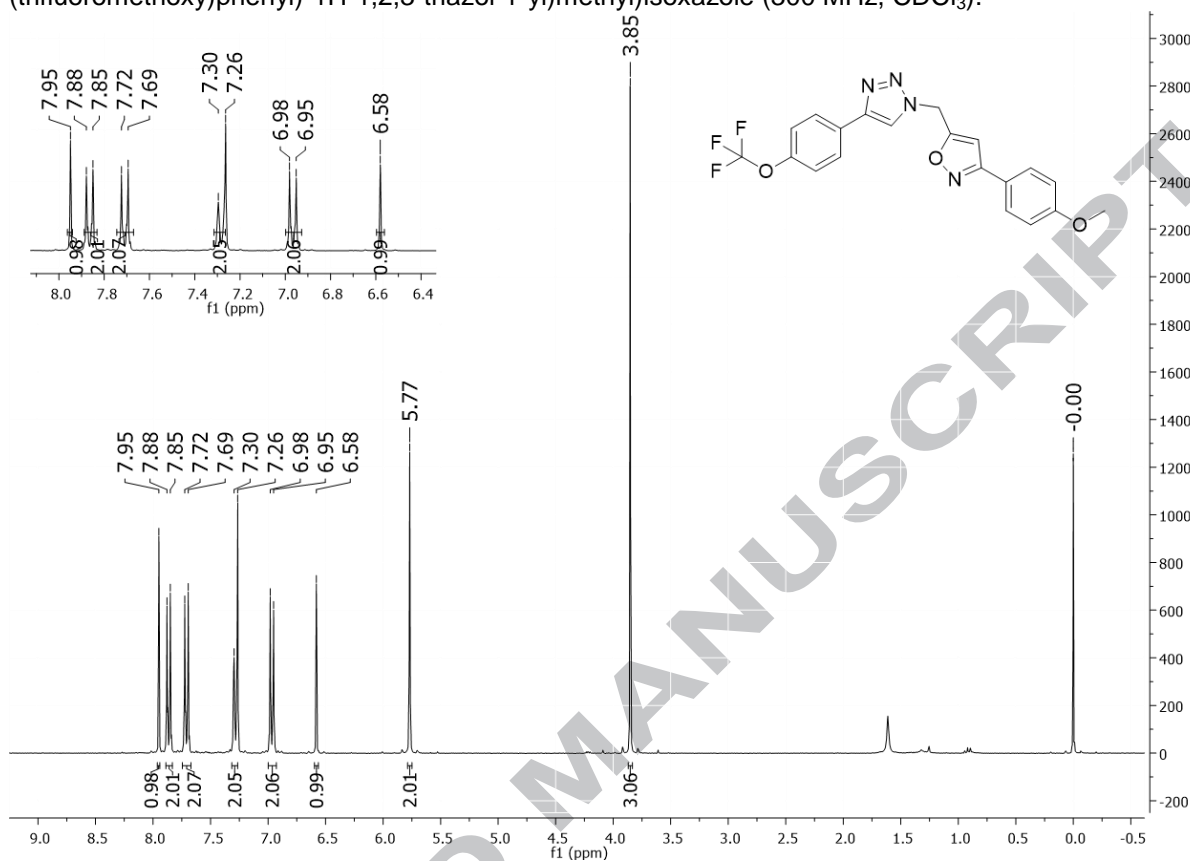


Fig. S83. $^{13}\text{C-NMR}$ spectrum of **compound 45**: 3-(4-methoxyphenyl)-5-((4-(trifluoromethoxy)phenyl)-1H-1,2,3-triazol-1-yl)methyl)isoxazole (125 MHz, CDCl_3).

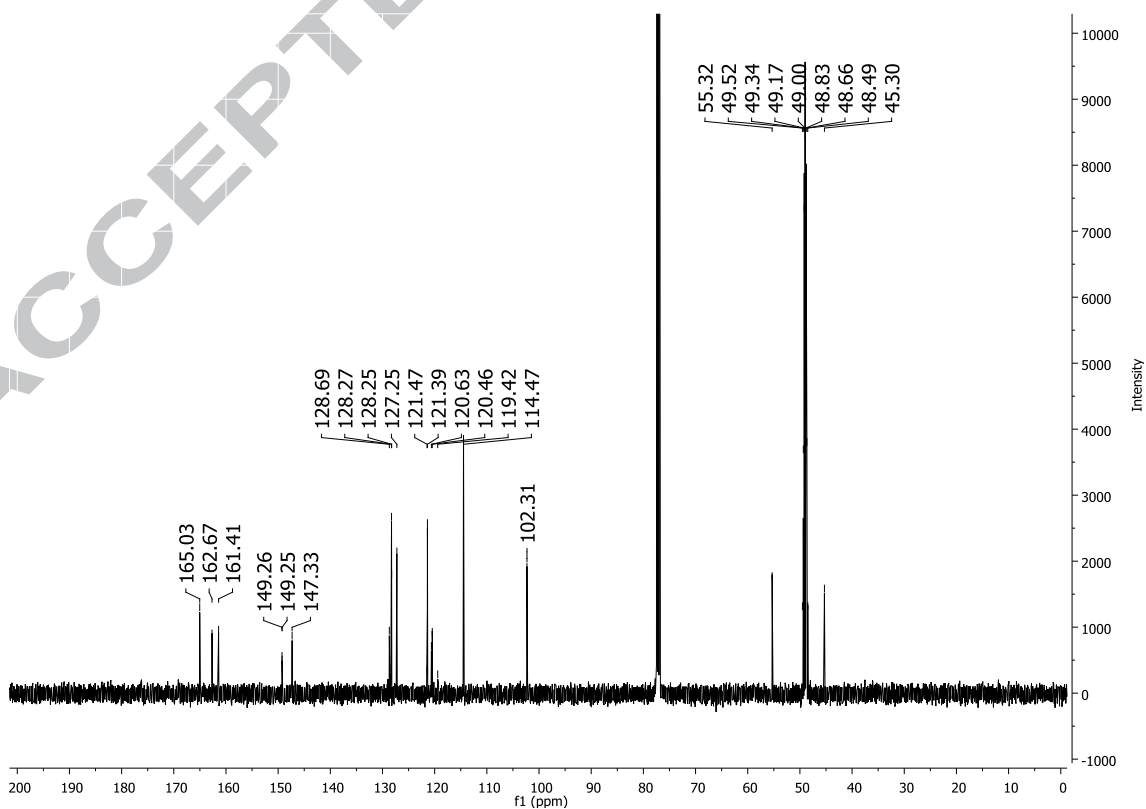


Fig. S84. $^1\text{H-NMR}$ spectrum of **compound 46**: 3-(benzo[d][1,3]dioxol-5-yl)-5-((4-(trifluoromethoxy)phenyl)-1H-1,2,3-triazol-1-yl)methyl)isoxazole (300 MHz, CDCl_3).

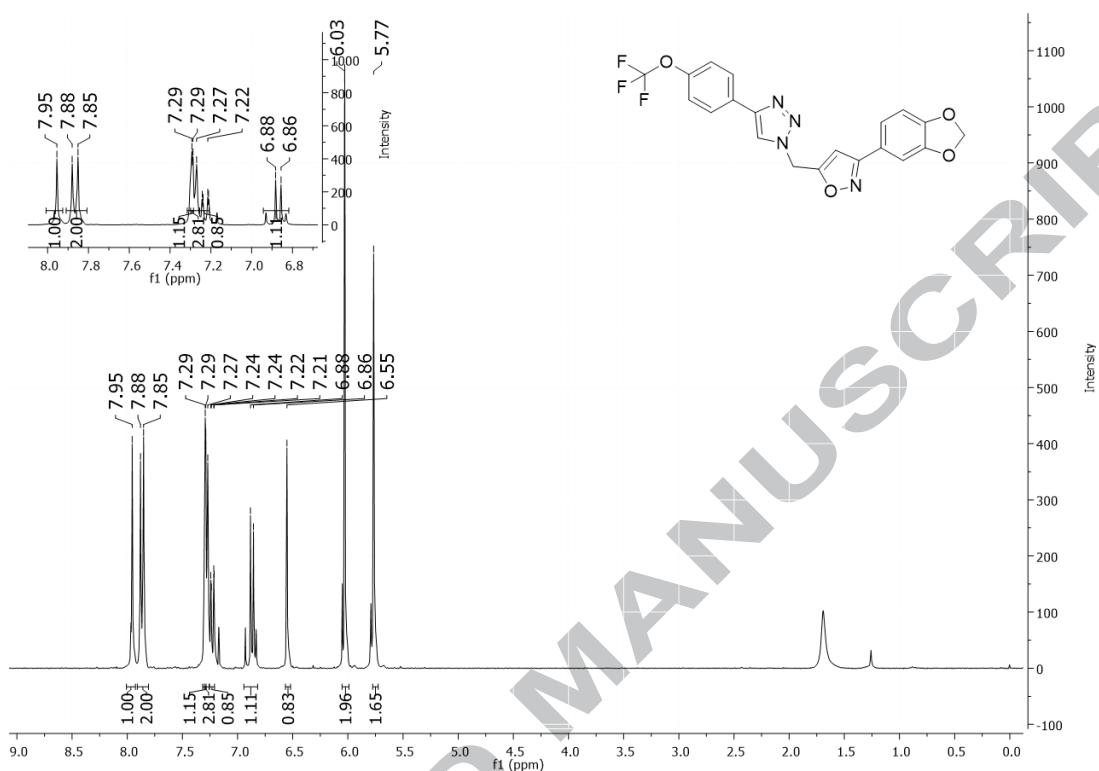


Fig. S85. $^{13}\text{C-NMR}$ spectrum of **compound 46**: 3-(benzo[d][1,3]dioxol-5-yl)-5-((4-(trifluoromethoxy)phenyl)-1H-1,2,3-triazol-1-yl)methyl)isoxazole (125 MHz, MeOD-d_4).

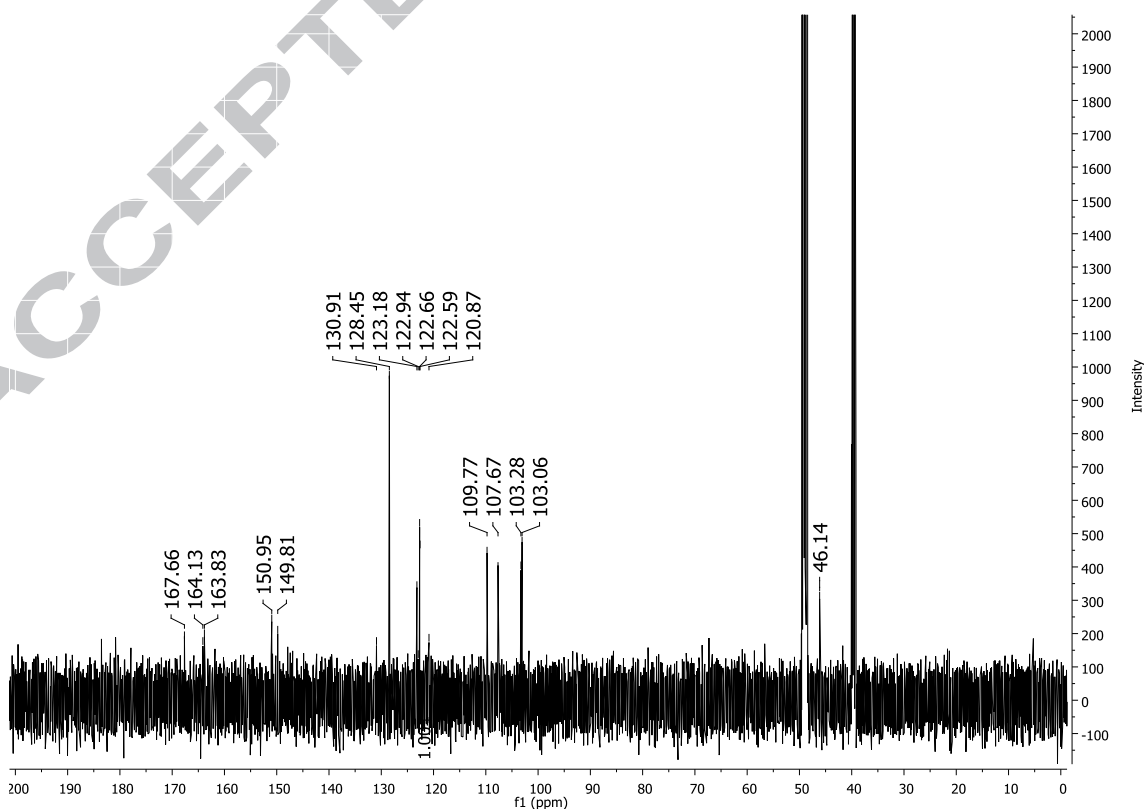


Fig. S86. $^1\text{H-NMR}$ spectrum of **compound 47**: 3-(4-methoxyphenyl)-5-((4-(4-pentylphenyl)-1H-1,2,3-triazol-1-yl)methyl)isoxazole (300 MHz, CDCl_3).

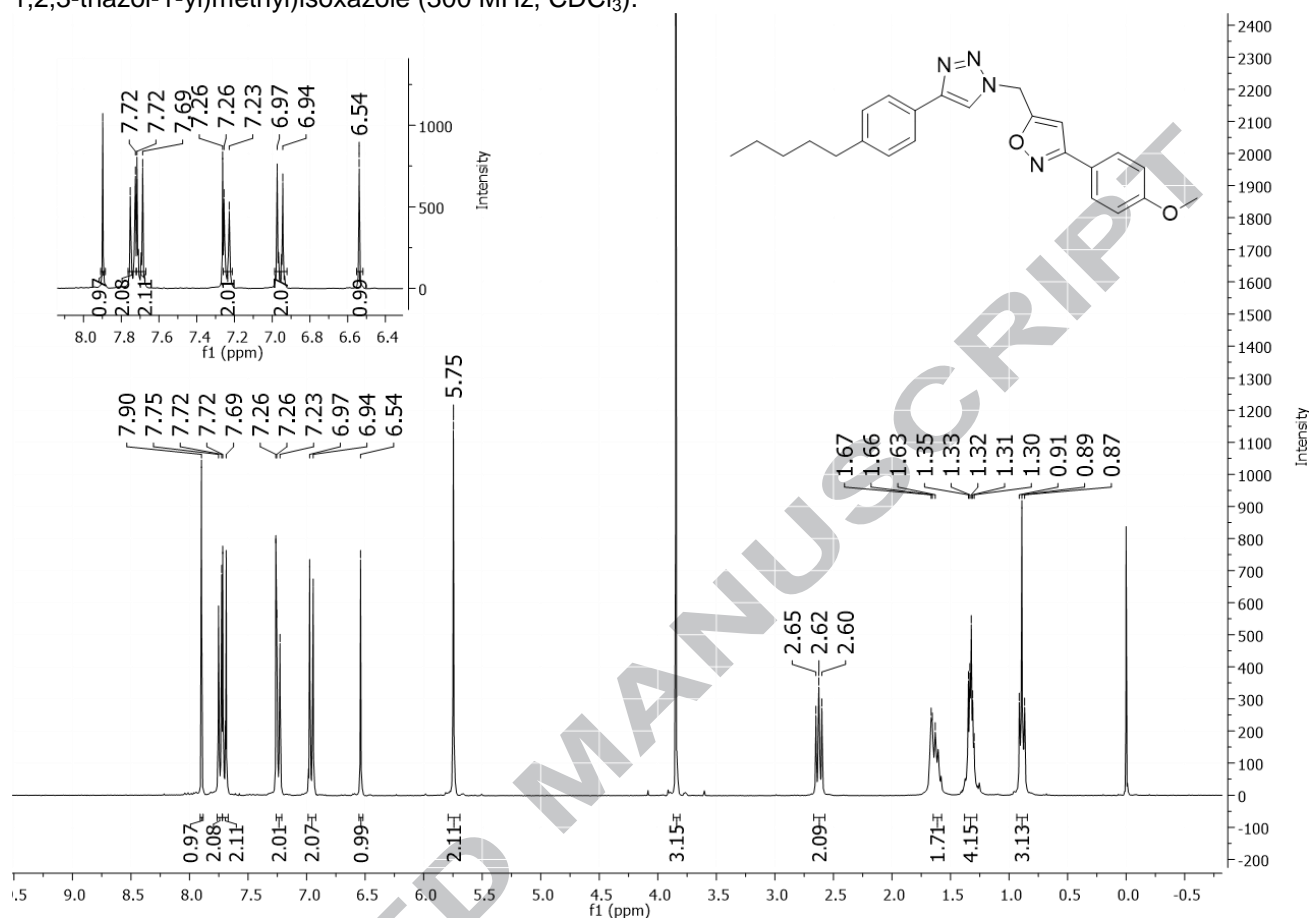


Fig. S87. $^{13}\text{C-NMR}$ spectrum of **compound 47**: 3-(4-methoxyphenyl)-5-((4-(4-pentylphenyl)-1H-1,2,3-triazol-1-yl)methyl)isoxazole (100 MHz, CDCl_3).

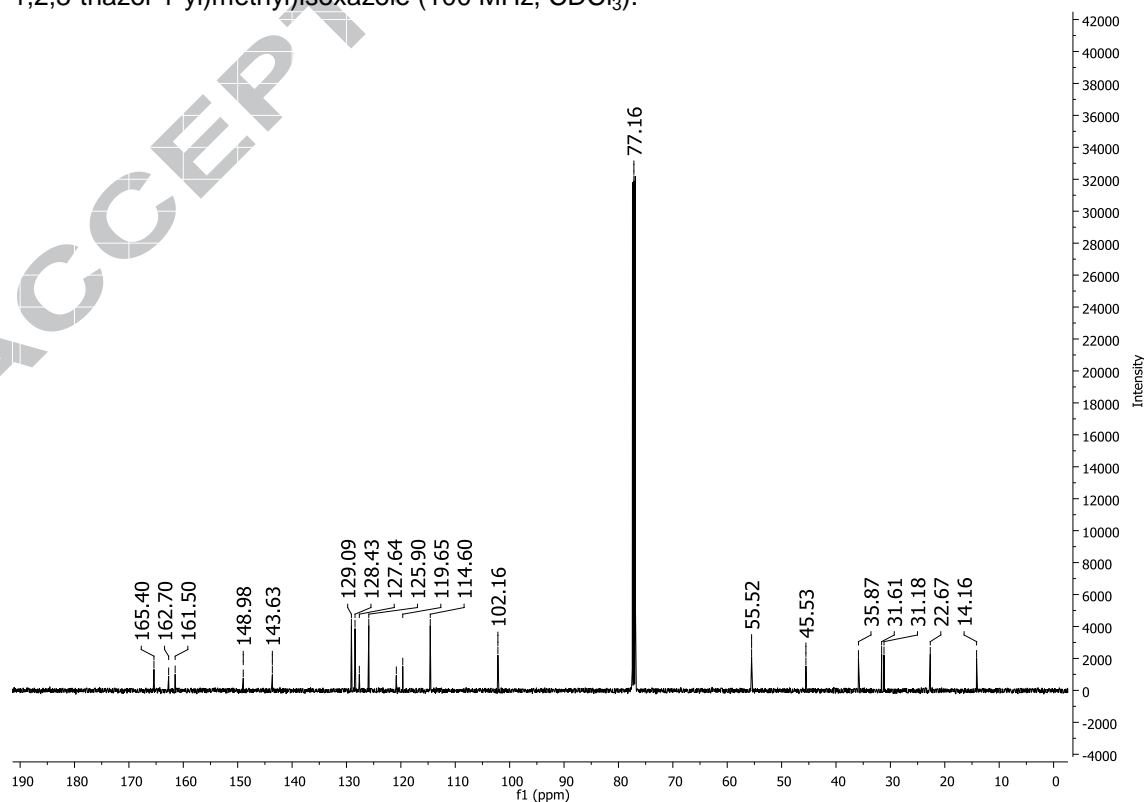


Fig. S88. $^1\text{H-NMR}$ spectrum of **compound 48**: 3-(benzo[d][1,3]dioxol-5-yl)-5-((4-(4-pentylphenyl)-1H-1,2,3-triazol-1-yl)methyl)isoxazole (500 MHz, DMSO-d_6).

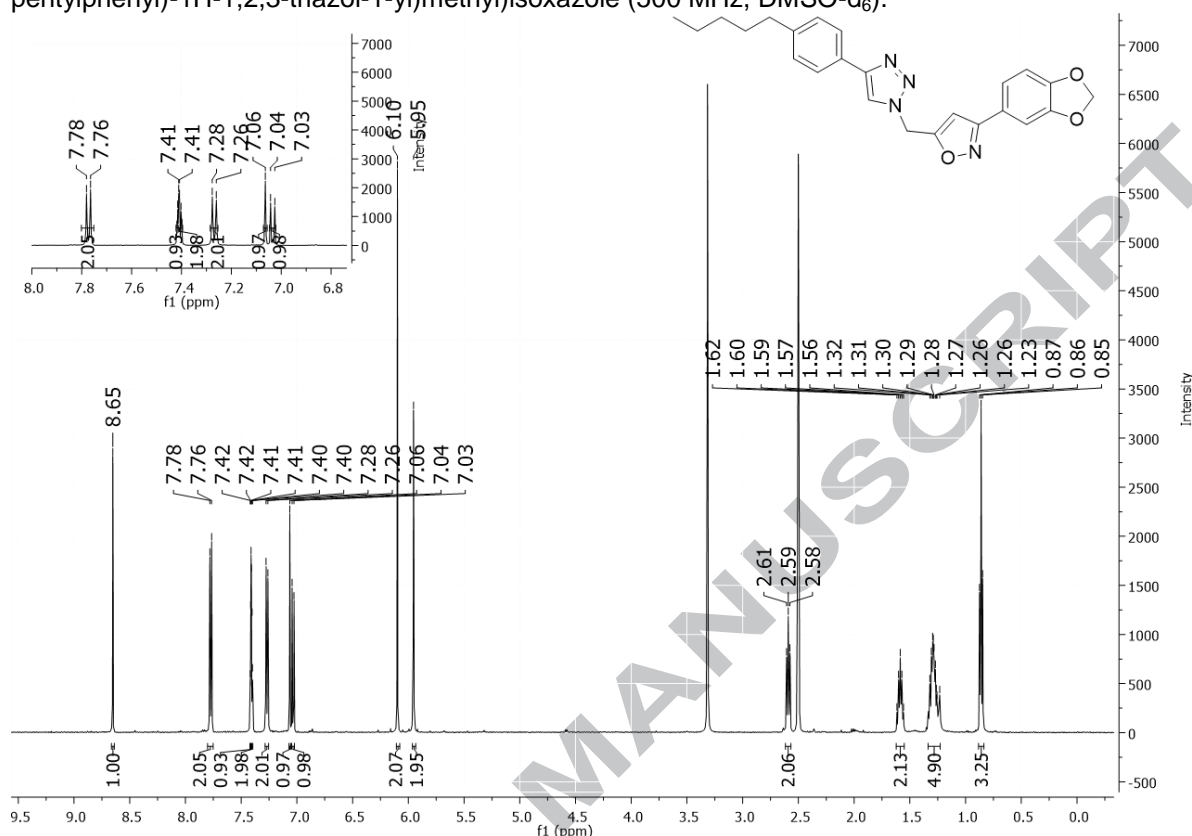


Fig. S89. $^{13}\text{C-NMR}$ spectrum of **compound 48**: 3-(benzo[d][1,3]dioxol-5-yl)-5-((4-(4-pentylphenyl)-1H-1,2,3-triazol-1-yl)methyl)isoxazole (100 MHz, DMSO-d_6).

